Elucidating mechanisms of transformation and tumorigenesis by Merkel cell polyomavirus tumor antigens

Kristine Nicole Dye

A dissertation

submitted in partial fulfillment of the

Requirements for the degree of

Doctor of Philosophy

University of Washington

2020

Reading Committee:

Denise A. Galloway (Chair)

Paul T. Nghiem

Jaisri R. Lingappa

Program Authorized to Offer Degree:

Pathobiology

University of Washington

Abstract

Elucidating mechanisms of transformation and tumorigenesis by Merkel cell polyomavirus tumor antigens

Kristine Nicole Dye

Chair of the supervisory committee

Denise A. Galloway

Pathobiology Program, Department of Global Health

In 2008, Merkel cell polyomavirus (MCPyV) was found to be the etiologic agent of 80% of Merkel cell carcinomas (MCC) through expression of two viral oncoproteins: the Small Tumor antigen (ST) and a truncated form of the Large Tumor antigen (LT-t). In order to elucidate mechanisms of transformation by these tumor antigens, we sought to define which of the tumor antigen(s) is responsible for transformation and tumorigenesis, the domains of the tumor antigen(s) responsible for this phenotype, and the cellular binding partners and pathways perturbed through interaction with the MCPyV tumor antigen(s). Various transformation assays using primary human foreskin fibroblasts (HFF), the potential host cell for natural MCPyV infection, transduced with MCPyV tumor antigens identified MCPyV ST as the dominant transforming protein, with LT-t showing no evidence of transforming potential in the assay. MCPyV ST expressing HFFs were also found to be tumorigenic when injected into NOD *scid* gamma mice, consistent with *in vitro* transformation assay

experiments. As MCPyV is the only human polyomavirus (HPyV) routinely found in a human cancer, we next sought to determine whether MCPyV ST is unique in its transforming ability. The ST antigens of two other skin tropic human polyomaviruses, Human Polyomavirus 7 (HPyV7) and Trichodysplasia spinulosa polyomavirus (TSPyV), were found to be non-transforming in HFFs, consistent with no association with these viruses and cancer. Mutational analysis of known MCPyV ST domains identified amino acids 116-120 and 91-95 as individually necessary for transformation. In order to identify the cellular binding partners and pathways necessary for transformation by MCPyV ST, TurboID Mass Spectrometry and Next-Generation RNA Sequencing (NGS) comparing the transforming MCPyV ST and non-transforming HPyV7 ST, TSPyV ST, MCPyV ST 116-120A and MCPyV ST 91-95A was performed. A total of 8 novel MCPyV ST interactors, with known oncogenic or tumor suppressive functions, were found to interact with ST, including Yes-associated protein 1 (YAP1), a transcriptional co-activator of the Hippo pathway. Interestingly, NGS found YAP target genes to be deregulated in ST compared to untransduced (UT) HFFs. Future experiments aim to further define the interaction between MCPyV ST and YAP, the role of this interaction in transformation and tumorigenesis by MCPyV ST, and YAP as a potential therapeutic target for the treatment of MCC.

TABLE OF CONTENTS

LIST OF FIGURES

LIST OF TABLES

LIST OF ACRONYMS

MCC – Merkel cell carcinoma

MCPyV – Merkel cell polyomavirus

VN-MCC – Merkel cell polyomavirus negative Merkel cell carcinoma

VP-MCC – Merkel cell polyomavirus positive Merkel cell carcinoma

LT – Merkel cell polyomavirus Large Tumor antigen

LT-t – Merkel cell polyomavirus truncated Large Tumor antigen

ST – Merkel cell polyomavirus Small Tumor antigen

MT – Murine polyomavirus Middle Tumor antigen

HFF – Primary Human Foreskin Fibroblasts

HPyV – Human Polyomavirus

HPyV7 – Human Polyomavirus 7

TSPyV - Trichodysplasia spinulosa polyomavirus

SV40 – Simian Vacuolating Virus 40

MuPyV – Murine Polyomavirus

Rb – Retinoblastoma protein

NLS – Nuclear localization sequence

NCRR – Non-coding regulatory region

PP2A – Protein phosphatase 2

YAP – Yes associated protein

LSD – Large Tumor Antigen Stabilization Domain

ΔLSD – Large Tumor Antigen Stabilization Domain 91-95 alanine substitution

116-120A – MCPyV ST amino acids 116-120 alanine substitution

NGS – Next Generation RNA Sequencing

UT – Untransduced

IHC – Immunohistochemistry

CK20 – Cytokeratin 20

PY – Person Years

ER – Early Region

LR – Late Region

ACKNOWLEDGMENTS

This project would not have been possible without the help of my many collaborators and support teams. The University of Washington's unique, interdisciplinary PhD program provided me with a platform to perform research applicable to my strengths and interests. I am grateful for the Fred Hutch and all the supportive faculty and resources provided through the center.

A special thank you to my mentor Denise Galloway for being my support, teacher, and exemplar through this process. I am also thankful for Ann Roman, who has been a co-mentor alongside Denise, and a fantastic resource and teacher. Additionally, I am grateful for all the members of the Galloway Lab who have each played an individual and influential role in my project and/or personal development, including Nick Salisbury, Sujita Khanal, Greg Wipf, Jody Carter, Robin Smith, and Leeya Pinder.

This would also have not been possible without the support of the Pathobiology PhD program and its director Lee Ann Campbell, and my committee members, Paul Nghiem (GSR, reading committee), Jaisri Lingappa (reading committee), Nina Salama, Gael Kurath, and Rachel Katzenellenbogen. They have supported me and my goals throughout this entire process, and I am incredibly grateful for their encouragement.

Last, but not least, the success of this project was greatly facilitated by our many collaborators who donated supplies, reagents, and/or protocols, including: Proteomics, Imaging, and Genomics Core Facilities (Fred Hutch), Jim DeCaprio Lab (Dana-Farber), Chris Buck (NIH), Jiaxin You Lab (University of Pennsylvania), and the John Lee Lab (Fred Hutch).

DEDICATION

I would like to dedicate this dissertation to my entire family. Your loving support is what kept me going.

CHAPTER 1. INTRODUCTION

1.1 CHARACTERIZATION AND EPIDEMIOLOGY OF MERKEL CELL CARCINOMA

Merkel cell carcinoma (MCC) is a rare, but extremely aggressive neuroendocrine skin cancer first characterized by the pathologist Cyril Toker in 1972 [1, 2]. Dr. Toker studied five tumors that appeared to be divergent from other known cutaneous malignancies, and termed these growths as "trabecular carcinomas of the skin." Dr. Toker described these tumors to originate from the dermis and possibly arise from sweat glands, have a trabecular architecture, contain cells with scant cytoplasm, arise in elderly patients of both sexes, and to be highly metastatic. In 1978 these original tumor samples were further investigated by Tang and Toker using electron microscopy [3]. Three out of the five original tumor samples were found to have dense-core granules that were indistinguishable from structures observed in cells derived from neurocrest origin, particularly Merkel cells. The overwhelming similarities between Merkel cells and these tumors eventually led to the belief of MCC arising from Merkel cells, and the subsequent renaming of trabecular carcinoma to Merkel cell carcinoma in 1982 [4, 5]. Although in the 1980's to early 2000's MCC was accepted to be its own unique carcinoma of the skin, tools that allowed for definitive diagnoses were limited. Upon the development and utilization of immunohistochemistry (IHC) on MCC tumors, cytokeratin 20 (CK20) was identified as a highly specific MCC biomarker useful for differentiating MCC from other morphologically similar carcinomas, as both MCCs and Merkel cells were found to have a unique dot-like pattern of CK20 expression [6].

Since the discovery of diagnostic markers and increasing recognition of MCC [7], there have been several epidemiological studies aimed to determine the incidence and distribution of MCC [8-13]. Collectively, these studies have found MCC to have a markedly lower incidence when compared

to other skin cancers (basal cell carcinoma 113 cases per 100,000 person years (PY), squamous cell carcinoma 38, melanoma 8.76 and MCC 0.28); however, the incidence and mortality of MCC have increased rapidly during the timeframe of these studies. Surprisingly, the incidence of MCC has increased by 95% since the year 2000 and is projected to continue rising. Although much rarer than melanoma, MCC has been found to have a 5-year survival rate of less than 45%, making MCC almost three times as lethal as melanoma. These epidemiological studies have also identified several risk-factors for developing MCC including old age, immunosuppression, additional cancer diagnoses, and high exposure to UV light [14-16].

1.2 IDENTIFICATION AND CLASSIFICATION OF MERKEL CELL POLYOMAVIRUS

Although MCC was first characterized in the early 1970's, it wasn't until 2008 that two distinct subtypes of MCC were identified [17]. A significant increase in MCC incidence was observed in immunosuppressed individuals such as the elderly, those infected with HIV-1 AIDS, and also those treated for autoimmune diseases such as rheumatoid arthritis or post-treatment solid organ transplantation by medically induced immunosuppression [18-21]. These findings led to the hypothesis that MCC may be associated with a pathogen. The investigation to identify a possible pathogen as the etiologic agent of MCC was led by Huichen Feng and Masahiro Shuda in the laboratory of Yuan Chang and Patrick Moore at the University of Pittsburgh [17]. Feng and Shuda, through utilizing next-generation RNA sequencing advances, performed digital transcriptome subtraction of several MCC tumors. After sequencing the entire transcriptome of these MCC tumors, and subtracting known human genes from the analysis, Feng and Shuda identified transcripts related to those of known polyomaviruses. Surprisingly, the polyomavirus identified in these tumors was distinct in sequence from known polyomaviruses and was therefore considered to be a novel polyomavirus which was subsequently termed Merkel cell polyomavirus (MCPyV).

Importantly, Feng and Shuda found MCPyV to be clonally integrated into the host genome of these MCC tumors, as similar integration patterns were observed for metastases in the lymph nodes of the same patient. Further, it was found that eight out of ten MCC tumors analyzed contained integrated MCPyV genome, suggesting that most, but not all, MCC tumors contained integrated MCPyV.

1.3 MERKEL CELL POLYOMAVIRUS

MCPyV, like other polyomaviruses, is a small, circular dsDNA virus with a genome of ~5.3kb [17, 22]. The circular viral genome consists of an early region (ER) and late region (LR) separated by a non-coding regulatory region (NCRR) containing a bidirectional promoter (Fig. 1) The LR encodes structural proteins necessary for the formation of the icosahedral capsid. Due to its constrained genomic size, MCPyV utilizes alternative splicing of the ER to generate several diverse tumor antigen proteins, including the large T-antigen (LT), 57kT, small T-antigen (ST), and alternate large tumor antigen open reading frame (ALTO). LT, ST and the 57kT share the same start codon, and encode the same N-terminal amino acids referred to as "common-T." LT and the 57kT then splice with a region downstream of the mRNA, whereas ST reads through this splice donor site

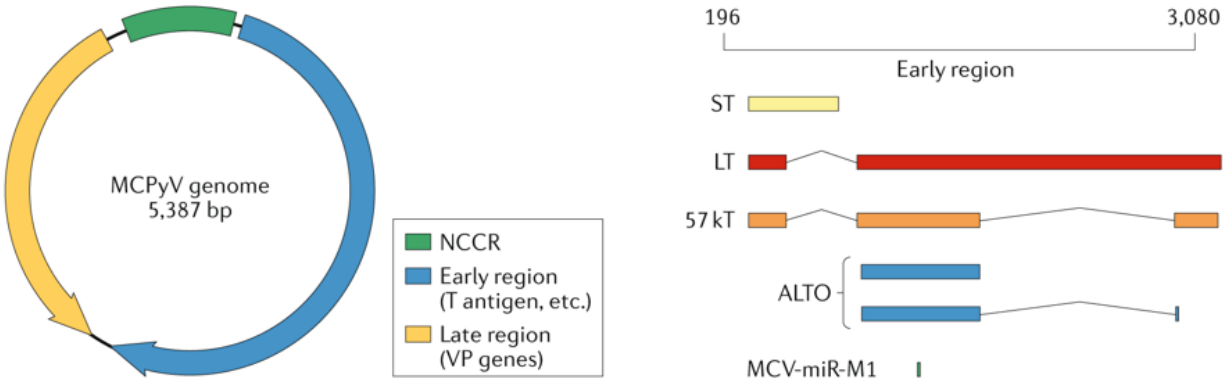

Figure 1. The organization of the MCPyV genome. The MCPyV genome is separated into an early and late region (ER and LR). The LR encodes structural proteins, and ER utilizes alternative splicing to generate the tumor antigens, including ST, LT, 57kT and ALTO. Figure adapted from Harms *et al.,* 2018.

before encountering its own stop codon prior the splice acceptor site of LT and 57kT. The region of ST encoded within the LT and 57kT intron is referred to as the "ST unique region." In contrast, the ALTO coding sequence begins at its own unique start codon and is overprinted on the +1 reading frame of the second exon of LT. The NCRR contains the origin binding domain (OBD) and separate bidirectional promoters for the transcription of the early or late regions.

The MCPyV viral life cycle begins with MCPyV interacting with heparin or chondroitin sulfate surface receptors and sialic acids co-receptors found on the surface of its target cell [23]. MCPyV then enters the cell by caveolar or lipid raft mediated endocytosis and travels to the endoplasmic reticulum via endosomes. Upon translocation into the nucleus, ER gene expression is immediately initiated, leading to expression of proteins necessary for S-phase cell cycle progression (LT and ST), and consequent upregulation of cellular proteins necessary for viral replication. High levels of LT expression also lead to the initiation of viral replication, as LT is responsible for interacting with and unwinding the DNA of the viral origin of replication through its origin binding domain (OBD) and helicase domain, respectively. This allows for cellular proteins and polymerases to be recruited to the viral origin and amplify the viral genome. LT binding to the origin of replication also blocks the ER promoter, leading to transcription of the structural proteins found in the LR and subsequent viral assembly and egress. Of note, the role of ALTO and 57kT in the viral life cycle is currently unclear [24]. Importantly, since its discovery MCPyV has been found to be ubiquitous in the human population. MCPyV is thought to be acquired in early childhood, as ~50% of children have circulating antibodies to MCPyV, and ~75% of adults are seropositive to MCPyV [25].

1.3.1 VIRUS POSITIVE VERSUS VIRUS NEGATIVE MERKEL CELL CARCINOMA

In 2008 it was discovered that MCC can be separated into two different subcategories: virus positive MCC (VP-MCC) and virus negative MCC (VN-MCC). VP-MCC refers to the 80% of MCC

tumors found to have integrated MCPyV genome and express the viral TAgs; however, the remaining 20% of MCC tumors are considered to be VN-MCC, as they do not have detectable integrated MCPyV genome. Instead, these VN-MCC tumors have an extensive UV mutational burden which is the highest of any cancer sequenced by the cancer genome atlas, and is 100-fold higher than the mutational burden of VP-MCC, which is the lowest of any epithelial cancer sequenced [26]. These findings suggest that in VN-MCC it is the accumulation of UV mutations that lead to the development of MCC, whereas in VP-MCC it is the integration of MCPyV and expression of its viral proteins that lead to the development of MCC. Surprisingly, regardless of the origin, VP- and VN-MCC are indistinguishable from each other to health care providers, suggesting that regardless of the cause, the heavy mutational burden or viral genome integration, they both lead to the development of the same cancer.

1.3.2 MERKEL CELL POLYOMAVIRUS IN MERKEL CELL CARCINOMA

After the discovery of MCPyV integration in MCC, MCPyV infection has been found to be ubiquitous in the human population, and is thought to be acquired in early childhood, as ~50% of children have circulating antibodies to MCPyV, and ~75% of adults are seropositive to MCPyV [25]. However, in normal, healthy individuals MCPyV is asymptomatic. Therefore, one of the most perplexing questions of MCC is how such a ubiquitous, innocuous virus can lead to the development of such a rare, aggressive cancer; however, more recently we are starting to appreciate the 'perfect storm' of events that must occur for the development of VP-MCC. In addition, these findings have also unambiguously proven MCPyV as the etiologic agent of VP-MCC.

Several differences have been observed between natural MCPyV infection and MCPyV caused MCC. For example, in MCPyV infection the viral genome is episomal; however, in VP-MCC the viral genome is integrated into the host genome of tumors [17, 23]. Importantly, the integration

of the MCPyV genome precedes, and is essential for, the development of VP-MCC [17]. Furthermore, the MCPyV genome integrated in MCC tumors is found to be consistently truncated due to the addition of a premature stop codon or deletion in the LT coding sequence, resulting in the expression of a truncated form of LT (LT-t) [24]. Although the exact location of this truncation is highly variable, they all have three things in common: 1) The truncation always deletes C-terminal helicase and ATPase domains, both of which are necessary for viral replication and thus deleterious for tumor formation due to cell lysis at the end of viral replication and potential clashing of replication forks. This truncation also deletes the C-terminal 100 amino acids of LT, which have been found to induce a DNA damage response and reduce cellular proliferation [27, 28]. 2) The MCPyV ER truncations always preserve the Rb binding domain of LT, and 3) the ST coding sequence is always intact, suggesting an importance for the LT Rb binding domain and the full, wild-type ST coding sequence for the development of VP-MCC tumors.

Finally, in contrast to the normal MCPyV viral life cycle, in MCC only the LT and ST antigens are expressed. Interestingly, the viability of VP-MCC tumors is dependent on both LT-t and ST expression, suggesting that these MCPyV TAgs are responsible for the aberrant proliferation and transformation of these MCC tumors cells [27]. Together, the integration and expression of the replication deficient MCPyV viral oncoproteins, LT-t and ST, present large bottlenecks in MCC development by MCPyV, and therefore present an explanation for the rarity of this cancer.

1.3.3 THE HOST CELL OF MERKEL CELL POLYOMAVIRUS INFECTION AND PROGENITOR CELL OF MERKEL CELL CARCIOMA

After the identification of MCPyV as the etiologic agent of MCC, several groups sought to define the mechanisms of transformation and tumorigenesis by MCPyV. However, our limited understanding of the host cell of MCPyV infection, and the progenitor cell of MCC has hampered

the success and relevance of these experiments. As the name would suggest, Merkel cell carcinoma was originally thought to occur upon MCPyV infection in Merkel cells [28, 29]. However, since their discovery, it has been found that Merkel cells are terminally differentiated and post-mitotic, therefore weakening the argument of Merkel cells as being the true progenitor of MCC, although MCPyV TAgs may be capable of inducing cell cycle progression of these quiescent Merkel cells. Eight years after the discovery of MCPyV, Jiaxin You's group at the University of Pennsylvania identified human dermal fibroblasts as a possible host cell of natural MCPyV infection, as dermal fibroblasts were the only skin cell capable of completing the full MCPyV viral lifecycle [30]. Whether dermal fibroblasts are also the progenitor cell of MCC is currently under debate, as several other groups have hypothesized epidermal stem cells, dermal stem cells, or pre-/pro- B cells as the MCC progenitor [31-34]. Further complicating the question, it appears that MCC progenitors may also differ between VP- and VN- MCC, as the progenitor of VN-MCC must reside in a cell that is exposed to UV radiation [28].

1.3.3.1 THE ANATOMY AND CELL TYPES OF THE SKIN

The skin is composed of three distinct layers: the epidermis, dermis, and hypodermis [35]. The epidermis is the top layer of the skin that is primarily composed of keratinocytes (~80%), but also contains dendritic cells, melanocytes, Langerhans cells and Merkel cells. Merkel cells are post-mitotic, mechanoreceptor cells found alongside epidermal stem cells in the basal epidermis, and concentrated in areas important for touch sensations such as the digits, lips, and hair follicles [36]. As single cells or clusters, known as touch-domes, Merkel cells are responsible for light touch sensation through their association with the terminal end of sensory neurons and neuroendocrine properties. Merkel cells can be distinguished from other cells in the basal epidermis by an array of immunohistochemical markers such as CK20, cytokeratins 8, 18, 19, and 20, chromogranin A,

synaptophysin, and neuron specific endolase. Below the epidermis, the dermis constitutes the majority of the skin, and is composed primarily of fibroblasts, but also contains pro- and pre- B-cells, macrophages, and mast cells [35].

1.4 POLYOMAVIRUSES AND DISEASE

In an effort to elucidate mechanisms of transformation by MCPyV LT-t and ST, many groups have turned to the studies of other known oncogenic polyomaviruses. The founding virus of the *polyomaviridae* family was discovered in 1953 as a filterable infectious agent that formed many different types of tumors in mice [37, 38]. Upon suspicion of the discovery of an oncogenic virus, the virus was named "polyomavirus" meaning "poly" - many "oma" - tumors. Approximately seven years later, in 1960, a primate polyomavirus was discovered as a contaminant of rhesus monkey kidney cell cultures used to produce the Salk poliovirus vaccine [39]. After its discovery, several reports implicated SV40 induced tumor formation in newborn rodents, and transformation of primary human cells [40-44]. As expected, these reports led to a growing public health concern, as the poliovirus vaccine contaminated with infectious SV40 had already been administered to over 98 million US residents between 1955 and 1963 [45]. As such, these reports led to intensive investigation into the oncogenic potential of SV40 that continues to this day, although currently no association has been found between SV40 exposure and human cancer [46, 47].

The first two HPyVs discovered were BK polyomavirus (BKPyV) and JC polyomavirus (JCPyV) [48, 49]. Both BKPyV and JCPyV are associated with disease of immunocompromised individuals; however, a clear association between these viruses and cancer has not yet been shown. With the rich history of polyomaviruses and cancer, the discovery of MCPyV as the first human polyomavirus (HPyV) to be associated with a human cancer initiated a search into identifying other possibly oncogenic human polyomaviruses. At the time of its discovery in 2008, MCPyV was the

fifth known HPyV, but now belongs to a family of 14 known HPyVs, none of when have been found to have a clear association with cancer, as is seen with MCPyV, although some HPyVs have been implicated in disease of immunosuppressed individuals. Similar to MCPyV most newly identified HPyVs are similarly ubiquitous in the population as measured by seroprevalence (Table 1), [50, 51].

Human Polyomavirus	Year of Discovery	Early Region Proteins	Known Diseases	Source of Isolation	Seroprevalence (%)
BK polyomavirus (BKPyV)	1971	LT, 17kT, ST	Polyomavirus associated nephropathy, hemorrhagic cystitis	Urine	82-92%
JC polyomavirus (JCPyV)	1971	LT, T' (165, 136, 135), ST	Progressive multifocal leukoencephalopathy	Urine, brain	40-55%
Karolinska Institute polyomavirus (KIPyV)	2007	LT, ST	None	Nasopharyngeal tissue	55-90%
Washington University polyomavirus (WUPyV)	2007	LT, ST	None	Nasopharyngeal tissue	70-90%
Merkel cell polyomavirus (MCPyV)	2008	LT, ST, 57kT, ALTO	Merkel cell carcinoma	Lesion	60-65%
Human polyomavirus 6 (HPyV6)	2010	LT, ST	None	Skin	70%
Human polyomavirus 7 (HPyV7)	2010	LT, ST	None	Skin	35%
Trichodysplasia spinulosa-associated polyomavirus (TSPyV)	2010	LT, MT, ALTO, ST	Trichodysplasia spinulosa, pilomatrix dysplasia	Lesion	70-80%
Human polyomavirus 9 (HPyV9)	2011	LT, ST	None	Skin, blood, urine	25-50%
Malawi polyomavirus (MWPyV)	2012	LT, ST	None	Stool, wart	Unknown
St. Louis polyomavirus (STLPyV)	2012	LT, MT, ST	None	Stool	Unknown
Human polyomavirus 12 (HPyV12)	2013	LT ST	None	GI Tract	Unknown
New Jersey polyomavirus (NJPyV)	2014	LT, alternative LT, ST	None	Muscle biopsy	Unknown
Lyon-IARC polyomavirus (LIPyV)	2017	LT, ST	None	Skin, stool	Unknown

Table 1. Human polyomaviruses. The 14 currently known human polyomaviruses and their year of discovery, ER proteins, associated diseases, tropism, and seroprevalence. Adapted from DeCaprio, 2017 and Moens, 2019.

The polyomavirus genome structure is very similar between human polyomaviruses and polyomaviruses of other species [52]. The ER of MuPyV, SV40, MCPyV and other skin trophic human polyomaviruses are similar, but also divergent in their splicing patterns and coding regions. The MuPyV ER encodes a large T antigen (LT), small T antigen (ST), and middle T antigen (MT). The SV40 ER encodes LT and ST. The MCPyV ER encodes LT, ST, and ALTO [24]. Interestingly, although ALTO is not found to be expressed in VP-MCC, and its role is not yet well understood in the MCPyV life-cycle, MCPyV ALTO is evolutionarily related to the transforming MT of MuPyV. Generally speaking, other known human polyomaviruses also encode LT and ST. Throughout this dissertation, HPyV7 and TSPyV will be representative of the additional 13 known HPyVs that have not yet been clearly associated with cancer. Due to their differential splicing patterns and divergent sequences, the TAgs from different species have shared and unique domains, and as such, have shared and unique functions (Fig. 2).

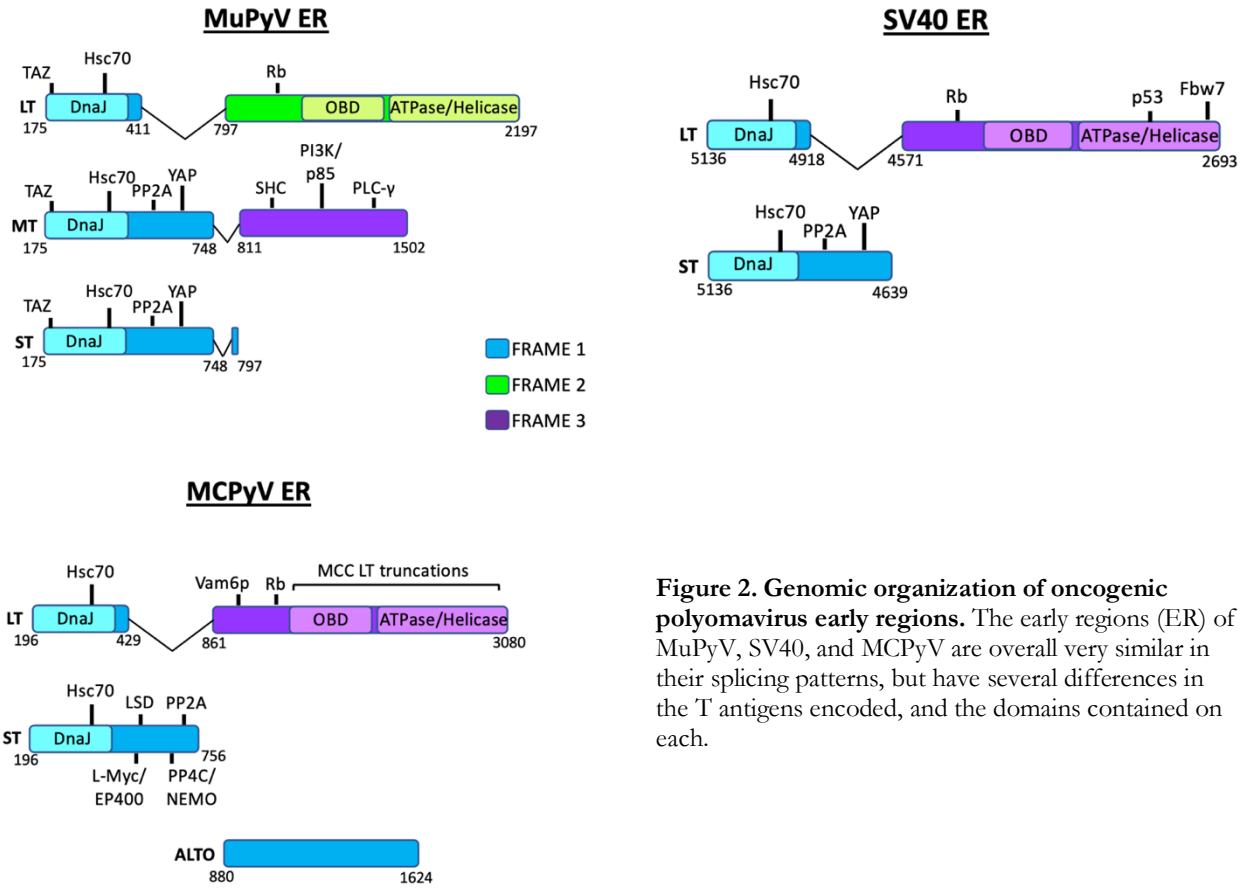

Figure 2. Genomic organization of oncogenic polyomavirus early regions. The early regions (ER) of MuPyV, SV40, and MCPyV are overall very similar in their splicing patterns, but have several differences in the T antigens encoded, and the domains contained on each.

Over the past 60 years, intensive research into the mechanisms of transformation by MuPyV and SV40 have revealed many mechanisms of cellular transformation. In MuPyV, MT has been found to be the dominant transforming protein, with ST playing more of a supportive role. However, in the case of SV40, LT is the dominant transforming protein, with ST also playing a supportive role [53]. Research into the binding partners and pathways perturbed by MuPyV and SV40 viral oncoproteins has revealed common themes in polyomavirus mediated transformation and tumorigenesis and has thus laid the groundwork for similar studies into MCPyV. Next, descriptions of the common pathways and proteins perturbed by polyomaviruses will be described, with an emphasis on our current understanding of the similarities and differences between polyomaviruses and these pathways.

1.4.1 RETINOBLASTOMA PROTEIN

The retinoblastoma protein (Rb) is an essential tumor suppressor that negatively regulates cellular proliferation, and is frequently mutated in a wide range of cancers [54]. In its active, hypophosphorylated form, Rb binds and sequesters E2F transcription factors. As E2F leads to transcription of genes necessary for cell cycle progression (G1→S), hypophosphorylated Rb inhibits cellular proliferation. Upon positive growth stimuli, cyclin D is expressed and activates the cyclin dependent kinase 4/6 (CDK4/6). The LxCxE motif of active cyclin D/CDK4/6 binds to and promotes the hyperphosphorylation of Rb, thereby inhibiting the association between Rb and E2F, leading to transcription of genes necessary for S-phase progression (Fig. 3) [55].

As Rb is frequently mutated in many cancers, it comes as no surprise that oncogenic polyomaviruses have evolved mechanisms to perturb this pathway to promote cell cycle progression, and consequently tumor formation in the rare event of viral genome integration. The LT of MuPyV, SV40, and MCPyV all contain an Rb binding domain (LxCxE motif) to known cellular regulators of

Rb such as cyclin D [56]. Indeed it has been found that MuPyV and SV40 LT bind Rb through their LxCxE motif, and this interaction is necessary for transformation [57]. In addition to the LxCxE motif, it has been found that an intact DnaJ domain is also necessary for inactivation of the Rb tumor suppressor by SV40 LT [58]. Functionally, the LxCxE motif is responsible for the physical interaction between LT and Rb, but the binding of heat shock proteins (Hsc70) to the DnaJ domain provides the energy to dissociate E2F from Rb, which together lead to increased transcription of E2F target cell cycle progression genes. Interestingly, the LxCxE motif and DnaJ domains are also conserved in other HPyV LT antigens [56]. For example, TSPyV a HPyVs not currently associated with cancer, is capable of binding and hyperphosphorylating Rb, leading to increased cellular proliferation [59]. Presumably, the other HPyV LT antigens also bind and dissociate Rb from E2F due to their LxCxE and DnaJ domain conservation, although binding and mechanistic studies between LT and Rb have not yet been performed for the majority of the remaining HPyVs. An importance for the Rb binding domain of MCPyV LT was also suspected, as all MCC LT truncating mutations conserve the LxCxE motif, suggesting an importance of this domain in the viability of MCC tumors [22]. Indeed, the LxCxE motif of MCPyV LT is necessary for cellular transformation,

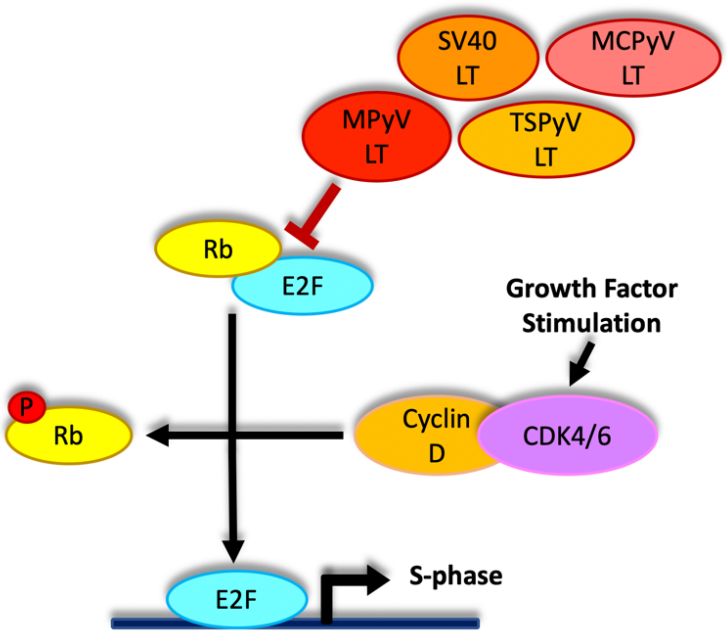

Figure 3. Polyomavirus perturbation of Rb. The LT antigen of many polyomaviruses have evolved to inhibit the interaction between Rb and E2F to progress into S phase.

and knockdown of LT-t in VP-MCC cells leads to cell death, but can be rescued upon Rb knockdown [60-62].

1.4.2 p53

The p53 tumor suppressor is frequently referred to as the "guardian of the genome" as p53 is a transcription factor that responds to various cellular stresses and regulates the expression of genes involved in cell cycle arrest and apoptosis [63]. In normal, healthy cellular conditions, p53 protein levels are low due to a negative feedback loop involving MDM2. Active p53 binds to the promoter of the MDM2 gene, thereby increasing its transcription. As MDM2 is an ubiquitin ligase that ubiquitinates and targets p53 for degradation by the proteasome, p53 levels are kept low in normal cells. However, cellular stresses, such as DNA damage or unscheduled upregulation of E2F responsive genes, can lead to the induction of the p53 activating proteins such as ARF [64]. ARF expression subsequently leads to activation of p53 through inhibition of MDM2 and consequent cell-cycle arrest or apoptosis (Fig. 4) [65].

Multiple steps in the lifecycle of DNA tumor viruses have been found to inadvertently trigger p53 activation, which could be devastating to viral replication as p53 activity results in growth arrest and apoptosis [66]. For

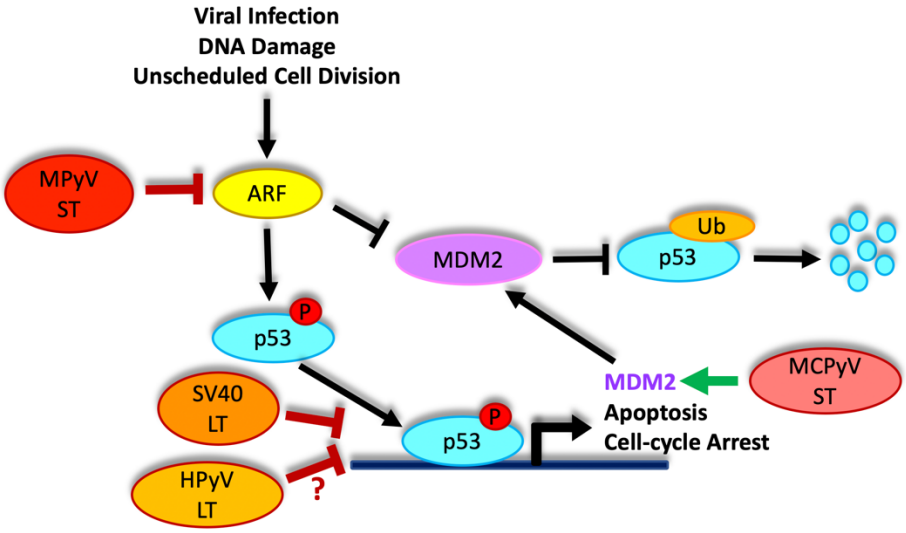

Figure 4. Polyomavirus perturbation of p53. Many polyomaviruses have evolved various mechanisms to disrupt the p53 tumor suppressor and inhibit cell-cycle arrest and apoptosis.

these reasons, polyomavirus TAgs have evolved various ways to combat p53 activation, which in turn increases the success of viral replication, but can consequently lead to cellular transformation upon viral integration and constitutive TAg expression. SV40 has been found to have the most direct mechanism of perturbing p53, as SV40 LT directly interacts with the DNA binding domain of p53 through the c-terminal ATPase/helicase domain of LT [67, 68]. This interaction inhibits the transcriptional activities of p53 that normally lead to cell death, arrest, and apoptosis. As such, the interaction with LT and p53 is necessary for transformation by SV40 [69, 70]. Unlike SV40, none of the MuPyV TAgs are capable of directly binding and inhibiting p53, even though MuPyV MT leads to activation of p53 through ARF induction [53]. Instead, MuPyV ST has evolved a mechanism dependent on PP2A binding to prevent ARF mediated activation of p53 [71, 72]. Accordingly, MT requires co-expression of ST to be transforming; or is transforming on its own if p52 or ARF are inactivated [71].

Similar to MuPyV, an interaction between MCPyV TAgs and p53 has never been observed [73]. This is consistent with MCPyV LT not encoding a p53 binding domain. Also, the c-terminal region of MCPyV LT, in which the SV40 LT p53 binding domain is located, is deleted in MCC due to MCC specific LT truncations, suggesting that even if the full-length MCPyV LT could interact with p53, this binding would be lost in MCC [22]. This is also consistent with the c-terminus of MCPyV LT having anti-proliferative functions [73-75]. Similar to MuPyV ST, it has been recently been suggested that MCPyV ST may also be responsible for inhibiting p53 activation, although through a different mechanism than MuPyV ST. Instead, it has been hypothesized that MCPyV ST, through binding of the transcription factor L-Myc and the histone acetyltransferase EP400, can lead to increased expression of MDM2 and MDM4, and consequent downregulation of p53 transcriptional targets [76]. Finally, except for MCPyV, TAgs from most other HPyVs are capable of

interacting with p53 through their conserved p53 binding domain, and may also be capable of a complex association with p53 inhibition, although further investigation is warranted [77].

1.4.3 PP2A

PP2A is a cellular phosphatase that is important for regulating the activity of several enzymes such as Akt, p53, c-Myc, and beta-catenin through dephosphorylation, therefore modulating many cellular pathways including those involved in cell cycle progression, DNA replication, transcription, protein translation, signal transduction, cytoskeletal dynamics, cell mobility, and apoptosis [78]. As such, PP2A dysregulation can lead to the development of cancer, and is therefore considered a tumor suppressor [79].

PP2A binding is a widely conserved function of polyomavirus ST proteins, although the exact PP2A subunits of this interaction differ between polyomaviruses, as well as the ultimate role of this interaction in transformation and tumorigenesis. PP2A is composed of a complex of three major subunits: the scaffold (A), regulatory (B), and catalytic (C) subunits. SV40 ST is only capable of interacting with the scaffold (A) subunit, whereas MuPyV ST and MT can interact with both the scaffold (A) and regulatory subunits (B) [80, 81]. In both cases, this interaction between ST and PP2A is thought to displace the regulatory (B) subunit from the holoenzyme, thereby inhibiting or deregulating the activity of PP2A [81, 82]. PP2A is the major target of SV40 ST, as this interaction is responsible for AKT activation, Myc stabilization, and 4E-BP1 hyperphosphorylation [83, 84]. The interaction between MuPyV MT and PP2A is essential for its interaction with Src family kinases, inactivation of p53, and is necessary for cellular transformation [71, 85].

MCPyV ST is similarly capable of interacting with PP2A A and C subunits to alter the substrate specificity through displacement of the B subunit [71]; however, this interaction has been found to be dispensable for transformation by MCPyV ST [27]. Other HPyVs TAgs have also been

found to interact and inhibit PP2A function, such as HPyV7 and TSPyV. The interaction between TSPyV MT and HPyV6 ST with PP2A leads to the activation of the mitogen activated protein kinase cascade, important for inducing cellular proliferation [86, 87].

1.4.4 YAP

Yes-associated protein (YAP) is an important transcriptional co-activator downstream of the HIPPO pathway which is important for regulating cellular proliferation and organ size [88, 89]. YAP activity is dependent on a few main factors including cell confluence, YAP localization, and YAP phosphorylation. Briefly, when cells are at low confluence, unphosphorylated YAP is found is located in the nucleus, where it binds to and activates transcription factors that are responsible for transcribing genes involved in cellular proliferation. When cells reach high confluence a signaling cascade leads to the phosphorylation of YAP and subsequent degradation or sequestration in the cytoplasm through interaction with 14-3-3 proteins. The lower protein levels or inability of YAP to translocate to the nucleus inhibits cellular proliferation (Fig. 5).

Because of the important role of YAP in regulating cellular proliferation and contact inhibition, YAP has been found to be mutated in many cancers [90]. It has been more recently appreciated that small DNA tumor viruses also perturb YAP as a means of transformation. SV40 encourages nuclear localization and transcription of YAP

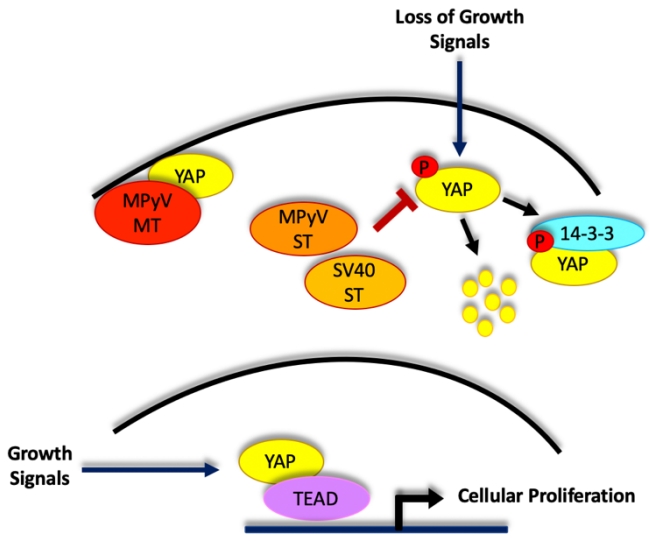

Figure 5. Polyomavirus perturbation of YAP. Both MuPyV and SV40 TAgs have evolved mechanisms to perturb YAP phosphorylation and localization to induce cellular proliferation.

target genes through activity of its ST antigen. Through interaction with both YAP and PP2A, SV40 ST can dephosphorylate YAP and retain it in the nucleus where it initiates transcription of genes to promote cellular proliferation, even at high cellular density [91]. Both the MT and ST antigens of MuPyV contain YAP binding domains, although their mechanisms of YAP perturbation are different. Similar to SV40 ST, MuPyV ST binds both YAP and PP2A, leading to decreased YAP phosphorylation and increased stability [92]. In contrast, MuPyV MT also binds and dephosphorylates YAP; however, MT also promotes YAP localization to the cellular membrane instead of the nucleus (Fig. 5) [93, 94]. The mechanism and role of MT mediated relocalization of YAP to the membrane is not currently well understood. Whether MCPyV perturbs YAP has not yet been explored.

1.4.5 FBW7

Fbw7 is the component of the SCF (Skp1, Cul1 and Fbox protein) ubiquitin ligases responsible for both substrate recognition and recruitment of the ubiquitination machinery. The substrate specificity of Fbw7 is regulated by the presence of a defined phosphorylated degron on the target protein. Fbw7 is responsible for the degradation of several cellular oncoproteins such as c-Myc and cyclin E. Interestingly, SV40 LT contains a decoy phosphodegron at its extreme C-terminus, which is capable of interacting with Fbw7 to decrease turnover of normal Fbw7 target substrates (Fig. 6)

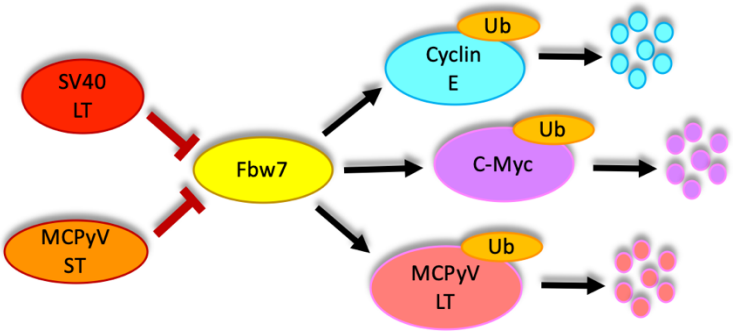

Figure 6. Polyomavirus perturbation of Fbw7. Both SV40 and MCPyV have been found to perturb Fbw7 to decrease turnover of cellular oncoproteins.

In contrast to SV40 LT, Kwun et al. have proposed MCPyV LT to be targeted for proteasomal

degradation through interaction with several ubiquitin ligases including Fbw7 and Fbw1 (β-TrCP) [27, 95, 96]. As MCPyV LT and LT-t play an important role in viral replication and tumor maintenance, respectively, their rapid turnover would be deleterious. However, amino acids 91–95 of MCPyV ST have been shown to increase LT protein levels, and was thus termed the Large-T Stabilization Domain (LSD). Currently, the ST LSD is thought to increase LT protein levels by binding and sequestering several ubiquitin ligases, including Fbw7, from LT and their other cellular targets, such as c-Myc, thereby decreasing their turnover. Such an activity, similar to SV40 LT, would suggest a possible role of the ST LSD in transformation and tumorigenesis, as increased concentrations of a MCPyV tumor antigen and cellular oncoproteins could lead to aberrant cellular proliferation, increased translation, and genomic instability [27]. Indeed, mutation of the LSD has been shown to ablate the ability of MCPyV ST expressing cells to form colonies in soft agar and promote epithelial hyperplasia in pre-term transgenic mouse embryos [97]. Furthermore, as MCPyV LT is necessary for viral replication, the activity of the ST LSD has also been proposed to initiate viral replication and exit from viral latency [98]. Taken together, perturbation of Fbw7 by the MCPyV ST LSD was the dominant theory for transformation by MCPyV ST before my dissertation research.

1.5 SUMMARY AND QUESTIONS TO ADDRESS

MCPyV, the etiologic agent of 80% of MCCs, is the first HPyV to be firmly associated with a human cancer. Although the viral oncoproteins of oncogenic polyomaviruses of other species, such as SV40 and MuPyV, have been extensively studied in their mechanisms of transformation, it appears that many of these known polyomavirus mechanisms are dispensable for transformation by MCPyV, or transformation by MCPyV may be accomplished through an unknown alternative mechanism. In order to elucidate common or unique mechanisms of transformation by MCPyV, I sought to address several questions including: 1) Which of the MCPyV TAgs is responsible for

transformation and tumorigenesis? 2) What are the domains on the MCPyV viral oncoproteins necessary for transformation and tumorigenesis? 3) What are the binding partners and pathways perturbed by MCPyV viral oncoproteins that lead to cellular transformation and tumorigenesis? Importantly, investigation into these questions will have immediate as well as far-reaching implications and consequences. Not only will research into these questions increase our understanding of how MCPyV can lead to the development of cancer and aid in the design of efficacious therapeutics, but also has broader implications in furthering our understanding of cancer, cellular, and molecular biology.

1.6 SIGNIFICANCE

Prior to 2016, the management of MCC included surgery, radiotherapy, and/or chemotherapy depending on the progression of disease [1, 99]. Unfortunately, these therapies come at the cost of the patient's quality of life, and only increase the progression-free survival by an average of three months. More recently, anti-PD-1 immunotherapy has been found to double the patient response rate of chemotherapy to ~60% [1, 100]. Although anti-PD-1 immunotherapy is a significantly more efficacious therapy than previous management tools such as chemotherapy, half of MCC patients still do not benefit from immunotherapy. Thus, there is still a large proportion of MCC patients that will benefit from the development of novel, efficacious MCC therapies [99].

Eighty-percent of MCCs are caused by the integration and expression of MCPyV TAgs [17]. Furthermore, the viability of these MCC tumors is dependent on MCPyV LT-t and ST expression, as knock-down of these TAgs leads to decreased proliferation and cell death [27]. The dependence on the expression of MCPyV TAgs for the viability VP-MCC suggests that direct targeting of these viral proteins and/or their associated cellular pathways could present a novel approach to the management of MCC. Therefore, the investigation into the mechanisms of transformation and

tumorigenesis by MCPyV TAgs described herein has implications not only for the virology of MCPyV, but also in the design of novel, efficacious, targeted MCC therapies, and more broadly cancer, cellular and molecular biology.

Although VP- and VN-MCC have different origins, the resultant disease is very similar in both cases. In order to identify how expression MCPyV TAgs leads to the development of MCC, many groups have assessed the mutations in VN-MCC in an effort to identify commonly mutated pathways that may also be perturbed by viral TAgs in VP-MCC [101]. Unfortunately, the extensive and unique mutational burden of individual VN-MCC tumors has made it difficult, if not impossible, to delineate the specific mutations responsible for the development of MCC. For these reasons, the complementary approach of elucidating mechanisms of transformation and tumorigenesis by MCPyV TAgs in VP-MCC may prove more feasible and informative for both the biology of VP- and VN-MCC. Therefore, the work described herein not only will facilitate in our understanding of the MCPyV TAgs to target in VP-MCC, but also the crucial cellular proteins and pathways that may be targeted for therapy of both VP- and VN-MCC.

CHAPTER 2. MATERIALS AND METHODS

2.1 HFF culturing and transductions

Dermal fibroblasts were isolated from human foreskin samples and cultured in DMEM supplemented with 10% (vol/vol) fetal bovine serum, penicillin-streptomycin (Life Technologies), GlutaMAX (ThermoFisher Scientific), and Non-Essential Amino Acids (ThermoFisher Scientific). All cell lines were maintained at 37°C in 5% CO_2. TAg sequences were cloned into the lentivirus transfer vector pLENTI through infusion (clontech).To generate lentiviruses, 293TN cells were transfected with psPAX, pMD2.G, and pLENTI using TransIT-293 Transfection Reagent (Mirus) at ~80% confluence. After two viral harvests at 48- and 72-hours post transfection, HFFs were

transduced with lentiviruses supplemented with polybrene. After 48 hours, transduced HFFs were selected with puromycin and cells were utilized for subsequent experimentation.

2.2 Transformation Assays

HFFs transduced with TAgs were assessed in various different transformation assays. Soft agar assays were performed as described in the JOVE soft agar colony formation assay online protocol [102]. Doubling time and saturation density experiments were performed by plating the same number of cells in 12 plates (4 timepoints and 3 triplicates), quantifying the number of cells at 2, 4, 8, and 14 days. Doubling time was calculated between days 2 and 4. Saturation density was determined by the day 14 timepoint.

2.3 Mouse Studies

$5x10^6$ HFF ST or GFP cells were implanted subcutaneously in NOD.Cg-*Prkdcscid Il2rgtm1Wjl*/SzJ (NSG) mice (Jackson Laboratories, USA). Prior to injection, cells were resuspended in 50% (v/v) growth factor reduced Matrigel (Corning, USA) in DMEM. 200 uL of cell/matrigel mixture was implanted in the dorsal flank using a 24-gauge needle. Mice were monitored daily for tumor growth and euthanized six weeks post-injection.

All animals were housed under the care of the Comparative Medicine facility at the Fred Hutchinson Cancer Research Center. Subcutaneous injection of cells was performed according to protocols approved by Fred Hutchinson Cancer Research Center's Institutional Animal Care and Use Committee.

2.4 Transfections and lentiviral shRNA knock-downs

Adenovirus-transformed human embryonic kidney cell lines (HEK293A) (Thermo Fisher Scientific) were cultured in DMEM supplemented with 10% (vol/vol) fetal bovine serum, penicillin-streptomycin (Life Technologies), GlutaMAX (ThermoFisher Scientific), and Non-Essential Amino Acids (ThermoFisher Scientific). All cell lines were maintained at 37°C in 5% CO_2. For transient transfection experiments, cells were plated in 10cm plates and transfected the next day using TransIT-293 Transfection Reagent (Mirus) at ~80% confluence. Cells were harvested 36–48 hours after transfection for subsequent experimentation. Fbw7 knock-down was performed by transducing 293A cells with lentiviruses containing shControl or shFbw7 (CAGAGAAATTGCTTGCTTT), followed by puromycin selection.

2.5 Plasmids and mutagenesis

T-antigens were subcloned into pCS2, and/or pCS2-HA vectors using the In-fusion HD Cloning Kit (Clontech). The pCS2-MCPyV.57kT plasmid was generated by GENEWIZ TurboGENE Gene Synthesis. The MCPyV LT alanine scan mutagenesis was performed by ThermoFisher Scientific GeneArt. MCPyV T antigen mutants were generated using New England BioLabs Q5 Site-Directed Mutagenesis Kit, with primers designed using the NEBase Changer tool (New England Biolabs). pCGN.HA-Fbw7 and pCGN.HA-Fbw7 R465C were provided by Patrick Moore and Yuan Chang (University of Pittsburgh).

2.6 Co-Immunoprecipitation, immunoblotting, and antibodies

Co-immunoprecipitations were performed using a modified protocol from Jianxin You (University of Pennsylvania). Briefly, 293A cells were harvested 36–48 hours after transfection and lysed with NP40 lysis buffer containing cOmplete, EDTA-free Protease Inhibitor Cocktail (Sigma-Aldrich) on

ice. Cell lysates were lightly sonicated and the lysates were rotated at 4°C for 1 hour. The BCA Protein Assay Kit (Pierce) was used to quantify the protein concentrations. 500µg of normalized cell lysates were pre-cleared with 25µl of equilibrized Protein A/G Magnetic Beads (Pierce) for 1 hour at 4°C with rotation. The A/G Magnetic Beads were removed from the cellular lysates and discarded, followed by incubation with 10µg of the immunoprecipitation antibody overnight at 4°C with rotation (XT10-donated from Chris Buck, CM2B4 (Santa-Cruz, sc-136172), Ab3-donated from Jim DeCaprio, Ab5-donated from Jim DeCaprio, anti-HA (BioLegend-MMS-101P), 9E10 (made in house), anti-FLAG M2 (Sigma-Aldrich, F1804), or anti-Fbw7 (Bethyl Labs, A301-720). 25µl of protein A/G magnetic beads, per sample, were also blocked in 1% BSA overnight at 4°C with rotation. The next morning, antibody/cellular lysates were added to the 25µl of pre-blocked A/G magnetic beads, and incubated at room temperature, with rotation, for 1 hour. Immunoprecipitated samples were washed several times with KCL buffer, resuspended in SDS sample buffer, boiled, separated by electrophoresis, and transferred to an Immobilon-P PVDF Membrane (Millipore) in parallel with 30µg of whole cell lysate. Membranes were blocked in 4% milk overnight at 4°C, followed by incubation with the primary antibodies described above, in addition to the 2T2 antibody which binds an epitope common to both MCPyV LT and ST (provided by Chris Buck; National Cancer Institute). After washing, a mouse IgG light chain specific HRP conjugated secondary antibody (Cell Signaling-D3V2A, #58802) was incubated with the membranes in 4% milk for one hour followed by washing and chemiluminescent detection with a ChemiDoc Imaging System (Bio-Rad). Actin immunoblotting was performed with β-Actin (Cell Signaling-13E5, #5125). c-Myc immunoblotting was also performed (Cell Signaling Technology, D84C12). A more detailed co-immunoprecipitation protocol may be viewed at: dx.doi.org/10.17504/protocols.io.v6ke9cw. Cell fractionation western blots were performed according to the subcellular fractionation protocol by Abcam.

2.7 RNA Extraction, qRT-PCR, and Next Generation RNA Sequencing

Total RNA was isolated from 293A cells 36–48 hours after transfection using a PureLink RNA Mini Kit (Thermo Fisher Scientific) with DNase I treatment. The SuperScript VILO cDNA Synthesis Kit (Thermo Fisher Scientific) was used to synthesize single-stranded complementary DNA (cDNA) from 1μg total RNA. Fbw7α, and GAPDH expression were evaluated in triplicate using diluted cDNA as template, gene-specific forward and reverse primers (0.3μM), and Power SYBR Green Master Mix (Thermo Fisher Scientific) in an Applied Biosystems StepOnePlus Real-Time PCR system (Thermo Fisher Scientific). Three biological and three experimental replicates of RNA isolated from HFFs expressing TAgs was submitted for TapeStation quality analysis, and then analyzed in the NovaSeq 6000 S1 flow cell. Individual genes with a FC>1.5 were grouped for hallmark gene sets (H), transcription factor targets (TFT), cancer gene neighborhoods (CGN), cancer modules (CM), and oncogenic signatures (C6) within the MSigDB collections.

2.8 TurboID Mass Spectrometry

Streptavidin agarose slurry was reductively methylated using a reductive alkylation kit (Hampton Research HR2-434). For each set of triplicates, 16 15cm plates at 90% confluency were incubated in DMEM with 500uM biotin for 30 minutes. After 30 minutes, cells were placed on ice and washed five times with ice-cold PBS to terminate the biotinylation reaction. Cells were then scrapped and spun down into cellular pellets that were resuspended in ice-cold lysis buffer and benzonase (Sigma), and rotated for 30 minutes at room temperature. Lysates were then spun at 10,800rpm for 15 minutes in an ultracentrifuge using an SW41 rotor, before collect the supernatant. Protein concentrations were normalized to 6mg/ml. For each 1ml replicate, 125ul of equilibrated reductively methylated streptavidin beads were added and rotated for 2 hours at room temperature, followed by

a series of washes. Finally, the beads were resuspended in digestion buffer and submitted to proteomics for mass spectrometry. A more detailed protocol will be shared upon request.

CHAPTER 3. IDENTIFICATION OF MERKEL CELL POLYOMAVIRUS TUMOR ANTIGENS RESPONSIBLE FOR TRANSFORMATION AND TUMORIGENESIS

3.1 INTRODUCTION

In order to elucidate the role of MCPyV in the development of MCC, the TAgs responsible for transformation and tumorigenesis must first be identified. The TAgs of related oncogenic polyomaviruses have been extensively studied and defined for their role(s) in transformation. For MuPyV, the MT antigen is thought to be the dominant transforming protein as it behaves as a catalytically inactive membrane signaling complex that interacts with signal transducers responsible for transformation such as TAZ, PP2A, PTK, Shc, 14-3-3, PI3K, PLC-gamma and YAP [103]. In the case of SV40, its LT antigen is the dominant transforming protein through its binding and perturbation of both Rb and p53 tumor suppressors [104]. Similarly, for both MuPyV and SV40, the ST antigen is thought to play a supportive role in transformation through the activity of its PP2A binding domain [105]. Therefore, it appears that the LT and MT antigens of SV40 and MuPyV, respectively, are the dominant transforming proteins, whereas the ST protein of both viruses plays an accessory role in transformation.

Although in most instances the MCPyV genome integrated in MCC has the capacity to express LT-t, ST, 57kT and ALTO, as far as we know only the LT-t and ST antigens are expressed, suggesting an importance for these TAgs in the development and/or maintenance of MCC [22, 24]. It has also been found that both LT-t and ST are necessary for the viability of VP-MCC tumors, as knock-down of LT-t and/or ST led to decreased proliferation and cell death of VP-MCC cell lines [27]. Several groups have sought to identify the viral oncoproteins of MCPyV necessary for

transformation; however, since our understanding of the host cell of MCPyV infection, and progenitor cell of MCC is limited, most of these transformation studies have been performed in less relevant cell lines such as immortalized rat fibroblasts (Rat-1 cells) [27, 96]. Eight years after MCPyV was discovered, Jiaxin You's group at the University of Pennsylvania identified human dermal fibroblasts as the host cell of MCPyV natural infection [106]. With this new finding, we first sought out to develop a robust, relevant, and reliable assay to determine the TAgs of MCPyV responsible for transformation and tumorigenesis.

Transformation is defined as the acquisition of expanded proliferation and/or survival potential of a cell [104]. Many *in vitro* transformation assays exist including, but not limited to, focus formation, doubling time, proliferation rate and soft agar assays, each of which assess different aspects and pathways involved in cellular transformation. For example, soft agar assays (SAA) assess anchorage independent growth, a feature of transformation highly correlated with tumorigenesis [104]. Fibroblasts are anchorage dependent, meaning that in order for fibroblasts to proliferate they must anchor to a solid surface. In SAAs the cells are suspended in semi-solid agarose in which normal fibroblasts are unable to proliferate and will die in suspension. In contrast, transformed fibroblasts are capable of bypassing anchorage inhibition, and will consequently proliferate and form colonies within the agarose, indicative of transformation. All transformation assays, including SAAs, are *in vitro* methods to predict whether a cell is tumorigenic *in vivo,* and therefore are considered a preliminary and more feasible first approach; however, for a transformed cell to be considered tumorigenic, further animal studies must be performed.

3.2 RESULTS

3.2.1 IDENTIFICATION OF THE TRANSFORMING MERKEL CELL POLYOMAVIRUS TUMOR ANTIGENS

3.2.1.1 THE SMALL TUMOR ANTIGEN IS THE DOMINANT TRANSFORMING PROTEIN OF MERKEL CELL POLYOMAVIRUS

The discovery of human dermal fibroblast as a probable host cell of natural MCPyV infection prompted us to investigate whether a cell permissive for MCPyV viral infection could also be transformed by the virus [30]. If so, this would present a much more relevant system to asses transformation by the MCPyV TAgs than the immortalized rat fibroblasts that have been used previously [27, 96]. Primary human foreskin fibroblasts (HFFs) isolated from foreskin tissue samples were transduced with lentiviruses encoding the MCPyV TAgs, including ER-t, LT-t, ST, ALTO, and the negative control GFP (Fig. 7A). After selection, these MCPyV TAg expressing HFFs were assessed in various transformation assays listed above. In SAAs, the negative control GPF expressing HFFs remained as single cells and were unable to bypass anchorage-inhibition (Fig. 7B and C). In some instances, MCPyV LT-t expressing HFFs became enlarged as if preparing to divide but rarely would successfully proliferate and form colonies. This was in stark contrast to MCPyV ST expressing HFFs, in which ST expression lead to robust colony formation in SAAs (Fig. 7B and C). ALTO, another MCPyV protein encoded within the ER was non-transforming in SAAs, consistent with ALTO not being expressed in MCC (data not shown). In VP-MCC both the MCPyV LT-t and ST antigens are expressed together and are both necessary for the viability of VP-MCC tumors [27]; therefore, we next sought to determine if expression of LT-t and ST together (ER-t) could synergize and result in colony formation greater than expression of ST alone. Surprisingly, HFFs expressing LT-t and ST together (ER-t) showed no significant difference in colony number above ST alone when normalized to ST protein levels (Fig. 7A-C).

The identification of ST as the dominant transforming protein of MCPyV also hints towards the location of the transforming domain of ST. MCPyV ST and LT-t are alternatively spliced forms

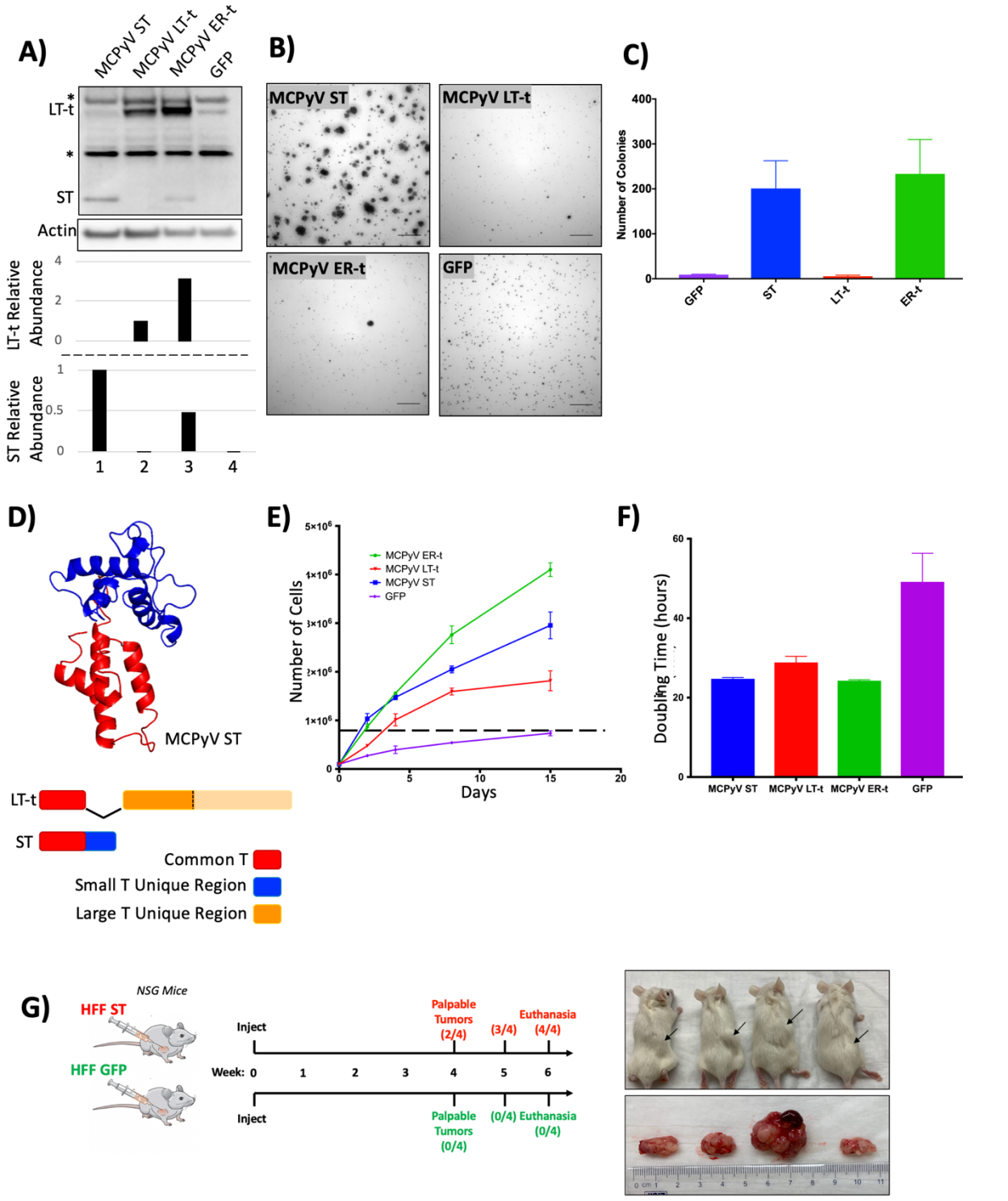

Figure 7. ST is the dominant transforming protein of MCPyV. (A) HFFs were transduced with lentiviruses encoding the MCPyV LT-t, ST, ER-t (LT-t and ST), or negative control GFP, and were assessed in anchorage independent growth (B and C), saturation density (E), doubling time (F), and *in vivo* tumorigenesis (G). The structure of MCPyV ST is divided between the common-T region shared with LT-t (red), and the ST unique region (red) (D).

of the same mRNA, resulting in both TAgs encoding a similar N-terminal region referred to as 'common-T', in addition to ST encoding its own unique region within the intron of LT-t referred to as the 'ST unique region' (Fig. 7D). Because MCPyV ST is transforming whereas MCPyV LT-t is non-transforming, one could hypothesize that the transforming domain of MCPyV ST resides with the ST unique region, as location of the transforming domain in the common-T region would most likely result in a similar transforming phenotype for MCPyV LT-t.

In addition to SAAs, we also investigated HFFs expressing various MCPyV TAgs in additional transformation assays such as saturation density and proliferation rate. Although HFFs expressing LT-t were unable to form colonies in SAA, these cells were capable of proliferating faster and reaching a saturation density higher than GFP expressing HFFs (Fig. 7E and F). Consistent with SAA experiments, ST expressing HFFs also had a shorter doubling time and higher saturation density than both GFP and LT-t expressing HFFs. Surprisingly, although the ER-t expressing HFFs did not have an advantage in colony formation above ST expression alone, ER-t HFFs surpassed ST expressing HFFs in both saturation density and doubling time experiments, suggesting a possible synergistic role of LT-t with ST leading to increased proliferation rate and saturation density (Fig. 7E and F).

The SAA is considered to be the strongest of the transformation assays, as SAAs have the highest correlation with being able to predict a cells ability to form tumors *in vivo* [104]. As such, we next investigated whether ST expressing HFFs, which formed robust colonies in SAAs, were indeed tumorigenic. Excitingly, 100% (4/4) of the NOD *scid* gamma (NSG) ST HFF injected mice and 0% (0/4) of the GFP HFF injected control mice formed large tumors *in vivo,* consistent with similar findings in *in vitro* SAAs (Fig. 7B, C and G). Currently, this *in vivo* tumorigenesis assay is being expanded to include LT-t and ER-t expressing HFFs.

Together, these data suggest that ST is the dominant transforming protein of MCPyV as it was the only MCPyV TAg found to form large colonies in SAAs, increase saturation density of HFFs, decrease the doubling time of HFFs, and form tumors in mice. As such, it can be hypothesized that the transforming domain of MCPyV ST most likely resides within its ST unique region. MCPyV LT-t is non-transforming in SAAs, but may play a supportive role to ST in bypassing contact-inhibition and decreasing cellular doubling time. Interestingly, co-expression of LT-t and ST together as is seen in VP-MCC did not increase colony formation above ST alone, further confirming ST as the dominant transforming protein of MCPyV.

3.2.1.2 MERKEL CELL POLYOMAVIRUS ST IS UNIQULEY TRANSFORMING AMONG HUMAN POLYOMAVIRUS ST ANTIGENS.

As mentioned earlier, MCPyV belongs to a growing family of known HPyVs, but is the only known HPyV clearly associated with cancer (Table 1)[50, 51]. To determine whether the transforming capabilities of MCPyV ST are unique to MCPyV, or shared among other HPyVs, we assessed the transforming capabilities of two other skin tropic HPyV ST antigens: HPyV7 ST, and TSPyV ST. HFFs expressing MCPyV ST, HPyV7 ST, TSPyV ST, or GFP were plated in SAAs followed by quantification of colonies after 4 weeks. Consistent with earlier experiments, MCPyV ST formed many robust colonies in the SAA, whereas the ST antigens of HPyV7 and TSPyV were non-transforming (Fig. 8A-C). These results are consistent with HPyV7 and TSPyV not being associated with cancer.

Additionally, comparisons in the saturation density and doubling time of HFFs expressing the ST antigen of MCPyV, HPyV7, and TSPyV were performed. Surprisingly, in saturation density and doubling time assays, TSPyV ST behaved similar to MCPyV ST, whereas HPyV7 ST had a saturation density and doubling time more similar to GFP (Fig. 8D and E).

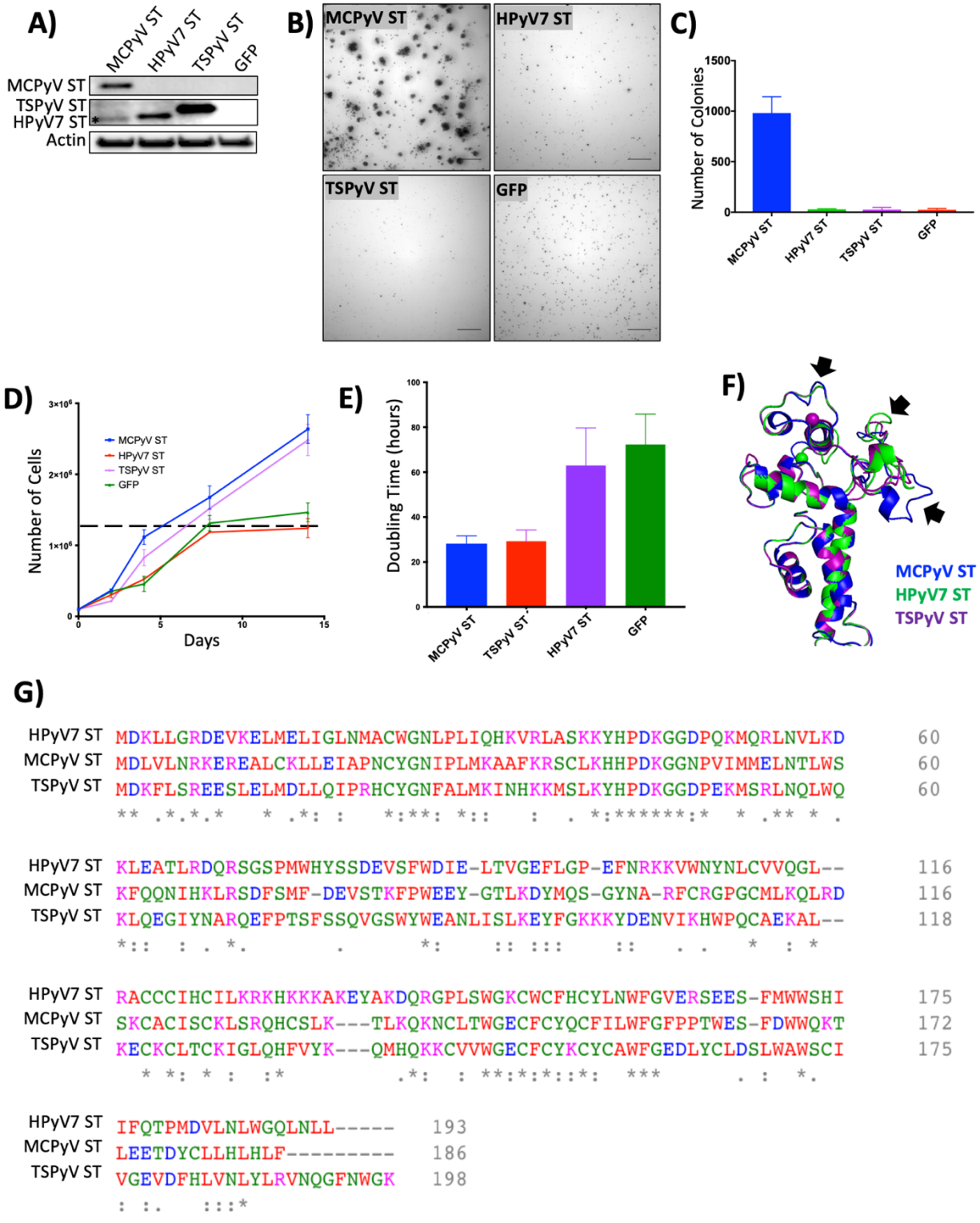

Figure 8. MCPyV ST is uniquely transforming among HPyV ST proteins. (A) HFFs were transduced with the ST antigens of MCPyV, HPyV7, TSPyV, or the negative control GFP, and assessed for anchorage inhibition (B and C), saturation density (D) and doubling time (E). A structural alignment between the transforming (MCPyV) and non-transforming (HPyV7 and TSPyV) ST proteins was performed to identify differences in the protein structure of the transforming and non-transforming ST proteins (arrows) (F). An amino acid alignment between MCPyV, HPyV7 and TSPyV ST antigens was performed through Clustal Omega (G).

In an effort to further elucidate the location of the unique MCPyV ST transforming domain, several comparisons were performed between the transforming MCPyV ST, and the non-transforming HPyV7 and TSPyV ST proteins including amino acid and structural alignments (Fig. 8F and G). Surprisingly, despite only ~30% amino acid similarity, the overall structure is predicted to be very similar between these ST proteins, with the exception of a few loops found at the C-terminal region of the protein. Therefore, these structurally dissimilar loops between the transforming and non-transforming ST proteins may contain the MCPyV ST unique transforming domain. Excitingly, these structurally dissimilar loops between the MCPyV ST and non-transforming ST proteins (Fig. 8F) are indeed found within the ST unique region predicted to contain the MCPyV ST transforming domain (Fig. 7D), and therefore may be the unique transforming domain of MCPyV ST not found in the non-transforming MCPyV LT-t, HPyV7 ST, and TSPyV ST. In conclusion, MCPyV ST is unique among HPyV ST antigens in that it is the only ST capable of inducing colony formation in SAA, consistent with MCPyV being the only known oncogenic HPyV. These data provide a powerful to identify differences between the transforming and non-transforming ST proteins to delineate the mechanism by which MCPyV ST transforms cells and leads to the development of MCC.

3.2.2 IDENTIFICATION OF MERKEL CELL POLYOMAVIRUS TUMOR ANTIGEN DOMAINS RESPONSIBLE FOR TRANSFORMATION

3.2.2.1 THE LXCXE MOTIF OF MERKEL CELL POLYOMAVIRUS LT-T IS IMPORTANT FOR CELLULAR PROLIFERATION

Unlike SV40, the MCPyV LT-t was unable to fully transform HFFs in SAAs, but did lead to modest alterations to the doubling time and saturation density of HFFs (Fig. 7). Others have shown

that MCPyV LT-t and its Rb binding domain are necessary for the viability of MCC tumors [27, 60]. Therefore, we were interested whether mutation of the MCPyV LT-t LxCxE motif would revert the decreased doubling time and increased saturation density of LT-t expressing HFFs. Both MCPyV LT-t E216K and S220A have been shown to disrupt the interaction between MCPyV LT-t and Rb [22, 61, 107]. Both direct and indirect mutation of the LxCxE motif of MCPyV LT-t led to dramatic decreases in saturation density, and slight increases in the doubling time of HFFs (Fig. 9A and B). Unfortunately, as wild-type MCPyV LT-t is non-transforming in SAAs, the role of the Rb binding domain in transformation by SAA cannot be performed; however, these data do suggest the Rb binding domain of MCPyV LT-t to be important for its effects on cellular proliferation rate and contact inhibition.

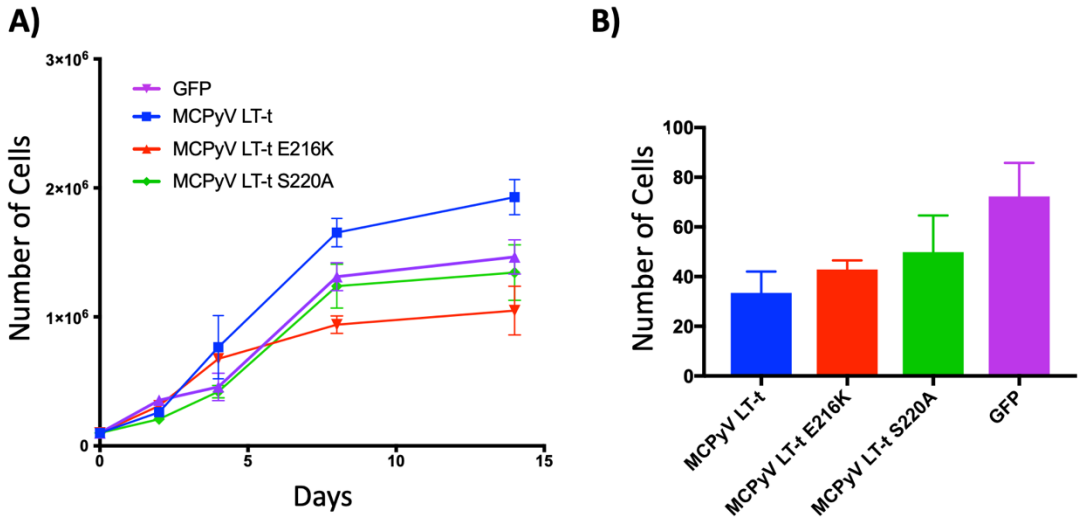

Figure 9. The Rb binding domain of MCPyV LT-t is important for increasing the saturation density and decreasing the doubling time of HFFs. HFFs expressing wild-type MCPyV LT-t, GFP, MCPyV LT-t S220A, or LT-t E216K were assessed in saturation density (A) and doubling time assays (B).

3.2.2.2 IDENTIFICATION OF MERKEL CELL POLYOMAVIURS SMALL T ANTIGEN TRANSFORMING DOMAINS

MCPyV contains several well-known functional domains that were identified through homology with other polyomavirus ST antigens, or unique to MCPyV ST (Fig. 10A and B) [108].

Several of these domains have been assessed for their role in transformation by MCPyV ST in less relevant systems; however, these domains remain to be assessed in our novel primary HFF SAA transformation assay. Many of the PP2A binding domains in MuPyV and SV40 ST are conserved in MCPyV ST, including R7, 95-111, 116-120, L142, and K134. These PP2A binding domains are necessary for the transforming properties of both MuPyV and SV40 ST antigens, but have been found to be insignificant for transformation by MCPyV ST [27, 108]. Another MCPyV ST domain identified through homology with other polyomaviruses is the Hsc70 binding domain, which is mutated by deletion of amino acids 17-27 (Δ17-27) or D44N [27, 109]. The Hsc70 binding domain is necessary for LT inhibition of Rb, and may also play a role in ST inhibition of the catalytic activity of PP2A [110, 111].

Unique domains identified through investigation of MCPyV ST include amino acids 91-95, also known as the Large T Stabilization domain (ΔLSD), EP400/L-Myc binding domain (4M), and the PP4C/Nemo binding domain (Δ95-111). In brief, amino acids 91-95 of MCPyV ST (LSD) have been found to increase LT protein levels through binding and perturbation of the ubiquitin ligase Fbw7 [96]. The interaction between amino acids 91-95 and Fbw7 is thought to be responsible for transformation by MCPyV ST, as perturbation of Fbw7 also increases concentrations of cellular oncoproteins that are targets of Fbw7 such as cyclin E and c-Myc. MCPyV ST has also been found to uniquely interact with the histone acetyltransferase EP400 and the transcription factor L-Myc through its 4M domain [112]. This interaction leads to broad transcriptional aberrations that increase metabolism, translation, cellular reprogramming, and degradation of p53, thereby contributing to cellular transformation. Finally, PP4C has been found to be a unique interactor of MCPyV ST [113]. The interaction between MCPyV ST and PP4C has been found to play a role in microtubule destabilization, cell motility, filopodium formation, and interference with the NFκB pathway.

A)

Name	Mutation	Interference	Reference
R7A	Alanine Substitution R7	PP2A Aα	Shuda, 2011
Δ17-27	Deletion of 17-27	Hsc70	Sullivan et al., 2002
D44N	Asparagine Substitution D44	Hsc70	Kwun, 2009
LSD	Alanine Substitution 91-95	Unknown	Kwun, 2013
Δ95-111	Deletion of 95-111	PP4C/Nemo/PP2A	Griffiths, 2013
116-120A	Alanine Substitution 116-120	PP2A	Kwun, 2015
L142A	Alanine Substitution L142	PP2A Aα and C	Shuda, 2011
K134A	Alanine Substitution K134	PP2A Aα	Kwun, 2015
4M	Serine Substitution E86,E87,K92,D93	EP400/L-Myc	Cheng, 2017

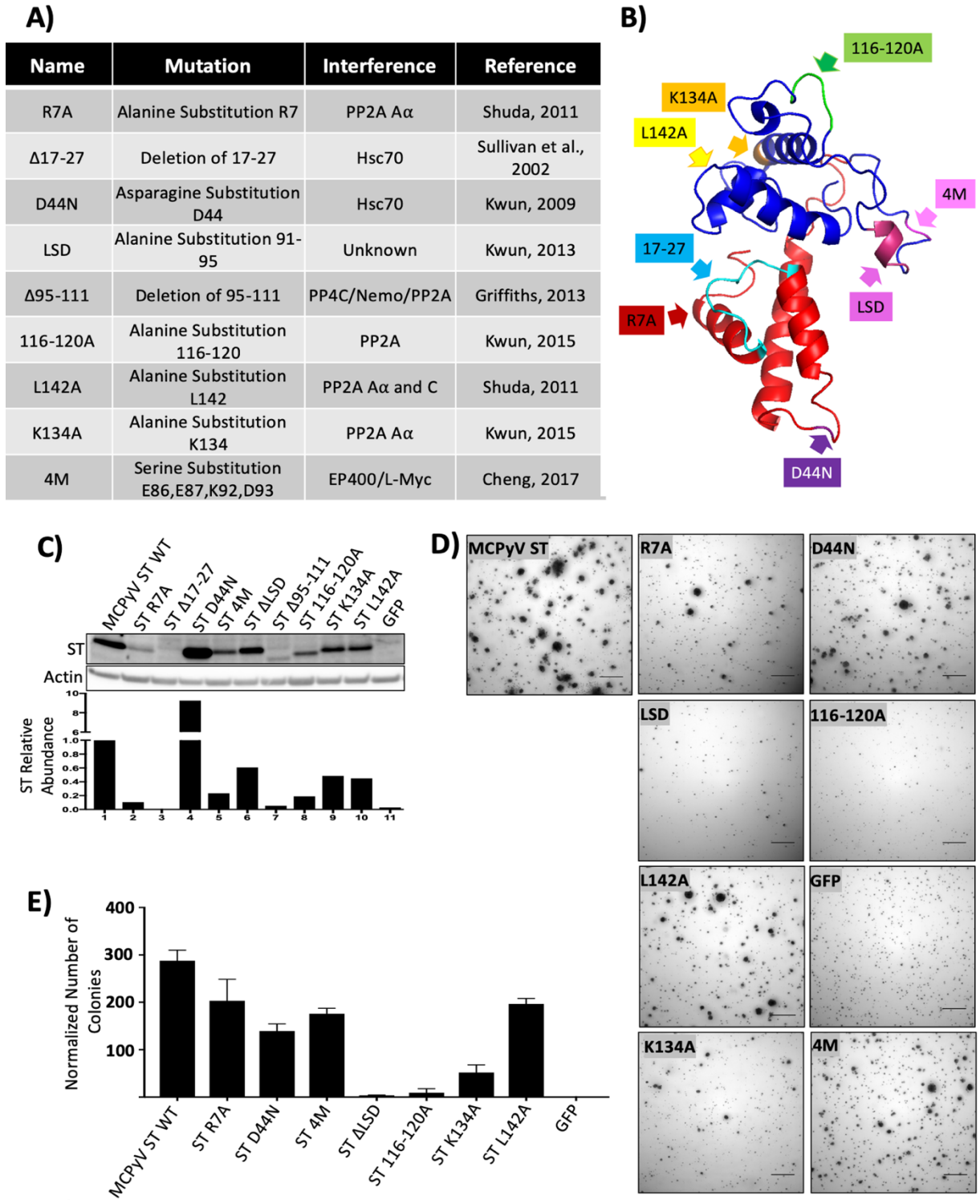

Figure 10. Amino acids 91-95 (LSD) and 116-120 are responsible for transformation. Known MCPyV ST functional domains (A and B) were assessed for their role in transformation. HFFs were transduced with the MCPyV ST mutants and protein levels were quantified by densitometry (C). HFFs expressing stable MCPyV ST mutants were assessed in SAA (D), and their colony numbers were quantified and normalized on protein levels (E). LSD = amino acids 91-95.

To determine whether these domains are responsible for the robust transforming phenotype of MCPyV ST, we assessed all of these MCPyV ST mutants in our novel HFF SAA. The protein levels for each of these mutants varied when transduced and expressed in HFFs, and these differences in protein levels were quantified by densitometry (Fig. 10C). The stable mutants were assessed for anchorage independent growth in SAAs, and the number of colonies formed by each of the MCPyV ST mutants was normalized based on their protein levels (Fig. 10C-E). All of the mutants had a reduced transforming capacity determined by colony number; however, alanine substitution mutants at positions 91-95 (ΔLSD) and 116-120 were completely ablated in their ability to form colonies in SAA, even though they were expressed at adequate levels in HFFs (Fig. 10C-E). Therefore, amino acids 91-95 (LSD) and 116-120 are responsible for transformation by MCPyV ST.

3.2.2.3 AMINO ACIDS 91-95 OF MCPYV ST ARE NECESSARY BUT NOT SUFFICIENT FOR TRANSFORMATION

Alanine substitutions of amino acids 91-95 of MCPyV identified this domain as being necessary for transformation. Therefore, we next sought to identify the specific residue necessary for transformation by testing individual MCPyV ST 91A, 94A, and 95A mutants. We omitted 92A and 93A from the analysis, as the MCPyV ST 4M mutant (E86S, E87S, K92S, D93S) overlaps the 91-95 mutant at residues 92 and 93 and was found to be transforming (Fig. 10C-E). Individual MCPyV ST 91-95 mutants were expressed at high levels and transformed similar to MCPyV ST WT when colony numbers were normalized to protein levels (Fig. 11A-C). To assess whether amino acids 91, 94 and 95 are all necessary, a MCPyV ST 91, 94, 95A mutant was constructed, but was not expressed at high enough levels for analysis (data not shown). Therefore, further investigation of amino acids 91-95 of MCPyV ST must be performed with the entire 91-95 alanine substitution.

Upon identification of amino acids 91-95 of MCPyV ST as being necessary for transformation, it was next investigated whether this domain is also sufficient for transformation. Earlier, it was shown that two other skin tropic human polyomavirus ST proteins (HPyV7 and TSPyV) were non-transforming when transduced into HFFs and assessed in SAAs (Fig. 8). Amino acid alignments of amino acids 91-95 of the transforming MCPyV ST and non-transforming HPyV7 and TSPyV ST proteins revealed that at the amino acid level these domains are surprisingly similar (Fig. 11D). To test whether amino acids 91-95 (LSD) are sufficient for transformation, a 'LSD swap' experiment was performed, in which amino acids 91-95 from the transforming MCPyV ST replaced amino acids 91-95 on the non-transforming ST proteins, and vice versa (Fig. 11E). All of these ST chimeras expressed when transduced in HFFs with the exception of 7:MLSD and 7:TLSD (Fig. 11F). The HFFs expressing stable ST 'LSD swap' chimeras were assessed for anchorage independent growth in SAAs, and the number of colonies formed by each chimera were quantified (Fig. 11G and H). Surprisingly, when amino acids 91-95 of the transforming MCPyV ST was replaced with amino acids 91-95 from the non-transforming HPyV7 or TSPyV ST (M:7LSD and M:TLSD) these chimeras were still capable of forming colonies, albeit to a lesser extent than the wild-type MCPyV ST. Furthermore, when amino acids 91-95 of MCPyV ST replaced amino acids 91-95 on the non-transforming TSPyV ST (T:MLSD), this chimera was not gain-of-function, in that it was still incapable of forming colonies. Therefore, it can be concluded that amino acids 91-95 of MCPyV ST are necessary, but not sufficient for transformation.

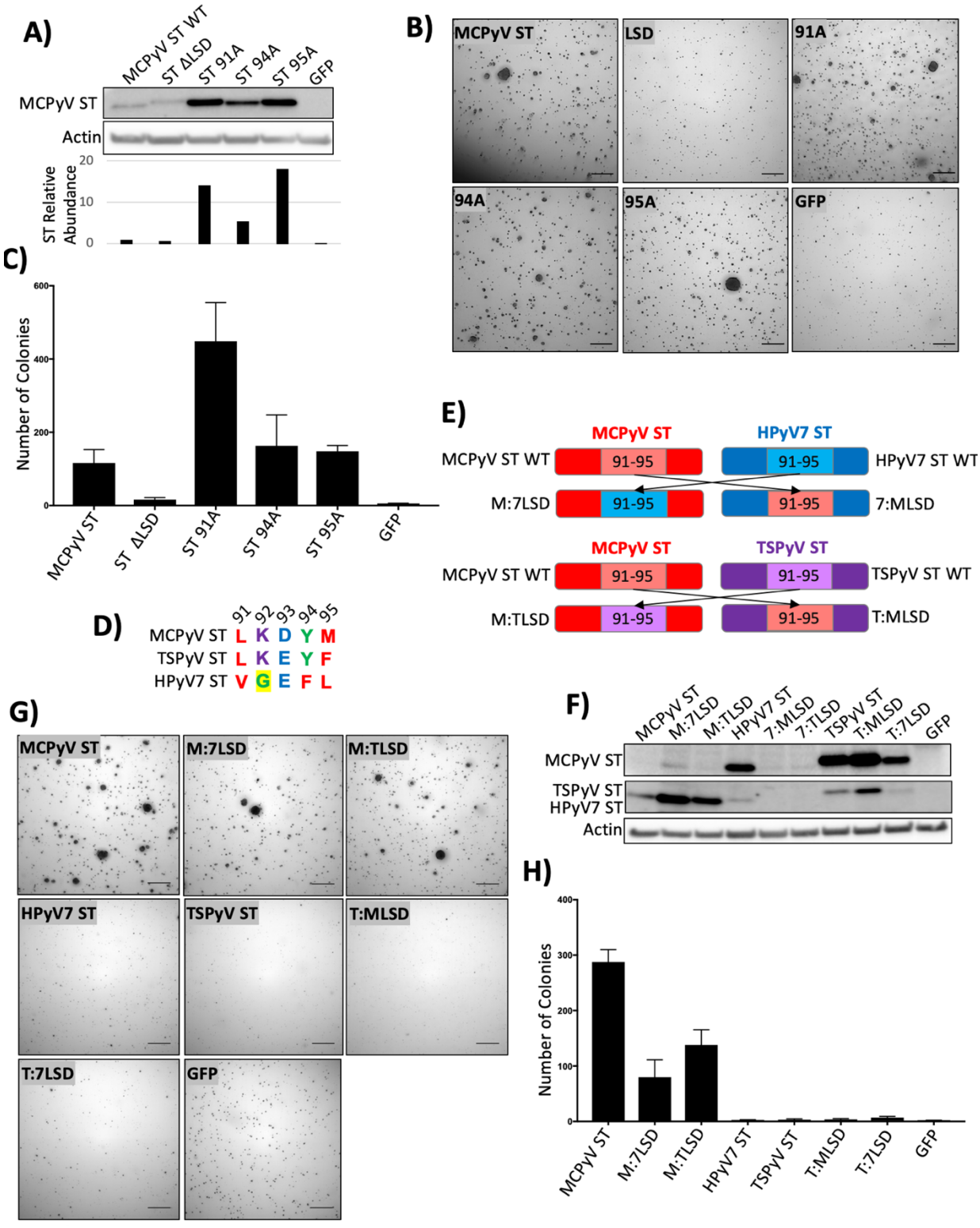

Figure 11. Amino acids 91-95 of MCPyV ST are necessary, but not sufficient for transformation. Individual residues of amino acids 91-95 of MCPyV ST were assessed for their role in transformation. The individual MCPyV ST 91-95 mutants were transduced and expressed in HFFs and protein levels were quantified by densitometry (A). Colony numbers were quantified and normalized based on protein levels (B and C). Amino acid alignments of amino acids 91-95 were compared (D) and swapped between MCPyV ST and the non-transforming HPyV ST proteins (E and F). These ST chimeras were assessed in soft agar assays (G) for the number of colonies formed from each chimera (H). LSD = amino acids 91-95.

3.2.2.4 AMINO ACIDS 116-120 ARE NECESSARY, BUT NOT SUFFICIENT FOR TRANSFORMATION BY MCPYV ST.

Amino acids 116-120 of MCPyV ST were also found to be necessary for transformation. Unlike amino acids 91-95, amino acids 116-120 were much more dissimilar between MCPyV ST and

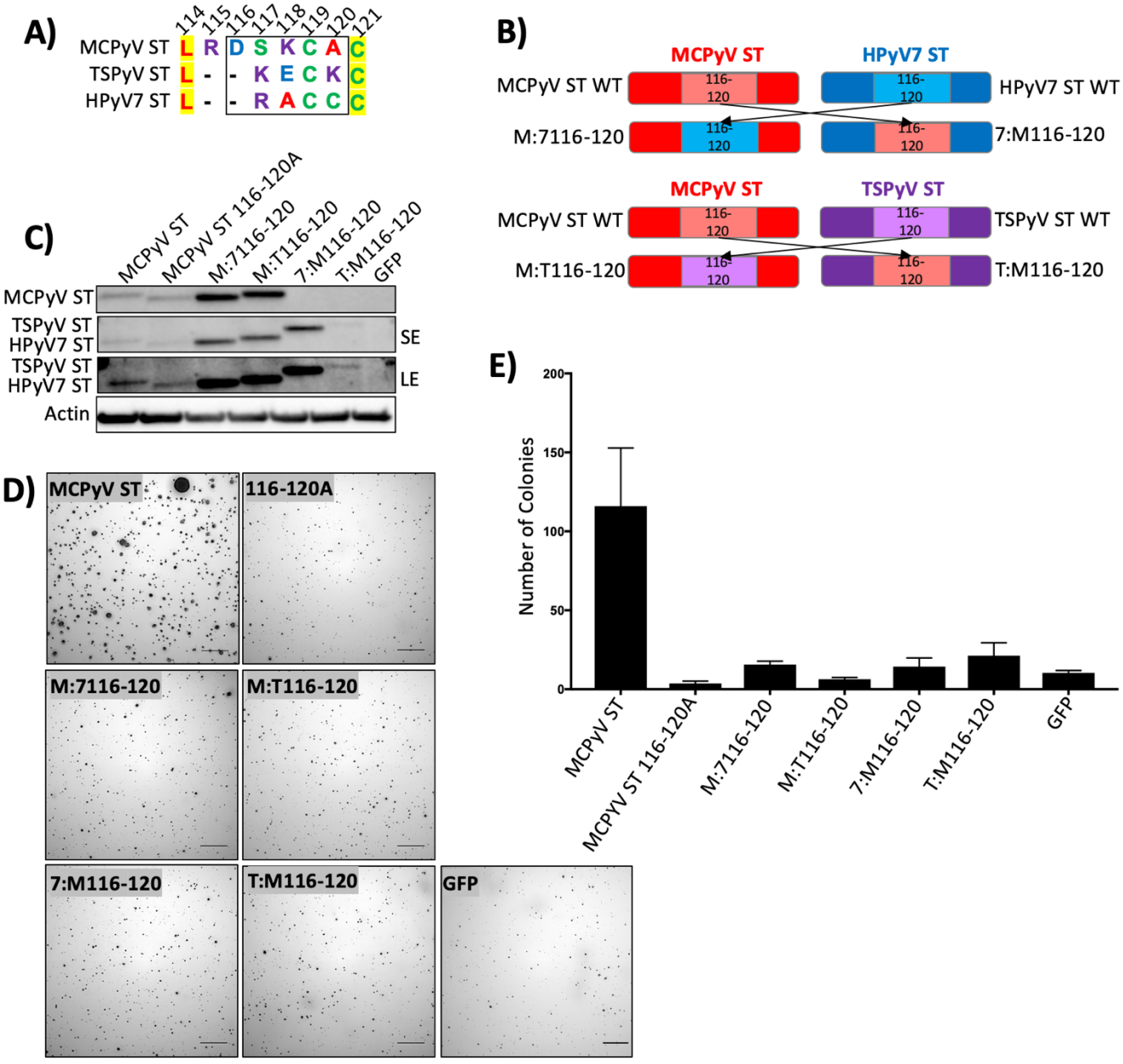

Figure 12. Amino acids 116-120 of MCPyV ST are necessary, but not sufficient for transformation. The amino acids within the 116-120 domain of the transforming MCPyV ST and the non-transforming HPyV7 and TSPyV ST proteins were aligned. Highlighted residues at position 114 and 121 refer to homology between all ST proteins. The box represents amino acids 116-120 (A). '116-120 swaps' were performed by swapping every residue between the conserved L114 and C121 between the transforming and non-transforming ST proteins (B). HFFs were transduced with the chimeras, and western blots of cellular lysates were probed with XT10 to confirm ST chimera expression (C). The ST chimera expressing HFFs were assessed in soft agar (D), where their colony numbers were quantified and compared (E).

the non-transforming HPyV7 and TSPyV ST proteins (Fig. 12A). Similarly, a '116-120 swap' was performed between the transforming and non-transforming ST proteins, in which all amino acids between the conserved leucine at position 114 and cysteine at position 121 were swapped between ST proteins (Fig. 12A and B). When transduced into HFFs, all chimeras expressed at varying levels (Fig. 12C); however, none of the chimeras were transforming (Fig. 12D and E). The loss of function seen when the transforming MCPyV ST 116-120 was swapped with a non-transforming 116-120 (M:7116-120 and M:T116-120) was consistent amino acids 116-120 of MCPyV ST being unique. However, as amino acids 116-120 of the transforming MCPyV ST did not confer HPyV7 or TSPyV transforming (7:M116-120 and T:M116-120) it can be concluded that amino acids 116-120 are necessary, but not sufficient for transformation.

3.3 DISCUSSION

Although MCPyV was discovered 12 years ago, the mechanism by which the integration of MCPyV leads to the development of 80% of MCC cases is still elusive. Unlike other oncogenic polyomaviruses such as MuPyV and SV40, in which the cellular tumor progenitors are understood and utilized in transformation studies, the progenitor cell of MCC is not well understood, and MCPyV is very poor at replicating in most cell types [114-116]. This has severely hampered our ability to identify the MCPyV TAgs responsible for the development of MCC and their mechanisms of transformation and tumorigenesis. Although some groups have observed transformation through expression of MCPyV TAgs, these experiments were done in cells of different species with many additional cellular perturbations [27, 96, 112]. Therefore, it is not known how representative these findings are to the activity of the MCPyV TAgs in MCC, and the additional cellular perturbations complicate mechanistic studies.

Upon identification of human dermal fibroblasts as a probable host cell of MCPyV infection, we were interested whether a permissive cell line could also be transformed by the virus [30]. Typically, permissive cell lines are not transformed by viruses, as these cells allow for viral replication and subsequent viral egress and cell death. However, lentiviral transduction and integration of the replication deficient MCPyV TAgs expressed in MCC allowed us to assess the transforming capacity of MCPyV TAgs independently in relevant, primary cells.

The discovery that MCPyV ST is capable of transforming primary HFFs in soft agar assays is important for several reasons. First, this finding provides a novel, relevant and robust assay to assess transformation by MCPyV TAgs. Second, through utilization of this assay we identified ST as the dominant transforming protein of MCPyV. Finally, this novel transformation assay identified MCPyV ST as being capable of transforming primary cells without any additional cellular perturbations, therefore highlighting the strength of MCPyV ST as a viral oncoprotein and providing a more appropriate tool to perform mechanistic studies. Importantly, the results of the *in vitro* soft agar assay were indeed correlated with the tumorigenicity of these cells *in vivo,* therefore proving TAg expressing HFFs in soft agar assays as a method reliably predictive of tumorigenesis by MCPyV ST. It should be noted that although we identified primary human dermal fibroblasts to be transformed by MCPyV TAgs, this finding is not intended as an argument to implicate dermal fibroblasts as the cell of origin for MCC.

Furthermore, the discovery of MCPyV ST as the dominant, and only transforming protein, of MCPyV in SAAs is very unique among known oncogenic polyomaviruses. The ST antigen of other related oncogenic polyomaviruses are thought to play only a supportive role, further suggesting that MCPyV is unique in its mechanism of transformation, as such a dominant transforming phenotype has never been observed by the ST antigen of other oncogenic polyomaviruses. Second, the MCPyV homologs of the dominant transforming proteins of MuPyV and SV40 were incapable of

transformation of HFFs in SAA. The LT antigen is the dominant transforming protein of SV40; however, MCPyV LT-t was unable to transform HFFs in SAA even though MCPyV LT-t contains the Rb binding domain necessary for transformation by SV40 LT [22, 69]. However, it has been shown that the interaction between Rb and MCPyV LT-t is necessary for the viability of VP-MCC tumors, therefore, it is likely that MCPyV LT-t and its interaction with Rb play an important role in tumor maintenance, that cannot be appreciated by assessment of anchorage-independent growth in SAAs [60]. This is supported by the fact that MCPyV LT-t expression alone, or in combination with ST led to faster HFF doubling times and higher saturation densities. Finally, the MT antigen is the dominant transforming protein of MuPyV. In contrast, MCPyV ALTO, the evolutionarily homolog of MuPyV MT, was non-transforming HFFs. Although ALTO is evolutionarily related to the transforming MuPyV MT, ALTO has never been found to be expressed in VP-MCC, suggesting ALTO may be evolutionarily distinct from MuPyV MT, and may be insignificant or deleterious to tumor formation.

The differences in transformation capacity of the MCPyV ER-t proteins not only identified MCPyV ST as the dominant transforming protein, but also suggested that the MCPyV ST transforming domain could be located in the ST unique region (Fig. 13A). Further, as MCPyV ST was found to be uniquely transforming among HPyV ST proteins, this provides us with a powerful tool to assess the differences between MCPyV ST and the non-transforming proteins to elucidate the unique domains and mechanisms of transformation of MCPyV ST. At the amino acid level, it is difficult to identify dissimilar domains between the MCPyV ST and non-transforming ST proteins, as they are ~30% identical in amino acid sequence. However, at the structural level these ST proteins are strikingly similar, despite the low level of amino acid similarity. The major dissimilarities in the predicted protein structures of MCPyV ST compared to the non-transforming ST proteins resides within loops at the C-terminal region of the protein, consistent with the earlier hypothesis of

the MCPyV ST transforming domain residing within the ST unique region not found in MCPyV LT-t (Fig.13A and B). For these reasons, it is possible that these structurally dissimilar loops contain the transforming domain unique to MCPyV ST, and not found in the non-transforming MCPyV LT-t, TSPyV ST, and HPyV7 ST antigens.

Many of the known functional domains of MCPyV were identified through homology with other polyomavirus proteins; however a few of these domains were identified as being unique to MCPyV ST. Herein we found most known functional MCPyV ST domains to be irrelevant for transformation by MCPyV ST, with the exception of and amino acids 91-95 and 116-120 of MCPyV ST. Excitingly, both 91-95 and 116-120 are found within the MCPyV ST unique region and correspond with the structurally dissimilar loops between MCPyV ST and the non-transforming ST proteins (Fig. 13A-C). However, these domains were subsequently found to be necessary but not

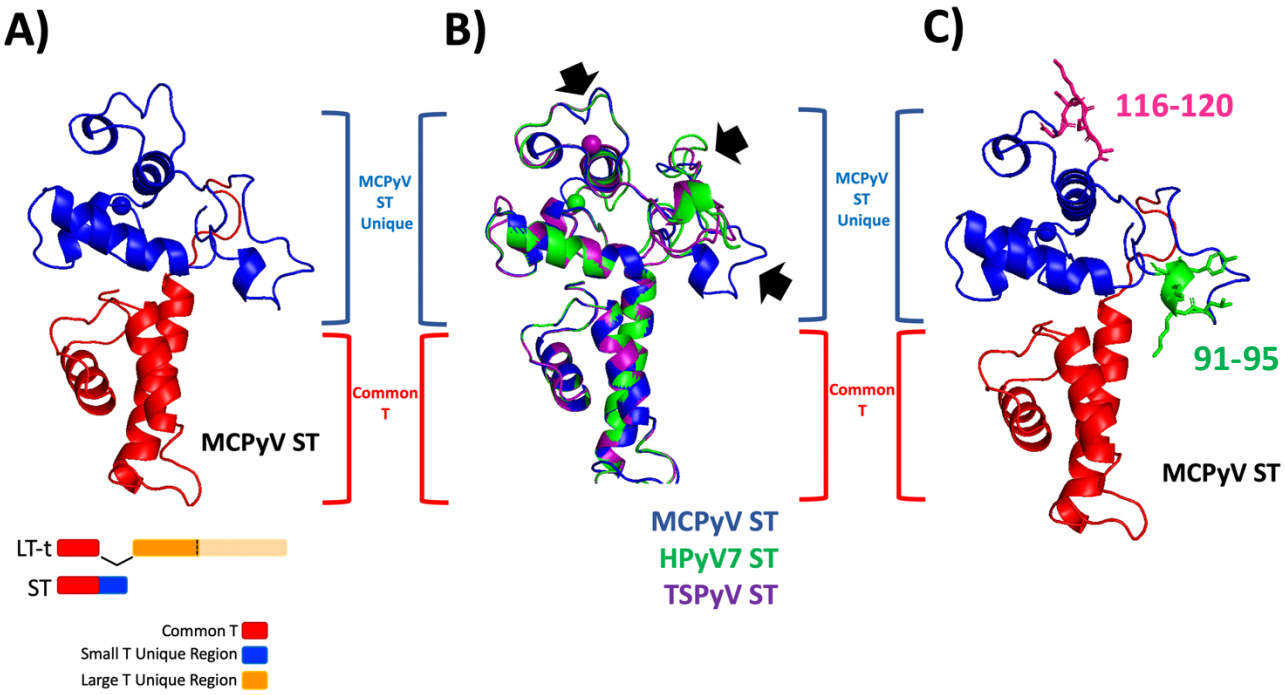

Figure 13. The MCPyV ST transforming domain most likely resides within the ST unique regions structurally dissimilar loops. The structure of MCPyV ST is split into two regions: common-T (red) which is shared with MCPyV LT-t, and the ST unique region (blue) which is encoded in within the LT-t intron (A). Structural alignments between the transforming MCPyV ST (blue), and the non-transforming HPyV7 ST (green) and TSPyV ST (purple) identified three structurally dissimilar loops that corresponded with the ST unique region (B). Amino acids 91-95 and 116-120, both of which were found to be necessary for transformation by MCPyV ST, are found within the MCPyV ST unique region and correspond with the structurally dissimilar loops between MCPyV ST and the non-transforming ST proteins.

sufficient for transformation. A few hypotheses exist for why this may be the case: 1) It is possible, if not likely, that transformation by MCPyV ST is dependent on a complex interaction between multiple domains and binding partners. Therefore, simply swapping one domain may not be sufficient to render a previously non-transforming protein transforming. 2) It is possible that the transforming domain or residue does not reside within amino acids 91-95 (LSD) or 116-120; however, mutation of these domains may cause structural changes that disrupt the nearby transforming domain. If this were the case, swapping amino acids within these domains would not be sufficient, as the actual transforming residue or domain is not actually being transferred. This hypothesis is supported by the fact that we were unable to narrow down the specific residue of amino acids 91-95 responsible for transforming, perhaps suggesting that the transforming domain does not actually reside within amino acids 91-95. This is further supported by the fact that amino acids 91-95 are very similar between the transforming MCPyV ST and non-transforming HPyV7 and TSPyV ST, suggesting that the actual transforming domain may reside within a region that is uniquely found in MCPyV ST and is structurally reliant on amino acids 91-95.

CHAPTER 4. THE SMALL T ANTIGEN OF MERKEL CELL POLYOMAVIRUS DOES NOT TRANSFORM HFFS THROUGH PERTURBATION OF FBW7 OR L-MYC

4.1 INTRODUCTION

In Chapter 3, ST was identified as the dominant transforming protein of MCPyV, and many known functional domains were assessed for their role in MCPyV ST induced transformation. Mutation of amino acids 91-95 or 116-120 ablated transformation by MCPyV ST. Although these domains were found to be necessary but not sufficient for transformation, the ablation of

transformation upon their mutation still makes them reliable tools to assess the binding partners and pathways associated with these domains in transformation. MCPyV ST 116-120A was first identified as being one of the many MCPyV ST mutants that no longer interacts with PP2A [108]. However, many groups have showed that PP2A binding is dispensable for transformation by MCPyV ST, and therefore there is most likely another unidentified purpose for this domain in transformation by MCPyV ST [27, 96, 97].

Two domains of MCPyV ST have gained most of the momentum in the literature for being responsible for transformation by MCPyV ST: the EP400/L-Myc binding domain (4M) and amino acids 91-95, also known as the Large T Stabilization Domain (LSD). It has been recently shown by James DeCaprio's lab at Harvard that MCPyV ST can bind and enhance the interaction between the histone acetyltransferase EP400 complex and the transcription factor, L-Myc through its 4M domains [112]. This leads to the recruitment of the EP400 complex to promoters targeted by L-Myc, many of which promote expression of genes involved in the generation of induced pluripotent stem cells (iPS), including the *MycL* promoter itself. Furthermore, overexpression of *MycL* is a hallmark of MCPyV positive MCC [117]. As we found mutation of the L-Myc binding domain (4M) to be dispensable for transformation by MCPyV, we sought to further investigate the proposed mechanism of transformation by MCPyV ST and L-Myc.

It has also been proposed that amino acids 91-95 of MCPyV ST (LSD) is responsible for transformation by MCPyV ST. Similarly, in our novel primary HFF transformation assay, amino acids 91-95 of MCPyV ST were indeed found to be necessary for transformation. Patrick Moore and Yuan Chang at the University of Pittsburg have shown amino acids 91-95 of MCPyV ST to perturb the functions of several cellular ubiquitin ligases, most notably SCF^{Fbw7}, to accomplish transformation [95, 96, 118]. SCF^{Fbw7} is a multi-protein complex responsible for binding and ubiquitinating target proteins for proteasomal degradation [119]. Fbw7 is the component of the SCF

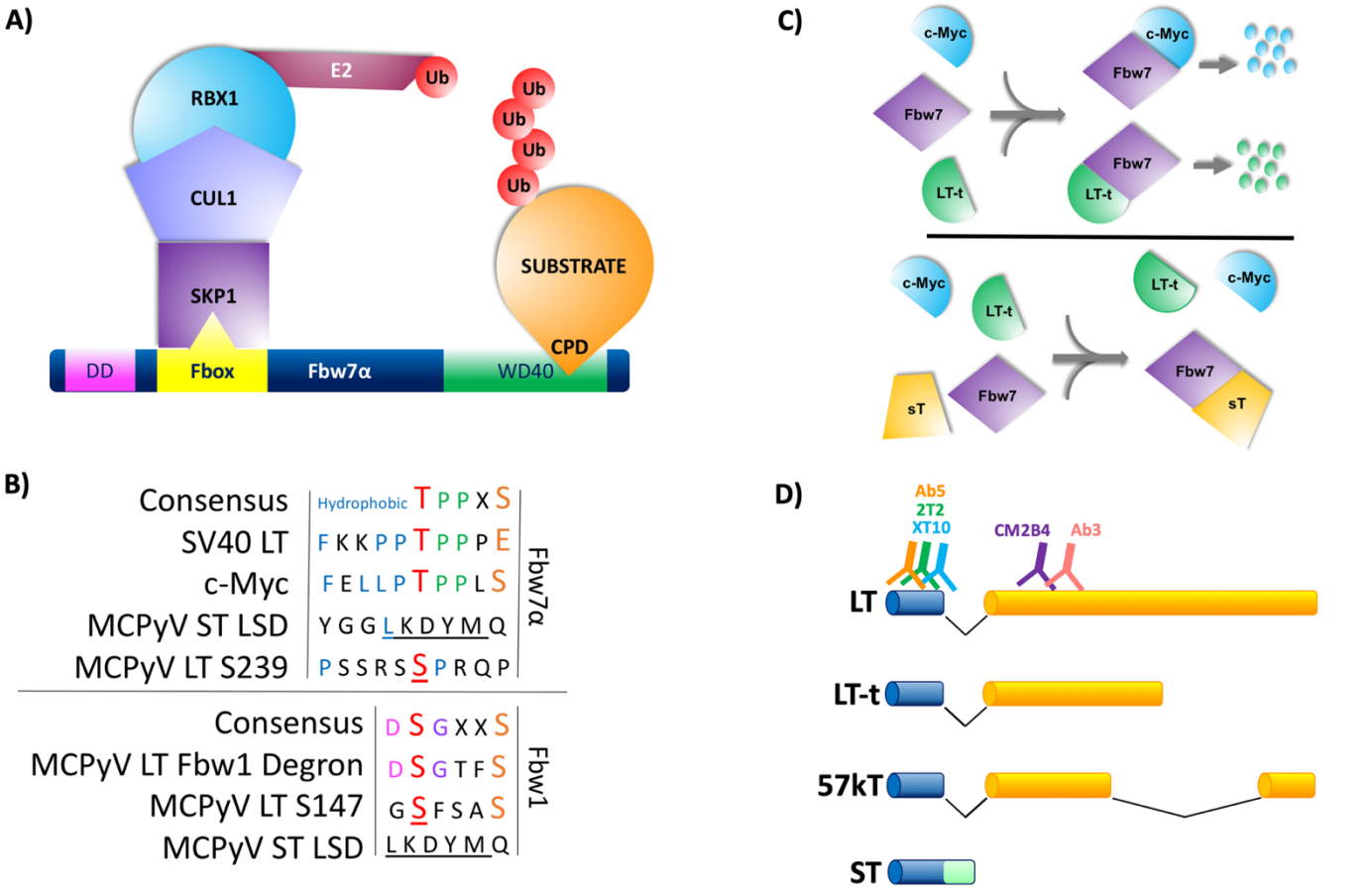

Figure 14. The mechanism of Fbw7 mediated ubiquitination. (A) The SCF^{Fbw7} ubiquitin ligase complex binds a target protein through the interaction of the WD40 domain of Fbw7 (green), and the Cdc4 phospho-degron (CPD) of the target substrate. The remaining SCF ubiquitination machinery, including the E2 ubiquitin conjugating enzyme, interacts with Fbw7 via the Fbox domain (yellow) leading to ubiquitination of the substrate protein. The dimerization domain (DD) (pink) mediates the formation of Fbw7 dimers. (B) Several proteins contain the conserved Fbw7 phospho-degron sequence (SV40 LT, c-Myc), whereas other proposed domains do not resemble either the Fbw7 or Fbw1 phospho-degron sequences (MCPyV ST LSD, MCPyV LT S239, MCPyV LT S147). Red and orange residues specify phosphorylated or negatively charged positions within the CPD (SV40 LT has a negatively charged glutamic acid at position +4), and underlined residues depict proposed residues essential for binding. Additional residues important for binding are also colored, such as hydrophobic residues preceding the central phosphorylated threonine (Fbw7-blue), two prolines after the central threonine (Fbw7-green), and the aspartic acid (Fbw1-pink) and glycine (Fbw1-purple) surrounding the central phosphorylated serine. (C) It has been proposed that in addition to its normal cellular targets, such as c-Myc, Fbw7 also targets MCPyV LT-t for proteasomal degradation (C-top panel); however, it is proposed that ST, through its Large-T Stabilization Domain (LSD) LSD, is able to bind and sequester Fbw7, thereby reducing turnover of MCPyV LT-t and its other cellular targets (C-bottom panel). (D) Due to alternative splicing, the MCPyV T antigens LT, LT-t, 57kT, and ST all contain a shared N-terminal domain (common-T, blue) that is recognized by several antibodies including Ab5 (IP, WB), 2T2 (WB), and XT10 (IP, WB). The MCPyV LT unique region (yellow), shared by LT, LT-t, and 57kT, is recognized by LT specific antibodies CM2B4 (IP, WB) and Ab3 (IP, WB). The MCPyV ST unique region is colored green. IP—immunoprecipitation, WB–western blot.

(Skp1, Cul1 and Fbox protein) ubiquitin ligases responsible for both substrate recognition and recruitment of the ubiquitination machinery. There are three isoforms of Fbw7 which localize to different subcellular compartments: Fbw7α is nucleoplasmic, Fbw7β is cytoplasmic, and Fbw7γ is nucleolar, with Fbw7α being thought to perform the majority of Fbw7 functions [120, 121]. All three Fbw7 isoforms contain three functional domains: 1) the Fbox domain binds Skp1, thereby linking Fbw7 to the SCF ubiquitination machinery, 2) the WD40 domain forms a β-propeller with two phosphate binding pockets that recognize target proteins containing phosphorylations within a conserved Cdc4 phospho-degron (CPD), named after the budding yeast Fbw7 homolog CDC4, and 3) the dimerization domain mediates the formation of Fbw7 dimers (Fig. 14A) [119, 121-124]. Most Fbw7 substrates share a dually phosphorylated degron with both phosphates spaced four amino acids apart (e.g. pTPPxpT/S), while the "+4" position can also be a negatively charged amino acid, and the "0" position is preceded by several hydrophobic amino acids (Fig. 14B) [121]. Of note, this CPD sequence is conserved among all currently known Fbw7 targets [125]. Three arginine residues within the WD40 domain of Fbw7 (R465, R479, and R505) make direct contacts with degron phosphates and are most critical for substrate interactions [119, 124]. Fbw7 is frequently mutated in cancers due to its tumor suppressive function of regulating protein levels of several cellular oncoproteins such as c-Myc and cyclin E [120, 121, 126-128]. Interestingly, Fbw7 function has also been shown to be perturbed by the LT protein of SV40. SV40 LT contains a decoy-CPD at its extreme C-terminus (pTPPPE), which can directly interact with the WD40 domain of Fbw7 and consequently decrease turnover of normal Fbw7 target substrates (Fig. 14B) [125].

In contrast to SV40 LT, Kwun et al. have proposed MCPyV LT to be targeted for proteasomal degradation through interaction with the WD40 domains of several ubiquitin ligases including Fbw7 and Fbw1 (β-TrCP) [95, 96]. As MCPyV LT and LT-t play an important role in viral replication and tumor maintenance, respectively, their rapid turnover would be deleterious.

However, amino acids 91–95 (LSD) of MCPyV ST have been shown to increase LT protein levels, and was thus termed the Large-T Stabilization Domain (LSD). Currently, the ST LSD is thought to increase LT protein levels by binding and sequestering several ubiquitin ligases, including Fbw7, from LT and their other cellular targets, such as c-Myc, thereby decreasing their turnover (Fig. 14C). Such an activity, similar to SV40 LT, would suggest a possible role of the ST LSD in transformation and tumorigenesis, as increased concentrations of a MCPyV tumor antigen and cellular oncoproteins could lead to aberrant cellular proliferation, increased translation, and genomic instability [96, 118, 129]. Moreover, mutation of the LSD has been shown to ablate the ability of MCPyV ST expressing cells to form colonies in soft agar and promote epithelial hyperplasia in pre-term transgenic mouse embryos [96, 97]. Indeed, we similarly found the LSD domain to be necessary for transformation by MCPyV ST, and therefore next sought to investigate if the proposed perturbation of Fbw7 was responsible for this phenotype. Furthermore, as MCPyV LT is necessary for viral replication, the activity of the ST LSD has also been proposed to initiate viral replication and exit from viral latency [95].

Herein, we aimed to investigate the current models of transformation and tumorigenesis (Fbw7 perturbation and L-Myc) in our novel MCPyV transformation assays using primary human foreskin fibroblasts. Of note, most of Chapter 4 was published in PLoS Pathogens on January 28, 2019 (Dye et al., 2019).

4.2 RESULTS

4.2.1 MERKEL CELL POLYOMAVIRUS TUMOR ANTIGENS EXPRESSED IN MERKEL CELL CARCINOMA FUNCTION INDEPENDENTLY OF THE UBIQUITIN LIGASES FBW7 AND β-TrCP

4.2.1.1 SV40 LT, BUT NOT MCPYV T ANTIGENS, CO-IMMUNOPRECIPITATE WITH FBW7

To first validate an interaction between Fbw7 and a well-established target, SV40 LT, co-immunoprecipitations were performed (Fig. 15A; Dye et al., 2019 S1 Table) [125, 127, 130]. In 293A cells FLAG tagged Fbw7α was co-transfected with HA tagged SV40 LT and immunoprecipitated with an anti-HA antibody. As expected, Fbw7α readily co-immunoprecipitated with SV40 LT (Fig. 15A, lane 4). SV40 LT was also found to co-immunoprecipitate the Fbw7α ΔFbox mutant, which is unable to ubiquitinate its substrate protein but is still capable of interacting with its substrate through an intact WD40 domain (Fig. 15A, lane 6). The interaction between SV40 and Fbw7α also displayed degron dependence as the SV40 LT CPD mutant, in which the central phosphorylated threonine of the CPD was substituted with an alanine, was incapable of co-immunoprecipitating wild-type Fbw7 (Fig. 15A, lane 5). Additionally, the interaction was disrupted by an Fbw7 WD40 mutant, in which a crucial arginine of the Fbw7 WD40 domain is mutated to a leucine (Fbw7α ΔFb R505L) (Fig. 15A, lane 7).

Having confirmed the reliability of the immunoprecipitation (IP) protocol utilized, the interaction between the CPD deficient MCPyV T antigens and Fbw7 was investigated. 293A cells were co-transfected with either HA-tagged MCPyV full-length LT, MCPyV truncated LT (LT-t), untagged MCPyV ST, or HA-SV40 LT, in combination with Fbw7α. Despite the fact that 293A cells express adenovirus E1A and E1B proteins, they were chosen as our experimental model to replicate the studies done by Kwun et al. [95, 96] and other Fbw7 substrate studies [120, 125]. Fbw7 proteins were pulled-down with an antibody recognizing a FLAG tag on the N-terminus of Fbw7, reciprocal to the IP performed in Figure 15A. Surprisingly, only SV40 LT co-immunoprecipitated with Fbw7α

in this IP, consistent with it being a bona-fide Fbw7 binding partner, whereas none of the MCPyV T antigens (LT, LT-t, and ST) interacted with Fbw7α even though their expression was confirmed in the cellular lysates (Fig. 15B). It should be noted that the alternatively spliced form of the full-length MCPyV LT, 57kT, was preferentially pulled-down in these assays; however, neither full-length LT nor 57kT are expressed in MCC tumors [22]. Also of note, the tumor expressed MCPyV LT-t was found to decrease Fbw7α protein levels, as seen in the protein lysate (Fig. 15B, lane 7). This decrease was not found to be a result of LT-t decreasing Fbw7α transcription by qRT-PCR (Dye et al., 2019 S2A Fig). Currently, the mechanism underlying this observation is not understood, and could either be a physiologically irrelevant consequence of artificial LT-t expression, or lead to the discovery of a novel role for MCPyV LT-t.

To ensure that the inability of FLAG tagged Fbw7 to pull-down the MCPyV T antigens is not a consequence of the tag used, we performed an identical experiment using Myc tagged Fbw7. Consistent with Figure 15B Myc tagged Fbw7 was capable of co-immunoprecipitating SV40 LT, but not the MCPyV T antigens (Fig. 15C), suggesting that the tag used to pull-down Fbw7 is not responsible for the inability to observe an interaction between the MCPyV T antigens and Fbw7.

It is possible that the HA tags found on MCPyV LT and LT-t could pose a steric hindrance to the interaction with Fbw7, although this would not explain the inability of MCPyV ST to bind Fbw7, as ST was untagged in these experiments. A similar co-immunoprecipitation to Figure 15B was performed by transfecting 293A cells with FLAG tagged Fbw7, and untagged SV40 and MCPyV T antigens, followed by pulldown of Fbw7 and XT10 immunoblotting to detect co-immunoprecipitated T antigens. Again, untagged SV40 LT was capable of co-immunoprecipitating with Fbw7; however, none of the untagged MCPyV T antigens co-immunoprecipitated (Fig. 15D).

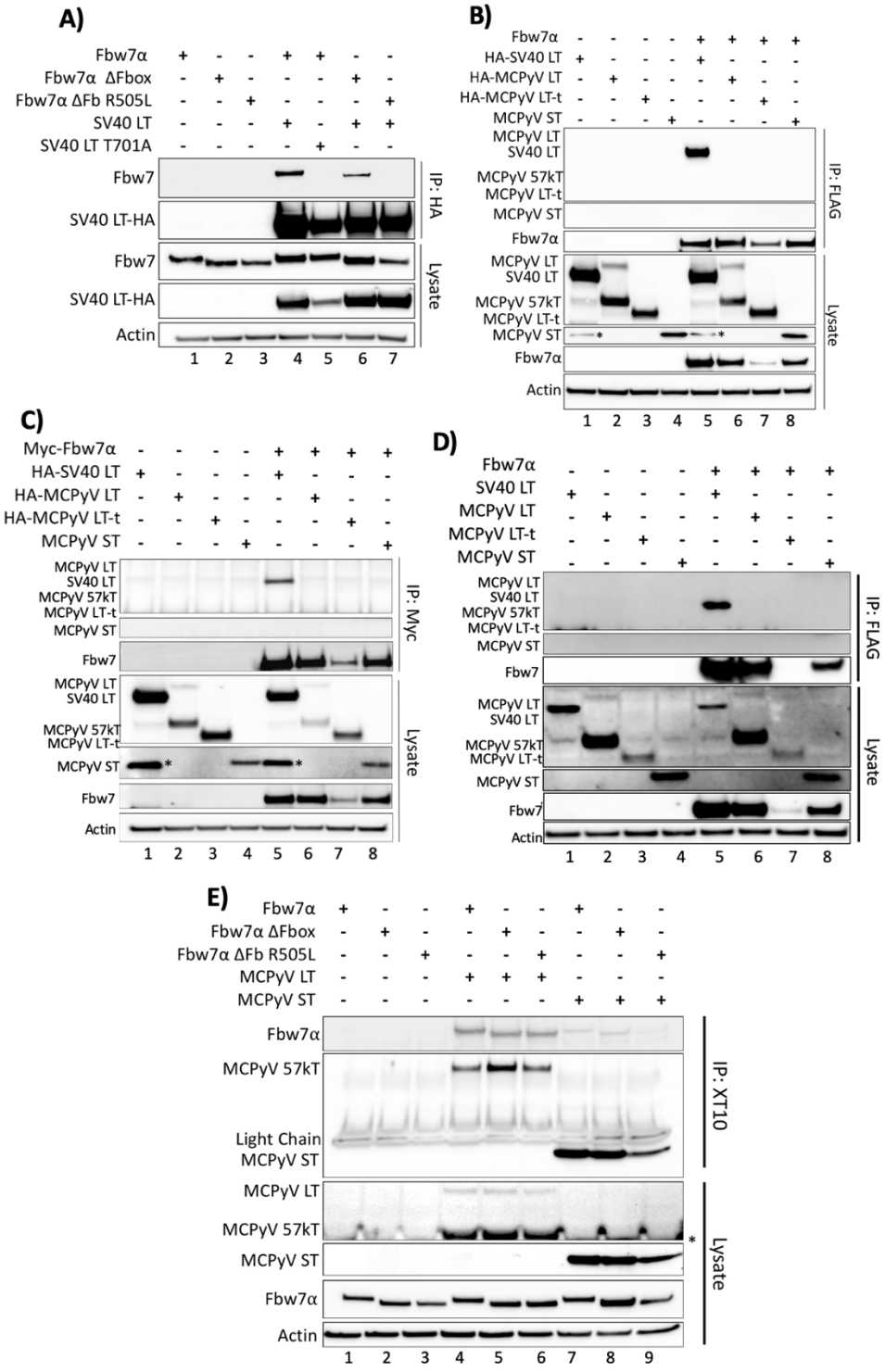

Figure 15. SV40 LT, but not the MCPyV T antigens, co-immunoprecipitate with Fbw7α.

(A) The SV40 LT antigen was pulled down with an anti-HA antibody from whole cell lysates of 293A cells expressing individual or combinations of HA-SV40 LT or the T701A mutant (5μg), wild-type FLAG-Fbw7 (4.5μg), or FLAG-Fbw7 ΔFbox/R505L mutants (3μg). Detection of co-immunoprecipitated Fbw7 was performed by immunoprecipitating with anti-HA, followed by immunoblotting with anti-FLAG. (B) The reciprocal IP to Fig 1A was performed with HA-SV40 LT, the MCPyV T antigens (HA-LT (5μg), HA-LT-t (10.5μg), and untagged ST (1μg)) and Fbw7, in which Fbw7 was pulled down (FLAG) and immunoblotted for interacting T antigens (anti-HA/2T2 (common-T antibody)). (C) An identical co-immunoprecipitation as Fig 1B was performed, except Fbw7 with an N-terminal Myc tag was pulled down from cellular lysates using a Myc tag specific antibody (9E10). (D) An identical co-immunoprecipitation as Fig 1B was performed with untagged SV40 and MCPyV T antigens. SV40 and MCPyV T antigens were detected by XT10 immunoblotting. (E) A co-immunoprecipitation between MCPyV T antigens (LT and ST) and Fbw7 was also performed through pull-down of the T antigens (XT10—common-T antibody) and detection of co-immunoprecipitated Fbw7 (anti-FLAG). Asterisks (*) denote non-specific bands.

Therefore, the N-terminal HA tag is not responsible for the inability of the MCPyV T antigens to co-immunoprecipitate with Fbw7.

In an effort to understand the discrepancies between our data and those of Kwun et al. [95, 96], a reciprocal co-immunoprecipitation was performed with an antibody that recognizes the J-domain of both SV40 and MCPyV T antigens, XT10. Immunoblotting for Fbw7 (FLAG) revealed an interaction between MCPyV LT and Fbw7α, and a very weak interaction between MCPyV ST and Fbw7α (Fig.15E). Furthermore, we were surprised to find that MCPyV LT and ST bound equivalently to wild-type Fbw7α and the Fbw7α WD40 mutant, R505L (Fig. 15E, lanes 6 and 9), which is unable to bind any other known Fbw7 substrates, including SV40 LT (Fig. 15A, lane 7). Although the interaction between MCPyV ST and Fbw7 R505L appears to be slightly fainter than the already weak interaction between Fbw7 and ST, this is most likely a consequence of less ST pulled-down in this lane (Fig. 15E, lane 9).

To determine whether XT10 was responsible for the contradictory binding results between co-immunoprecipitations performed in different directions, immunoprecipitations were performed with additional antibodies specific for the region shared by MCPyV LT, LT-t, 57kT and ST (common T–Ab5) (Dye et al., 2019 S3A Fig), or LT, 57kT and LT-t only (CM2B4, Ab3) (Fig. 14D; Dye et al., 2019 S3B Fig).

MCPyV LT co-immunoprecipitated Fbw7 with each MCPyV T antigen antibody used for the pulldown (Dye et al., 2019 S3A and S3B Fig, lane 3). Similarly, MCPyV ST again very weakly co-immunoprecipitated Fbw7 (Dye et al., 2019 S3A Fig, lane 7). As seen with XT10 pull-down (Fig. 15E), LT was found to co-immunoprecipitate with the Fbw7 WD40 mutant (Fbw7 ΔFb R505L) (Dye et al., 2019 S3A and S3B, lane 5). Taken together, it appears that MCPyV LT and ST interact with Fbw7 nonspecifically when pulled-down with antibodies specific for the MCPyV T antigens,

and this interaction is not reproducible when pulled-down with an Fbw7 anti-tag antibody (FLAG or Myc).

4.2.1.2 MCPYV ST INCREASES LT PROTEIN LEVELS INDEPENDENTLY OF FBW7, BUT DEPENDENT ON THE LSD

The LSD of MCPyV ST has been proposed to be responsible for binding Fbw7α even though this domain does not contain a recognizable conserved CPD (Fig. 14B) [96]. To assess the role of the ST LSD in the weak interaction between ST and Fbw7, a ST ΔLSD mutant was constructed and tested in similar co-immunoprecipitation experiments. In our hands, the ST ΔLSD mutant was still capable of interacting with Fbw7, and appeared to bind more strongly to Fbw7α than wild-type ST, most likely a consequence of greater amounts of ST ΔLSD mutant being expressed (Fig. 16A, lane 4). Similar results were found when the ST ΔLSD mutant was immunoprecipitated with Ab5 (Dye et al., 2019 S3A Fig, lane 8).

The current model proposes MCPyV ST preferentially binds and sequesters Fbw7 away from MCPyV LT and its other cellular targets, suggesting ST has a higher affinity for Fbw7 than LT (Fig. 14C) [95, 96]. However, since the unidirectional interaction between MCPyV ST and Fbw7α was found to be weaker than that of LT (Figs 15E and 16A; Dye et al., 2019 S3A Fig), and independent of the ST LSD (Fig. 16A; Dye et al., 2019 S3A Fig), we examined whether ST was capable of increasing MCPyV LT protein levels in the absence of Fbw7. Knockdown of Fbw7 in 293A cells was performed with lentiviruses containing either an shControl or shFbw7, and the knockdown was confirmed by pulldown and immunoblotting of endogenous Fbw7 (Fig. 16B). To investigate the described perturbation of Fbw7 by MCPyV ST, a downstream target of Fbw7, c-Myc, was analyzed in 293A cells expressing shControl, shFbw7, and/or MCPyV ST. As expected, Fbw7

knockdown led to increased c-Myc protein levels (Fig. 16C, lane 3); however, MCPyV ST expression in shControl 293A cells did not increase endogenous c-Myc protein levels (Fig. 16C, lane 2).

Therefore, MCPyV ST's inability to stabilize a downstream Fbw7 target, c-Myc, is contrary to the model of ST sequestration of Fbw7. As has been described previously, MCPyV LT protein levels were increased by co-expression of MCPyV ST, but not the ST ΔLSD mutant (Fig. 16D, lanes 1–3) [96]. However, in Fbw7 knockdown cells MCPyV ST also increased LT protein levels (Fig. 16D, lane 5). Therefore, the LSD sequence in ST is capable of increasing LT protein levels independent of Fbw7, supporting the lack of functional significance of the LSD sequence in the unidirectional interaction between MCPyV ST and Fbw7. Taken together, MCPyV ST does not perturb the function of Fbw7, and thus opens the door for further investigation into the mechanism by which the ST LSD increases LT protein levels.

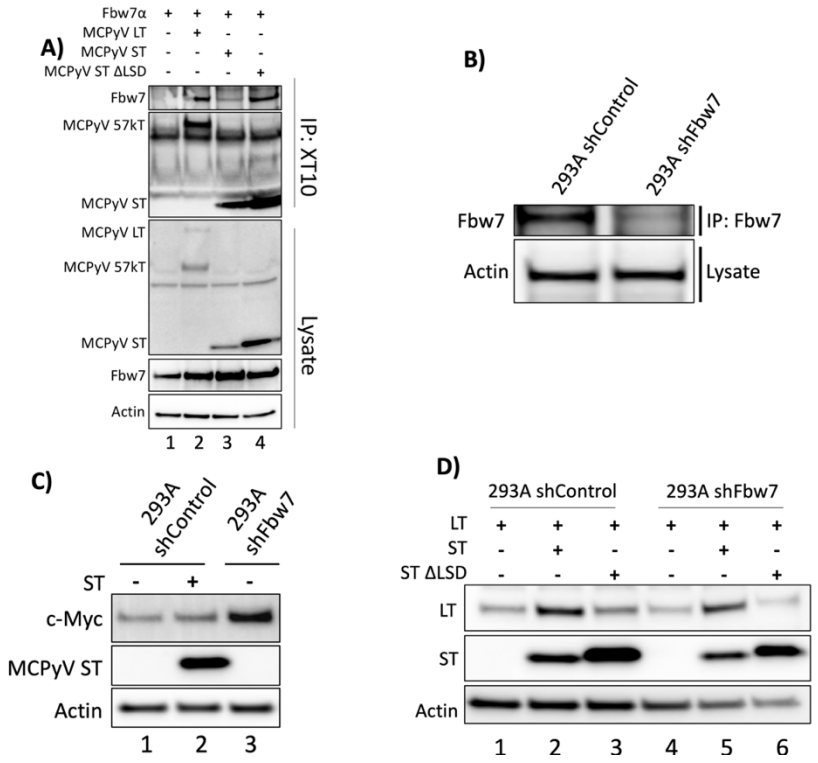

Figure 16. MCPyV ST increases LT protein levels independently of Fbw7, but dependent on the LSD.
(A) A co-immunoprecipitation between MCPyV T antigens (LT, ST, ST ΔLSD) and Fbw7 was performed through pull-down of the T antigens (XT10—common-T antibody) and detection of co-immunoprecipitated Fbw7 (anti-FLAG). (B) Fbw7 knockdown was confirmed in 293A cells transduced with lentiviruses containing shControl or shFbw7 by pulling down and immunoblotting for Fbw7 (A301-720). (C) Endogenous c-Myc protein levels were assessed by western blot in 293A expressing shControl, shFbw7, and/or MCPyV ST. (D) MCPyV LT protein levels were assessed in control and Fbw7 knockdown 293A cells with and without ST or ST ΔLSD co-expression.

4.2.1.3 MCPYV LT-T IS NOT BOUND OR DESTABILIZED BY FBW7

In MCPyV positive MCC only ST and LT-t are expressed [17, 22]. Since ST sequestration of Fbw7α away from LT-t is a proposed mechanism of ST induced transformation and tumorigenesis [96], we next sought to determine whether LT-t is bound and destabilized by Fbw7α. MCPyV LT-t or SV40 LT were immunoprecipitated with either the XT10, Ab3, or Ab5 antibodies from whole cell lysates of 293A cells transfected with the T antigens and Fbw7α. Unlike SV40 LT, MCPyV LT-t was unable to co-immunoprecipitate with Fbw7α (Fig. 17A, lane 5; Dye et al., 2019 S3A and S3B Fig, lane 6). The interaction between MCPyV LT-t and Fbw7α has been described as extremely transient due to rapid degradation and is, therefore, only observable after treatment with the broad proteasome inhibitor MG132 [96]. Similar to Kwun et al., we were able to see an interaction between MCPyV LT-t and Fbw7α when treated with MG132; however, an even stronger interaction was observed between our negative control, SV40 LT-T701A, and Fbw7α with MG132 treatment, suggesting that pleiotropic effects of MG132 treatment can lead to false positives (compare Fig. 15A with Dye et al., 2019 S2B Fig) [96]. A more direct and reliable way to assess binding partners of Fbw7α uncoupled from turnover is through the utilization of the degradation incompetent Fbw7α ΔFbox mutant. MCPyV LT-t was also unable to co-immunoprecipitate with Fbw7α ΔFbox, further suggesting the inability of these two proteins to interact, even in the absence of turnover (Fig. 17A, lane 6).

To determine if MCPyV LT-t is destabilized by co-expression of Fbw7α, cells were co-transfected with identical amounts MCPyV LT-t and increasing amounts of either Fbw7α or the degradation incompetent Fbw7α ΔFbox mutant. Consistent with Fbw7α not binding LT-t, co-expression of Fbw7α did not reduce LT-t protein levels (Fig. 17B). This is in contrast to c-Myc, which was readily destabilized by Fbw7α, but was not destabilized by the Fbw7α ΔFbox mutant (Fig.

17C). Together, these results suggest that the LT-antigen found in MCC, LT-t, is neither bound nor destabilized by Fbw7α.

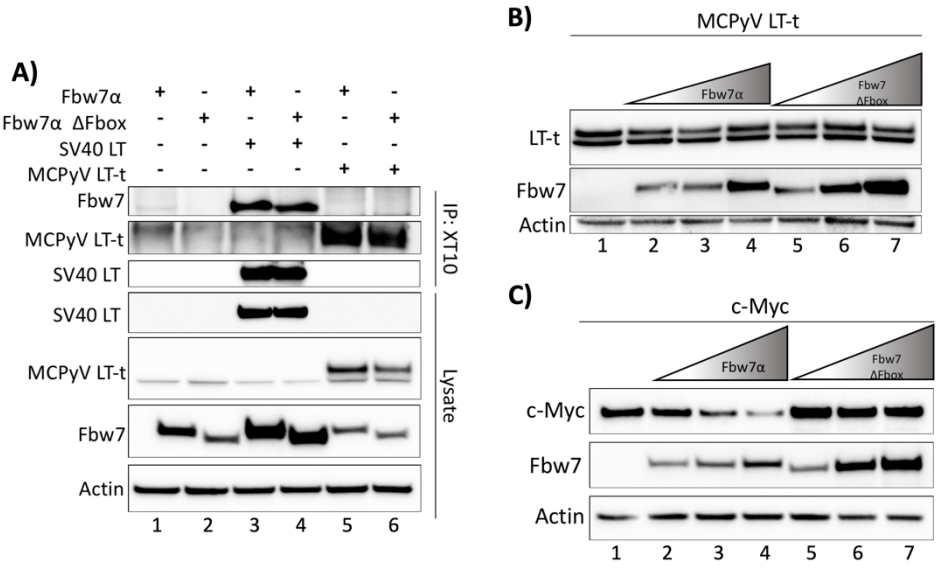

Figure 17. MCPyV LT-t is not bound or destabilized by Fbw7.
(A) Whole cell lysates of 293A cells transfected with individual or combinations of FLAG-Fbw7 (4.5μg), ΔFbox (3μg), HA-SV40 LT (5μg), MCPyV LT-t (10.5μg), were pulled-down with XT10, and immunoblotted with anti-FLAG. (B) 293A cells were transfected with a constant amount of MCPyV LT-t (10μg) and increasing amounts of Fbw7 (2.5μg, 5μg, 10μg) or the stable, degradation incompetent, Fbw7 ΔFbox (1.25μg, 2.5μg, 5μg). MCPyV LT-t protein levels were compared by 2T2 immunoblotting (common-T antibody). (C) Similar to Fig 3B, 293A cells were transfected with consistent amounts of HA-c-Myc (2μg) and increasing amounts of Fbw7 (0.1μg, 0.25μg, and 0.5μg). c-Myc protein levels were compared through detection of c-Myc by immunoblotting with anti-HA.

4.2.1.4 MCPYV LT UNIDERECTIONALLY BINDS FBW7 THROUGH AN UNIDENTIFIED DOMAIN

Kwun et al. mapped the domain of MCPyV LT-t targeted by Fbw7α to residues around S239, although this domain does not resemble a canonical Fbw7 CPD (Fig. 14B) [95]. Because we did not detect an interaction between LT-t and Fbw7, the S239A mutation was constructed in full-length LT; however, this mutant was still capable of co-immunoprecipitating Fbw7α (Fig. 18A; Dye et al., 2019 S3A and S3B Fig, lane 4). Therefore, since MCPyV LT does not contain a canonical

degron, and the proposed degron, S239, was found to be dispensable, it is unknown how or where the unidirectional interaction between MCPyV LT and Fbw7 is occurring. The MCPyV T antigen specific antibodies used in these immunoprecipitations can pull-down both MCPyV LT and 57kT since they are identical in sequence with the exception of a spliced-out intron of the 57kT (Dye et al., 2019 S4A Fig). Therefore, it is unclear whether or not the observed interaction between MCPyV LT/57kT and Fbw7α is specific to MCPyV LT, 57kT, or a domain shared by both. However, a construct that could only express the 57kT also readily co-immunoprecipitated with Fbw7 independent of the WD40 domain (Fig. 18B).

Since MCPyV LT and 57kT, but not LT-t, were capable of binding Fbw7α, the Fbw7α binding domain of MCPyV LT and 57kT must reside in the C-terminal 100 amino acids common to both proteins (Dye et al., 2019 S4A Fig). Although the decoy-CPD of SV40 LT is found at its extreme C-terminus [125], the entire full-length MCPyV LT does not contain a canonical Fbw7 CPD. To identify the domain within the C-terminal 100 amino acids of MCPyV LT responsible for binding Fbw7α, an alanine scan in which sequential 5 amino acids were substituted with alanines was performed. Every stable mutant of the alanine scan was capable of co-immunoprecipitating Fbw7α (Dye et al., 2019 S4B-S4E Fig) though we cannot rule out interactions with sequences that when mutated destabilized LT. It is also possible that there are multiple weak degrons in the C-terminus of MCPyV LT, though this type of binding has been refuted [127, 131] and would nevertheless be inconsequential to MCPyV transformation as this region of LT is not expressed in MCCs. Therefore, the MCPyV LT domain responsible for the unidirectional interaction observed between LT and Fbw7α is still unresolved.

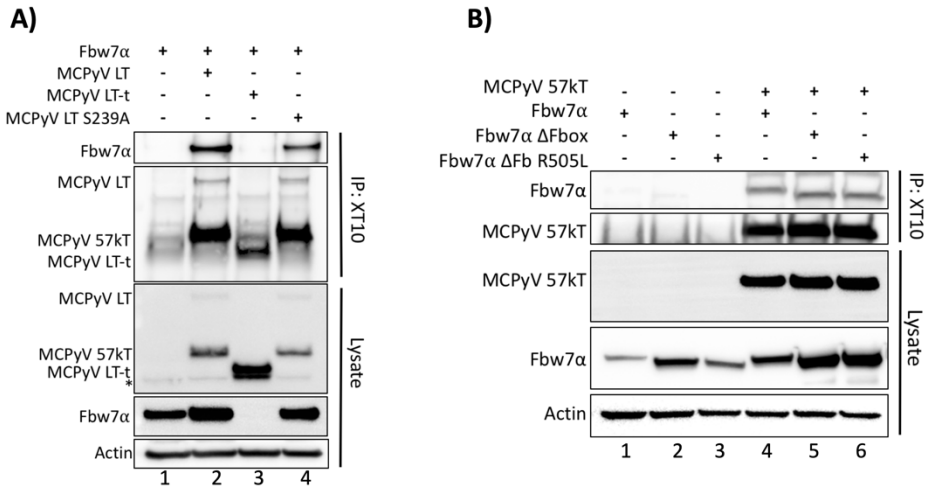

Fig 18. MCPyV LT and 57kT bind Fbw7α independently of its WD40 domain and MCPyV LT S239.
(A, B) MCPyV LT was pulled-down with XT10 from whole cell lysates of 293A cells transfected with individual or combinations of full-length MCPyV LT S239A (5μg), MCPyV LT-t (10.5μg), MCPyV 57kT (5μg), Fbw7 (4.5μg), ΔFbox (3μg), or R505L (3μg), and immunoblotted with anti-FLAG to detect co-immunoprecipitated Fbw7. (B) A plasmid encoding only the sequence of MCPyV 57kT was similarly pulled-down and co-immunoprecipitated Fbw7 was detected. Asterisks (*) denote non-specific bands.

4.2.1.5 THE SITE ON FBW7 TO WHICH BINDING OF MCPYV T ANTIGENS OCCURS IS UNKNOWN

After unsuccessful identification of the MCPyV LT domain responsible for binding Fbw7α, we decided to also investigate the domain of Fbw7α responsible for binding MCPyV LT. As was shown in Figure 15E, MCPyV LT and ST were capable of interacting with an Fbw7α WD40 domain mutant, R505L, which has not been reported for any other known Fbw7 substrates. In contrast, the proposed interaction between MCPyV LT and Fbw7α was reported to be WD40 dependent, as an R465C mutation ablated this interaction [96]. Since all three arginine residues (R465, R479, R505) are necessary for the function of the Fbw7α WD40 domain, experiments were conducted to

determine whether an Fbw7 R465C mutation would interfere with binding to LT. HA-tagged Fbw7α and the mutant R465C (gifts from Patrick Moore and Yuan Chang) in addition to FLAG-tagged Fbw7α and R505L were studied for their ability to interact with MCPyV LT or LT-t. Both wild-type Fbw7α constructs, regardless of having an HA or FLAG tag, were able to co-immunoprecipitate with MCPyV LT, but not the tumor-specific LT-t with XT10 pull-down (Fig. 19A, lanes 5,6, 9, and 10). However, we found both WD40 domain mutants, R505L and R465C, to co-immunoprecipitate with MCPyV LT, further supporting that the unidirectional interaction observed between MCPyV LT and Fbw7 occurs independently of residue R465 in the WD40 domain (Fig. 19A, lanes 7 and 8) [96]. Furthermore, the interaction between Fbw7α and MCPyV LT did not lead to destabilization of LT (Fig. 19B). Thus, the interaction observed between MCPyV LT and Fbw7α is independent of the WD40 domain, and is consistent with the inability of Fbw7 to degrade LT, as the WD40 domain is responsible for positioning the substrate for ubiquitination and subsequent degradation [119, 121, 124].

The region of Fbw7α responsible for binding MCPyV LT mapped to the common C-terminal region shared by all Fbw7 isoforms (Dye et al., 2019 S5A and S5B Fig) which is known to contain three functional domains: the dimerization, Fbox, and WD40 domains [121]. As shown thus far, the Fbw7 Fbox and WD40 domains are dispensable for this interaction (Figs. 15E, 18B, 19A; Dye et al., S3A and S3B Fig); therefore, the dimerization domain was also assessed. A double Fbw7α mutant containing a deletion of both the Fbox and dimerization domain (Fbw7α ΔFD) was still capable of co-immunoprecipitating with both MCPyV LT and ST (Dye et al., 2019 S5C Fig). Therefore, it is unclear which domain of Fbw7α is responsible for the unidirectional interaction observed with MCPyV LT and ST.

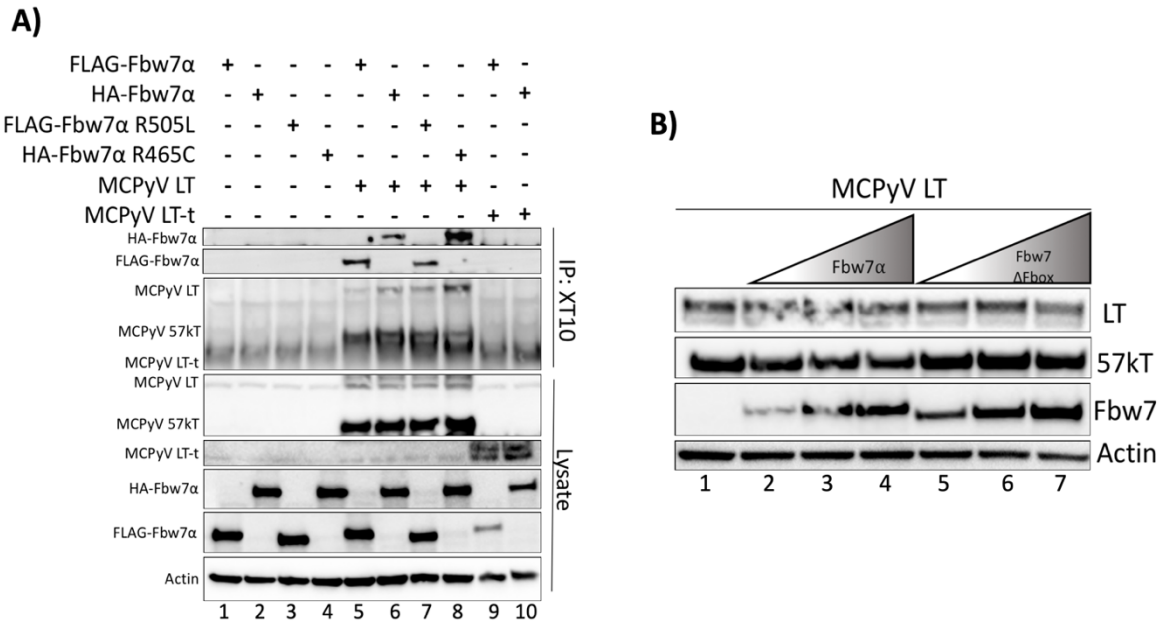

Fig 19. MCPyV LT is not bound or destabilized by the WD40 domain of Fbw7.
(A) MCPyV LT was pulled-down from whole cell lysates of 293A cells transfected with MCPyV LT (5μg), LT-t (10.5μg) and either the FLAG-Fbw7α (4.5μg), or HA-Fbw7α construct (8μg). In addition, the FLAG-tagged WD40 mutant (FLAG-Fbw7α-R505L) (3μg), and the HA-tagged WD40 mutant provided by Kwun et al. (HA-Fbw7α-R465C) (8μg) were tested for their ability to co-immunoprecipitate with MCPyV LT and LT-t (17). (B) Consistent amounts of MCPyV LT (5μg) were co-expressed with increasing amounts of Fbw7 (2.5μg, 5μg, 10μg) or the degradation incompetent Fbw7 ΔFbox mutant. Immunoblotting with 2T2 was performed to compare MCPyV LT protein levels in each condition.

4.2.1.6 MCPYV LT-T AND ST DO NOT INTERACT WITH THE E3 UBIQUITIN LIGASE FBW1

In addition to Fbw7, it has also been proposed that MCPyV LT is targeted for destruction by several other ubiquitin ligases including another Fbox containing E3 ubiquitin ligase, Fbw1(β-TrCP) [95]. The phospho-degron for Fbw1 recognition is also well defined and contains the sequence DpSGXXpS/pT [132], which is present at the extreme C-terminus of MCPyV LT. However, the reported domain of MCPyV LT responsible for the interaction with Fbw1 was mapped to S147 [95], which is missing several components of the canonical Fbw1 phospho-degron sequence (Fig. 14B). Further, it has been hypothesized that MCPyV ST promiscuously binds several

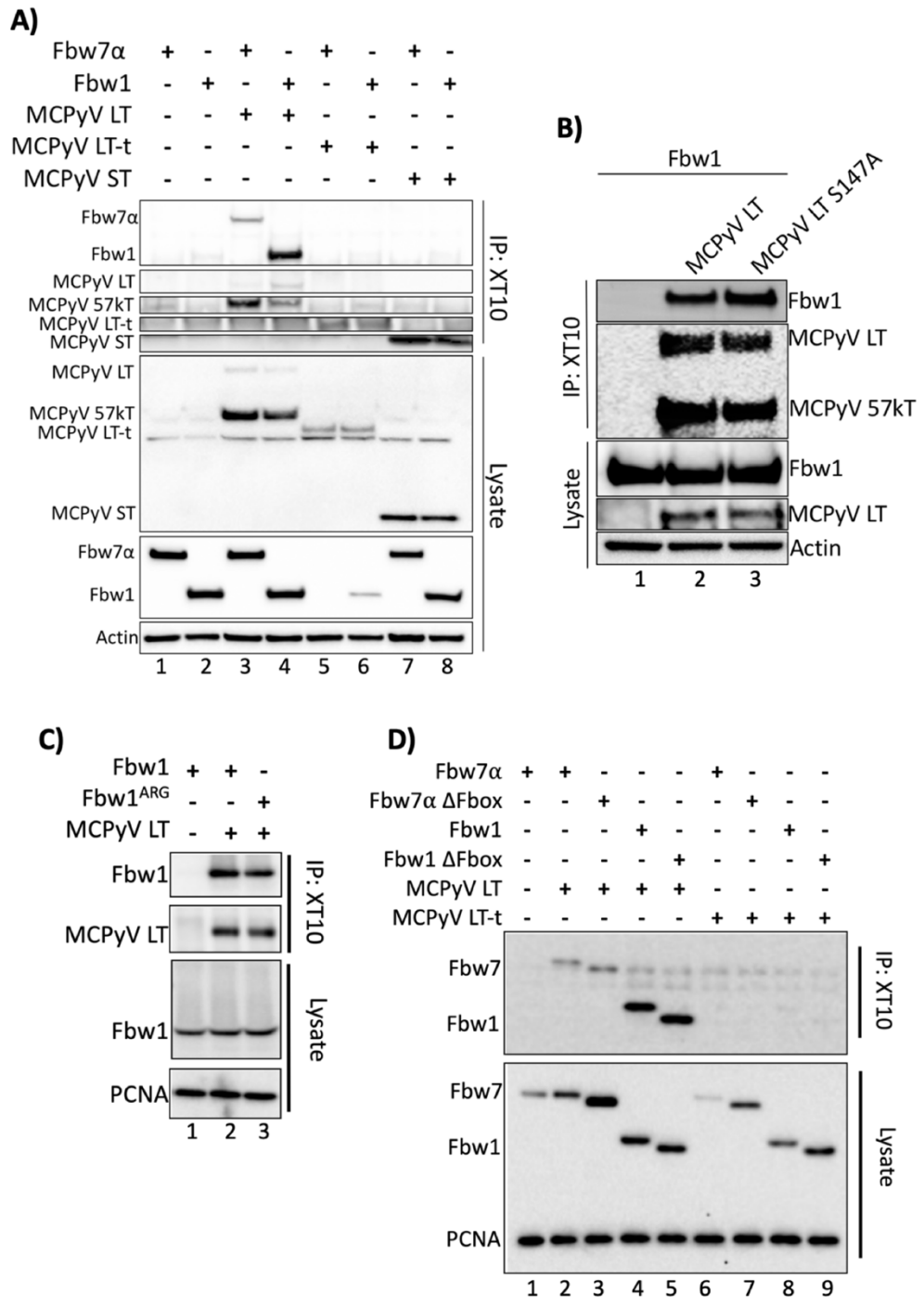

Figure 20. MCPyV LT-t and ST do not interact with the E3 ubiquitin ligase Fbw1 (β-TrCP).
(A) Fbw1, was assessed for its ability to co-immunoprecipitate MCPyV T antigens. 293A cells co-transfected with individual or combinations of Fbw7 (4.5μg), Fbw1 (3μg), MCPyV LT (5μg), MCPyV LT-t (10.5μg), or MCPyV ST (1μg). MCPyV T antigens were pulled down with XT10, and Fbw7 or Fbw1 co-immunoprecipitation was detected by immunoblotting with anti-FLAG. (B) A mutation in the proposed Fbw1 binding domain of MCPyV LT-t, S147A, was also assessed for its ability to co-immunoprecipitate Fbw1. (C and D) MCPyV LT and LT-t were immunoprecipitated with XT10 and stained for co-immunopreciptated Fbw7, Fbw1, ΔFbox, or WD40 ($Fbw1^{ARG}$) mutants (FLAG).

immunoprecipitations were performed in which the T antigens were pulled-down and co-

immunoprecipitated Fbw7 or Fbw1 was detected. MCPyV LT bound both Fbw7α and Fbw1; however, LT-t and ST failed to bind Fbw1 (Fig. 20A). Furthermore, an alanine MCPyV LT mutant, S147A [95], was still capable of co-immunoprecipitating Fbw1 (Fig. 20B). Similar results were found when the immunoprecipitation was performed with additional MCPyV T antigen specific antibodies (Dye et al., 2019 S6A and S6B Fig). Similar to Fbw7, MCPyV LT was capable of binding to both Fbw1 WD40 and ΔFbox mutants (Fig. 20C, lane 3, 20D lane 5), again suggesting the interaction between MCPyV T antigens and Fbw1 to be non-specific. Of note, MCPyV LT-t was also capable of decreasing Fbw1 protein levels, as was seen with Fbw7, (compare Figure 15B to 20A) even though MCPyV LT-t was not found to bind either proteins. Therefore, this either novel function of MCPyV LT-t, or irrelevant consequence of artificial LT-t expression, is broadly acting.

4.2.2 MCPYV ST TRANSFORMS HFFS INDEPENDENT OF L-MYC

More recently an additional mechanistic model of MCPyV ST mediated transformation has been proposed. James DeCaprio's group at Harvard has shown by that MCPyV ST can bind and enhance the interaction between the histone acetyltransferase EP400 complex and the transcription factor, L-Myc. This leads to the recruitment of the EP400 complex to promoters targeted by L-Myc, many of which promote expression of genes involved in the generation of induced pluripotent stem cells (iPS), including the *MycL* promoter itself [112]. In contrast to c-Myc, L-Myc is a much less understood Myc isoform. Unlike c-Myc, L-Myc is only expressed during embryonic development, and is limited to certain tissues [133]. However, overexpression of *MycL* is a hallmark of MCPyV positive MCC, and more recent research has found *MycL* to also be amplified in another neuroendocrine cancer, small cell lung cancer (SCLC), and that the viability of these tumors is dependent on continual *MycL* expression [112, 117, 134]. It has been shown that knockdown of *MycL*, EP400, or ST leads to decreased MKL-1 proliferation; however, soft agar analysis has been limited to using human foreskin keratinocytes (HFK) expressing hTERT, OCT4, SOX2, and KLF4

in addition to *MycL* or MCPyV ST, or IMR90 cells expressing hTERT and dominant negative p53, in addition to MycL or MCPyV ST. In our novel HFF-ST SAA, mutation of the binding domain of L-Myc and EP400 (4M) had no effect on transformation by MCPyV ST (Fig. 10). Therefore, as we are the only group successful in transforming primary HFFs with only MCPyV ST, it is important to also assess whether overexpression of *MycL* is necessary for transformation by MCPyV ST in this transformation model to evaluate the applicability of HFF-ST transformation to actual MCC cell lines.

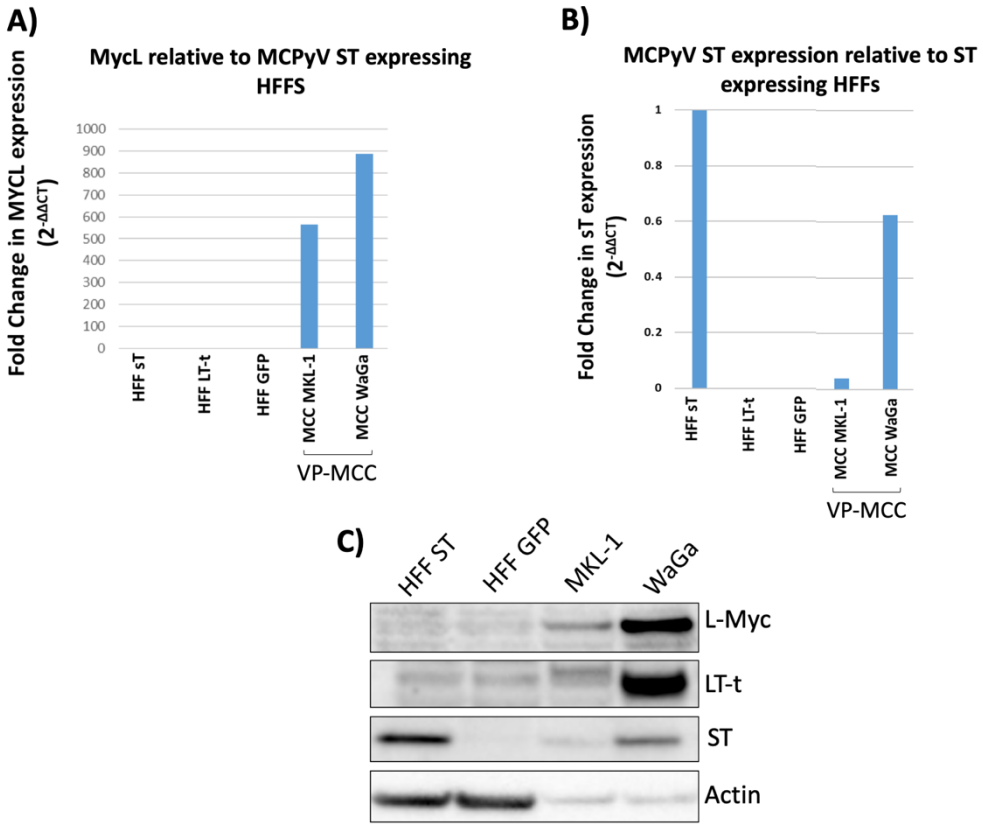

Figure 21. MCPyV ST does not transform HFFs through overexpression of *MycL*. qRT-PCR of HFFs expressing ST, LT-t or GFP, compared to the VP-MCC cell lines MKL-1 and WaGa was performed to compare *MycL* (A) and ST (B) mRNA expression levels. For each comparison, mRNA levels were compared relative to HFFs expressing ST. Protein lysates from HFFs expressing MCPyV ST or GFP, and the VP-MCC cell lines MKL-1 and WaGa were western blotted and immunoblotted for L-Myc protein levels and the MCPyV TAgs (C).

To assess the role of MCPyV T-antigens on the expression of *MycL,* mRNA levels were assessed by qRT-PCR in HFFs expressing MCPyV ST, LT-t or GFP, and the VP-MCC cell lines MKL-1 and WaGa. As reported by others, *MycL* expression is elevated in MKL-1 and WaGa VP-

MCC cell lines [112], whereas *MycL* mRNA levels HFFs expressing MCPyV ST or LT-t were not significantly different from GFP expressing HFFs (Fig. 21A). To ensure that differences in *MycL* mRNA levels were not due to differences in MCPyV ST expression levels between cell lines, qRT-PCR was also performed to compare MCPyV ST mRNA levels in HFFs transduced with MCPyV ST, LT-t, or GFP, and the VP-MCC cell lines MKL-1 and WaGa. Surprisingly, MCPyV ST mRNA levels were significantly higher in the HFFs transduced with MCPyV ST than the VP-MCC cell lines (Fig. 21B), concluding that the absence of *MycL* expression in HFFs cannot be attributed to the amount of ST expressed in these cells. Finally, western blots were performed on cell lysates from HFFs expressing MCPyV ST, GFP, MKL-1 and WaGa. Consistent with the qRT-PCR results, MKL-1 and WaGa had detectable L-Myc protein, whereas L-Myc protein levels HFFs expressing ST or GFP was undetectable (Fig. 21C). Therefore, although it is understood that L-Myc plays a role in MCC cell lines, ST is not transforming HFFs through overexpression of *MycL*, consistent with positive transformation of the MCPyV ST EP400/L-Myc binding mutant (4M) (Fig. 10).

4.3 DISCUSSION

Herein we investigated the two current models of MCPyV ST mediated transformation and tumorigenesis using our novel, relevant primary HFFs. Both MCPyV ST perturbation of Fbw7 and overexpression of *MycL* have been proposed to be responsible for the induction of transformation and tumorigenesis by MCPyV ST [96, 112]. Integration and expression of MCPyV T antigens accounts for 80% of MCC cases [17]; therefore, elucidating the true mechanisms by which LT-t and ST accomplish transformation and tumorigenesis is paramount for the design of novel therapeutics to treat VP-MCCs. Furthermore, such insight could also have implications not only for understanding polyomavirus oncogenesis and disease, but also for cellular pathways, homeostasis, and broad disease pathology. MCPyV ST has been shown to increase protein levels of MCPyV LT, LT-t, and several other cellular oncoproteins involved in proliferation, such as c-Myc and cyclin E

[96]. This has been proposed to be a consequence of ST sequestration of several ubiquitin ligases, including Fbw7 and β-TrCP, and underlies the proposed mechanisms of ST enhancement of viral replication, and induction of transformation and tumorigenesis [95, 96, 118, 129].

Since many cellular pathways, processes, and fates are sensitive to, and directed by, the amount of a given protein, and ubiquitin-mediated proteolysis is irreversible, this process is tightly regulated [135]. To be targeted by Fbw7, and subsequently ubiquitinated for proteasomal degradation, a protein must 1) contain a specific and highly conserved amino acid sequence called a CPD, and 2) include multiple site-specific phosphorylations performed by other tightly regulated kinases within the cell [119, 124, 126, 127]. For these reasons, it was surprising that both MCPyV LT-t and ST have been reported to bind Fbw7, as neither viral protein contain the well-known, conserved, Fbw7 CPD.

The concept of viral oncoprotein perturbation of ubiquitin ligases is well-established [125, 136-140]. Although evolutionarily related, several significant differences lie between the interaction of SV40 LT and Fbw7, and the proposed interaction between MCPyV LT-t and Fbw7. SV40 LT binds the WD40 domain of Fbw7 through its canonical CPD sequence, leading to the stabilization of SV40 LT and Fbw7 targets, and mislocalization of the nucleolar Fbw7γ isoform [123]. In contrast, MCPyV LT-t has been proposed to also bind the WD40 domain of Fbw7, leading to its destruction despite the absence of a canonical CPD [95, 96]. While not impossible, it is difficult to rationalize how MCPyV LT-t is binding to the WD40 domain of Fbw7 in the absence of a CPD. Also, why MCPyV LT-t, a protein necessary for tumor viability, would retain sequences that would ultimately lead to its destruction, and therefore rely on the activities of another viral protein, ST, to avoid degradation is counter-intuitive [95, 96].

The interaction between MCPyV T antigens and ubiquitin ligases have been implicated in regulating both viral latency in normal, asymptomatic, viral infection (LT and ST), and

transformation in the setting of MCC (LT-t and ST) [95, 96]. In this report, we provide several lines of evidence that oppose both proposed models.

It has been proposed that MCPyV ST promiscuously binds and sequesters several E3 ubiquitin ligases through its LSD; however, as each of these ubiquitin ligases recognize distinct phospho-degrons, it is difficult to imagine how one domain could interact with several different highly specific proteins [95, 96, 118, 119, 132]. In our hands, weak ST binding to Fbw7 was only observed unidirectionally and independent of the Fbw7 WD40 and ST LSD domains. Moreover, an interaction between MCPyV ST and Fbw1 was never observed. Therefore, we hypothesized that MCPyV ST, which lacks a canonical CPD and does not bind to the WD40 domain of Fbw7, may possess an alternative mechanism for binding and perturbing the function of Fbw7 independent of the WD40 domain. For instance, binding to another component of the SCF complex, as has been proposed for the adenovirus E1A protein [140], could explain the proposed ubiquitin ligase binding promiscuity of MCPyV ST. However, this hypothesis is also not supported by our data, as MCPyV ST also unidirectionally co-immunoprecipitated the Fbw7 ΔFbox mutant, which cannot recruit the remaining SCF complex. Furthermore, others have hypothesized that MCPyV ST may inhibit the formation of dimers to perturb Fbw7 function, as the dimerization domain of Fbw7 has been found to enhance binding to low affinity substrates [96, 122]. However, as we have also shown MCPyV ST capable of binding a dimerization domain Fbw7 mutant, it is unlikely that MCPyV ST utilizes this mechanism to perturb Fbw7 targeting of low affinity substrates, such as LT. Therefore, thorough investigation of several mechanisms by which MCPyV ST could perturb the function of ubiquitin ligases failed to uncover or support the proposed promiscuity of MCPyV ST ubiquitin ligase perturbation.

The proposed model of MCPyV ST mediated transformation suggests that MCPyV LT-t and other cellular oncoproteins are stabilized through MCPyV ST sequestration of Fbw7, leading to

aberrant cellular proliferation and transformation [96]. Although our studies confirmed the ability of ST to increase LT protein levels through the LSD, this was accomplished independently of Fbw7. This is supported by the fact that MCPyV LT-t was never found to interact with, or be destabilized by, Fbw7. This suggests that MCPyV LT-t is not targeted by Fbw7, and is consistent with MCPyV ST not specifically binding to, or perturbing the function of Fbw7 to increase LT-t protein levels. Furthermore, MCPyV ST had no effect on c-Myc protein levels, a bona-fide Fbw7 substrate, further confirming no association between MCPyV ST and Fbw7. Thus, it can be concluded that the mechanism(s) by which ST increases LT-t protein levels, and transforms cells, does not involve sequestration and/or perturbation of Fbw7.

MCPyV LT destabilization by ubiquitin ligases has been proposed to play a role in maintaining viral latency in a normal infection, as reduced LT protein levels decreases viral replication [95]. Unlike tumor expressed MCPyV LT-t, we were able to observe a weak interaction between MCPyV LT and Fbw7; however, this interaction was only observed unidirectionally, was independent of proposed LT binding domains and the Fbw7 WD40, did not lead to destabilization of LT, and has no relevance to transformation and tumorigenesis. Although neither MCPyV LT nor ST contain a canonical Fbw7 CPD, one could hypothesize that the unidirectional interaction observed between LT, ST and Fbw7 could occur through a novel degron sequence found on these T antigens. However, such an interaction would still be dependent on an intact Fbw7 WD40 domain, which we found to be dispensable for binding. In addition, we were unable to identify the domains of the T antigens nor Fbw7 responsible for the unidirectional interaction through both direct mutagenesis of the proposed binding domains and comprehensive mutational screens. Thus, the proposed model of ST sequestration of ubiquitin ligases to stabilize LT protein levels and induce viral replication in the setting of a normal viral infection can not be confirmed at the level of the interaction itself or functionally.

To directly evaluate the discrepancies between our data and those of Kwun et al., plasmids were exchanged and tested in parallel. Here, both Fbw7 expressing constructs were capable of co-immunoprecipitating with MCPyV LT, but not the tumor expressed MCPyV LT-t. Also contrary to previous reports, the interactions observed between MCPyV LT and the provided Fbw7 constructs were independent of the WD40 domain. Thus, it is unlikely that the observed weak, unidirectional, destabilization and CPD/WD40 independent interaction observed between MCPyV T antigens and Fbw7 is relevant to the role of the T antigens in either the viral life-cycle or tumorigenesis.

In conclusion, we thoroughly investigated the specific interaction and downstream consequences of the proposed involvement of MCPyV T antigens and Fbw7. A likely artifactual interaction between MCPyV LT, ST and Fbw7 was observed, but not with LT-t, thereby dismissing the relevance of the proposed model in MCC tumorigenesis. It should be noted that ST is capable of increasing LT protein levels through its LSD; however, the mechanism by which this is accomplished by MCPyV ST is not fully understood, as Fbw7 was found to play no role in this interaction. Furthermore, HFFs expressing MCPyV ST did not lead to increases in *MycL* expression as has also been proposed as a mechanism of MCPyV ST mediated transformation and tumorigenesis. In conclusion, we propose MCPyV ST to be capable of transformation and tumorigenesis independent of ubiquitin ligase perturbation and L-Myc, and therefore open the door for further investigation into the mechanisms by which MCPyV ST and amino acids 91-95 contribute to viral replication, latency, and induce transformation and tumorigenesis.

CHAPTER 5. IDENTIFICATION OF CELLULAR BINDING PARTNERS AND PATHWAYS PERTURBED BY MCPYV ST.

5.1 INTRODUCTION

In order to appreciate the mechanisms by which a disease develops and is maintained, the understanding of protein-protein interactions and consequent downstream pathway perturbations is critical. The earlier chapters of this dissertation have found MCPyV ST to be uniquely transforming among HPyV ST proteins, and that this transforming function is dependent on amino acids 91-95 and 116-120. Although these domains were found to be necessary but not sufficient for transformation, the 91-95A and 116-120A MCPyV ST non-transforming mutants are still powerful tools to identify unique MCPyV ST cellular binding partners and pathways necessary for transformation. By comparing the differences in cellular binding partners and perturbed pathways between the transforming MCPyV ST and the non-transforming HPyV7 ST, TSPyV ST, MCPyV ST 91-95A, and MCPyV ST 116-120A, we hope to identify the unique mechanism of transformation by wild-type MCPyV ST.

As our understanding of protein-protein interactions is paramount to understand the development of disease, many experimental approaches have been developed to identify and assess these interactions, such as mass spectrometry. Mass spectrometry has been utilized by others in an attempt to identify MCPyV ST cellular interactors [112, 113]; however, these experiments were limited to using less relevant cell lines such as 293 cells. Furthermore, these experiments were performed using traditional co-IP/mass spectrometry approaches which are dependent on antibody-based co-immunoprecipitations and also the rate of dissociation of protein-protein complexes, therefore limiting the identification of transient or weak protein interactors. Interestingly, neither of these experiments identified Fbw7 as an MCPyV ST cellular interactor, consistent with our disproving of the Fbw7 perturbation transformation mechanism described in Chapter 4. Previous mass spectrometry attempts have identified NEMO and L-Myc as MCPyV ST interactors responsible for transformation by MCPyV ST [112, 113]. Unfortunately, in HFFs, the MCPyV ST NEMO binding domain mutant (Δ95-111) was expressed at levels too low to assess for

transformation in soft agar assays. However, mutation of the L-Myc binding domain (4M) did not ablate transformation, suggesting these two MCPyV ST interactors are not responsible for the robust transforming phenotype of MCPyV ST in our novel, relevant, and robust transformation assays.

More modern mass spectrometry approaches have increased our ability to identify prey proteins which have weak or transient interactions with the bait protein. For example, in the past 8 years enzyme-catalyzed proximity labeling has become a popular approach to study protein interactions [141]. TurboID is a proximity labeling mass spectrometry approach in which your protein of interest (bait) is fused in frame with a modified version of an *E. coli* biotin ligase (BirA). The mutant BirA enzyme catalyzes the formation of activated biotin molecules (biotinoyl-5'-AMP), which creates a "cloud" of activated biotin around the bait. These activated biotin molecules then react with free amines of proteins associated with the bait. Because this reaction is immediate, this not only allows for the biotinylation of stable interactors, but also weak or transient interactors, all of which can be captured through streptavidin-based affinity purification and identified through mass spectrometry. Therefore, TurboID eliminates epitope blocking common to antibody-based co-immunoprecipitation methods, and is capable of identifying both stable and transient protein interactors.

The ultimate goal is to identify MCPyV ST cellular interactors that disrupt associated pathways resulting in cellular transformation. Next generation RNA sequencing is a powerful tool to assess global transcriptional changes that may occur downstream of MCPyV ST expression. Similarly, RNA sequencing of primary HFFs expressing MCPyV ST has never been performed, and therefore can be used as a useful and relevant tool to complement mass spectrometry experiments in the same cells. Herein we aimed to identify novel and unique MCPyV ST interactors in primary HFFs responsible for transformation through TurboID mass spectrometry. We further sought to

identify MCPyV ST interactors with downstream cellular perturbations as assessed by next generation RNA sequencing. Together, these approaches may identify the unique mechanism(s) by which MCPyV ST transforms primary HFFs and leads to the development of VP-MCC, both of which are paramount for the development of novel and efficacious MCC therapeutics.

5.2 RESULTS

5.2.1 IDENTIFICATION OF MCPYV ST BINDING PARTNERS AND PATHWAYS NECESSARY FOR CELLULAR TRANSFORMATION

5.2.1.1 TURBO ID MASS SPECTROMETRY INDENTIFIED SEVERAL POSSIBLE MCPYV ST CELLULAR INTERACTORS IMPLICATED IN CANCER

The history of utilizing mass spectrometry to identify MCPyV ST cellular interactors responsible for transformation and the development of MCC has yet to elucidate a protein interaction responsible for the robust transforming capacity of MCPyV ST. This is surprising, as MCPyV ST has been found to be a very strong viral oncoprotein. For these reasons, we hypothesized that the use of irrelevant cell lines and traditional co-immunoprecipitation methods in previous approaches could be to blame. Mass spectrometry of co-immunoprecipitated MCPyV ST cellular interactors has not yet been performed in primary HFFs, a more relevant cell line in which MCPyV ST is independently and robustly transforming. Furthermore, the previously used MCPyV antibody immunoprecipitations are useful for identifying stable and strong MCPyV ST interactors, but less useful in identifying transient protein interactions. For these reasons, we decided to implement a modern proximity-dependent mass spectrometry approach called TurboID [141]. The mutant BirA biotin ligase enzyme was fused in frame on the N-terminus of MCPyV ST with a 4xGS

linker separating the proteins and a V5 epitope tag (TID-ST). Since we have predicted the transforming domain of MCPyV ST to be found within the ST unique region found in the C-terminal region of the protein, we hypothesized fusion of the biotin ligase on the N-terminus of MCPyV ST would lessen the possibility of interference with MCPyV ST interactors responsible for transformation.

Because the size of MCPyV ST greatly increased upon fusion of the biotin ligase (18kDa to ~60kDa), we first sought to compare the subcellular localization between MCPyV ST and TID-ST to confirm the exposure of TID-ST to proteins of the correct subcellular compartment necessary for transformation. Whole cellular protein lysates were fractionated and the prevalence of MCPyV ST and TID-ST was compared for each subcellular compartment. Similar to MCPyV ST, TID-ST predominantly localized to the nucleus, and is therefore exposed to similar proteins as the transforming MCPyV ST (Fig. 22A).

TurboID was performed on HFFs expressing TID-ST as well as HFFs expressing negative controls such as a biotin ligase fused GFP with a nuclear localization sequence (NLS) to mimic the subcellular compartment of TID-ST (TID-GFP-NLS), and the biotin ligase expressed alone (TID). TurboID was performed twice for HFFs expressing TID-ST, and once for each negative control. Biotinylated proteins for each experiment were captured by streptavidin beads and identified by mass spectrometry.

A)

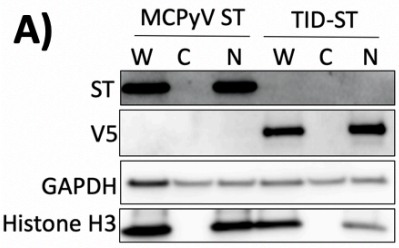

B)

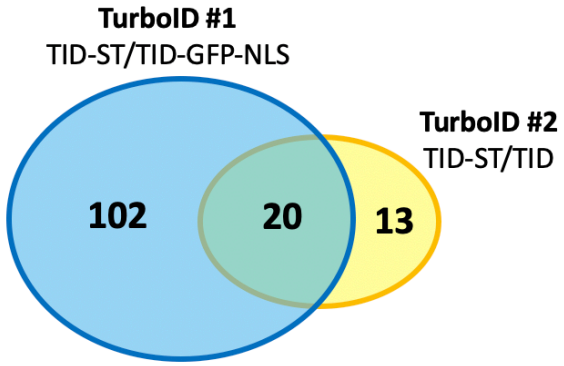

C)

calcyclin binding protein	progesterone receptor membrane component 2
ST13, Hsp70 interacting protein	alpha-2-macroglobulin
LIM domain 7	laminin subunit gamma 1
RNA polymerase II associated protein 3	myosin light chain 12A
cysteine and histidine rich domain containing 1	chloride intracellular channel 1
coiled-coil and C2 domain containing 1A	VPS37A, ESCRT-I subunit
pleckstrin homology like domain family B member 1	RuvB like AAA ATPase 1
stress induced phosphoprotein 1	glomulin, FKBP associated protein
E1A binding protein p400	sorting nexin 1
exocyst complex component 4	catenin delta 1
trinucleotide repeat containing 6A	proteasome subunit alpha 4
immunoglobulin binding protein 1	K1C10
5'-3' exoribonuclease 1	matrin 3
baculoviral IAP repeat containing 6	nucleosome assembly protein 1 like 1
CDV3 homolog	NECAP endocytosis associated 2
translocase of outer mitochondrial membrane 20	family with sequence similarity 193 member A
mitochondrial ribosomal protein S31	thioredoxin like 1
protein phosphatase 6 regulatory subunit 3	serine and arginine rich splicing factor 11
family with sequence similarity 120A	triosephosphate isomerase 1
H0Y858	Mab-21 domain containing 2
tetratricopeptide repeat domain 1	protein disulfide isomerase family A member 3
annexin A5	adaptor related protein complex 4 subunit epsilon 1
tetratricopeptide repeat domain 9C	pleckstrin homology like domain family B member 2
SEC23 interacting protein	multivesicular body subunit 12A
slingshot protein phosphatase 1	transforming growth factor beta 1 induced transcript 1
epidermal growth factor receptor pathway substrate 15	coiled-coil domain containing 6
serine/threonine kinase 38	mediator complex subunit 15
aldolase, fructose-bisphosphate A	La ribonucleoprotein domain family member 6
tyrosine kinase non receptor 1	enhancer of polycomb homolog 1
angiomotin	talin 2
golgin A3	protein tyrosine phosphatase, non-receptor type 13
tetratricopeptide repeat domain 4	synaptopodin
myopalladin	phosphoglycerate mutase 1
SCY1 like pseudokinase 1	TBC1 domain family member 5
proline rich coiled-coil 1	EH domain binding protein 1
prolyl 4-hydroxylase subunit beta	dynein cytoplasmic 1 light intermediate chain 2
prune homolog 2	heterogeneous nuclear ribonucleoprotein R
TRAF family member associated NFKB activator	pleckstrin homology domain containing A2
signal transducing adaptor molecule	LIM domain 7
FK506 binding protein 5	eukaryotic translation initiation factor 5
solute carrier family 25 member 5	nascent polypeptide associated complex subunit alpha
eukaryotic translation initiation factor 2A	zinc finger FYVE-type containing 16
NCK adaptor protein 1	palladin, cytoskeletal associated protein
coenzyme Q3, methyltransferase	PDZ and LIM domain 1
zinc finger protein 148	synaptojanin 2
suppression of tumorigenicity 5	PDZ and LIM domain 5
USO1 vesicle transport factor	phosphatidylinositol binding clathrin assembly protein
serpin family H member 1	5'-nucleotidase, cytosolic II
WD repeat domain 36	signal recognition particle 54
isoleucyl-tRNA synthetase 2, mitochondrial	NIMA related kinase 1
A-kinase anchoring protein 13	proline rich coiled-coil 2A

D)

NudC domain containing 2
STIP1 homology and U-box containing protein 1
striatin
SWI/SNF related, matrix associated, actin dependent regulator of chromatin,
ADAM metallopeptidase with thrombospondin type 1 motif 15
WW domain containing transcription regulator 1
chromosome 1 open reading frame 68
prostaglandin E synthase 3
collagen type XII alpha 1 chain
collagen type III alpha 1 chain
inhibitor of growth family member 3
nexilin F-actin binding protein
methylcrotonoyl-CoA carboxylase 1

E)

SGT1 homolog, MIS12 kinetochore complex assembly cochaperone
DnaJ heat shock protein family (Hsp40) member C7
aryl hydrocarbon receptor interacting protein
NudC domain containing 3
BCL2 associated athanogene 2
FK506 binding protein 4
striatin 4
heat shock protein family A (Hsp70) member 1B
heat shock protein family A (Hsp70) member 4
heat shock protein family A (Hsp70) member 9
Yes associated protein 1
heat shock protein family A (Hsp70) member 8
DnaJ heat shock protein family (Hsp40) member B1
heat shock protein family H (Hsp110) member 1
protein phosphatase 6 regulatory subunit 1
heat shock protein 90 alpha family class B member 1
DnaJ heat shock protein family (Hsp40) member B4
nuclear distribution C, dynein complex regulator
RNA binding motif protein 14
heterogeneous nuclear ribonucleoprotein M

F)

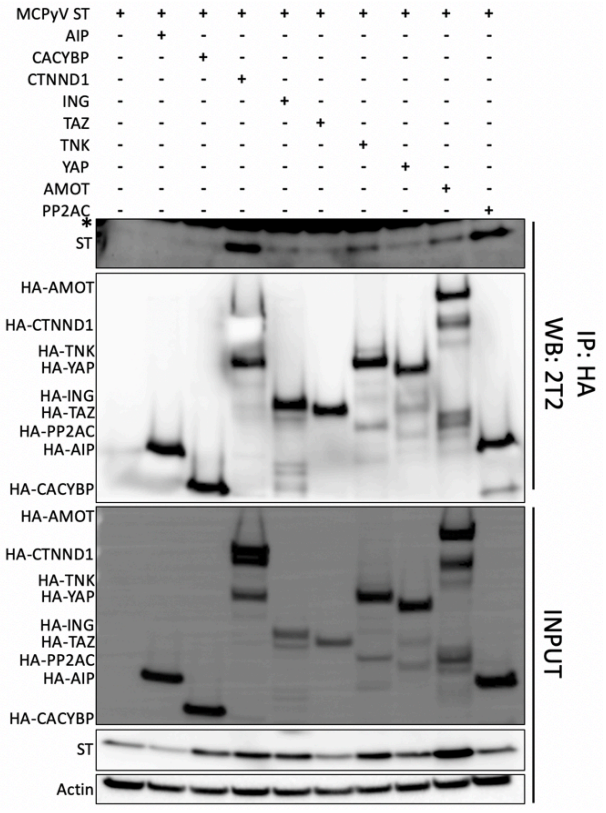

Figure 22. TurboID identified many known and novel MCPyV ST cellular interactors. HFFs expressing MCPyV ST or TID-ST were compared in the subcellular localization of the ST protein through subcellular fractionation western blotting. MCPyV ST was immunoblotted with 2T2, whereas TID-ST was immunoblotted with a V5 antibody. Cytoplasmic and nuclear fractions were confirmed by GAPDH and histone H3 immunoblotting (A). Potential MCPyV ST interactors were defined as proteins with a FDR<0.01 and a FC>2 ST/Ctrl. Between TurboID #1 (blue) and #2 (yellow), twenty proteins were identified as potential MCPyV ST interactors in both experiments (D), whereas TurboID #1 identified 102 (C), and TurboID #2 identified 13 unique potential MCPyV ST interactors (E). Together, TID-ST expressing HFFs in TurboID #1 and #2 significantly identified nine known MCPyV ST interactors (blue). Out of the 135 identified potential MCPyV ST interactors, eight were selected for further analysis for their role in transformation by MCPyV ST (red). Validation co-immunoprecipitation experiments were performed by co-transfecting HA tagged binding partners with MCPyV ST in 293A cells. Potential binding partners were pulled down with anti-HA conjugated beads, and immunoblotted for MCPyV ST.

Since TurboID has never been utilized as a method to identify MCPyV ST cellular interactors, we first investigated whether TurboID identified known ST cellular interactors [142]. Together, both TurboID experiments identified a total of 18 already known MCPyV ST interactors, 9 of which were significantly enriched in the ST expressing HFFs (Fig. 22C-E, blue highlight). The first TurboID experiment (TurboID #1) comparing HFFs expressing TID-ST and TID-GFP-NLS identified a total of 635 proteins, 121 of which were enriched in ST expressing HFFs defined as a False Discovery Rate (FDR) <0.01 and Fold Change (FC) >2 (Fig. 22B and C). TurboID #2 comparing TID-ST and TID identified a total of 674 proteins, with 34 proteins found to be enriched in the ST expressing HFFs (Fig. 22B and D). Twenty potential MCPyV ST cellular interactors were found to overlap between TurboID #1 and #2 (Fig. 22B and E).

The identification of several well-known MCPyV ST interactors validated the reliability of TurboID as a method to identify novel MCPyV ST cellular interactors. Out of 135 potential MCPyV ST cellular interactors, 126 have yet to be characterized in the literature. In an effort to identify potential MCPyV ST interactors that may play a role in transformation by MCPyV ST, the remaining 126 TurboID identified MCPyV ST interactors were analyzed for proteins that could predictively be responsible for the robust transforming capacity of MCPyV ST, such as known oncoproteins, tumor suppressors, transcription factors, etc.. Eight of the TurboID identified potential MCPyV ST interactors were selected for further investigation, as these proteins are known to be associated with

cancer, and may be bound and targeted by MCPyV ST leading to transformation and the development of MCC (Fig. 22C-E, red highlight).

Because TurboID is a proximity-dependent mediated biotinylation identification method, the amount of noise in the system is generally higher than with other mass spectrometry approaches. In an effort to lessen the background noise the TurboID experiment was performed twice with two different controls, and potential MCPyV ST interactors were limited to proteins identified with a FDR<0.01 and FC>2 when comparing HFFs expressing MCPyV ST to the control. However, it is still possible that a proportion of the 135 TurboID identified MCPyV ST interactors do not indeed interact with MCPyV ST, rather are false positives. For these reasons, validation co-immunoprecipitation experiments were performed to confirm the direct interaction. All eight potential MCPyV ST interactors identified through TurboID were cloned into the transfectable vector pCDNA3.1(+) with an N-terminal HA-tag, and co-expressed individually in 293A cells with MCPyV ST. The potential binding partners were pulled down from whole cellular lysates using HA antibody conjugated beads, and the co-immunoprecipitates were immunoblotted for MCPyV ST. Surprisingly, MCPyV ST co-immunoprecipitated with the majority of TurboID identified potential interactors, in addition to the positive control PP2A (Fig. 22F). Therefore, TurboID successfully identified several novel MCPyV ST interactors with potential roles in transformation by MCPyV ST.

5.2.1.2 IDENTIFICATION OF PATHWAYS PERTURBED BY MCPYV ST EXPRESSION IN HFFS

We next sought to identify MCPyV ST confirmed cellular interactors with downstream consequences that may result in cellular transformation. Most cellular pathways result in known downstream transcriptional changes. Therefore, transcriptional aberrations downstream of the TurboID identified MCPyV ST binding partners were assessed in HFFs expressing MCPyV ST by

A)

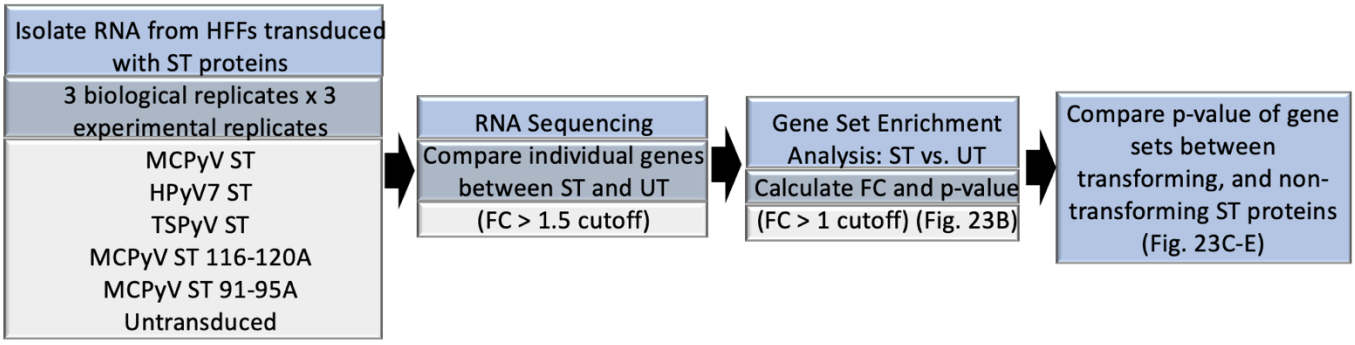
Isolate RNA from HFFs transduced with ST proteins
3 biological replicates x 3 experimental replicates
MCPyV ST
HPyV7 ST
TSPyV ST
MCPyV ST 116-120A
MCPyV ST 91-95A
Untransduced
RNA Sequencing
Compare individual genes between ST and UT
(FC > 1.5 cutoff)
Gene Set Enrichment Analysis: ST vs. UT
Calculate FC and p-value
(FC > 1 cutoff) (Fig. 23B)
Compare p-value of gene sets between transforming, and non-transforming ST proteins (Fig. 23C-E)

B)

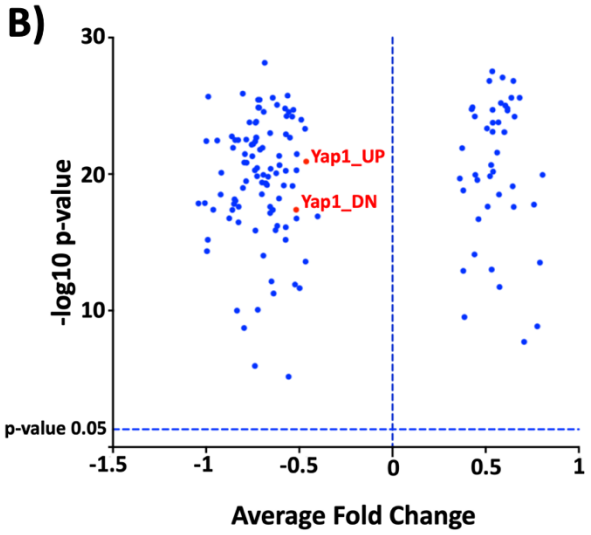
-log10 p-value
Yap1_UP
Yap1_DN
p-value 0.05
Average Fold Change

C)

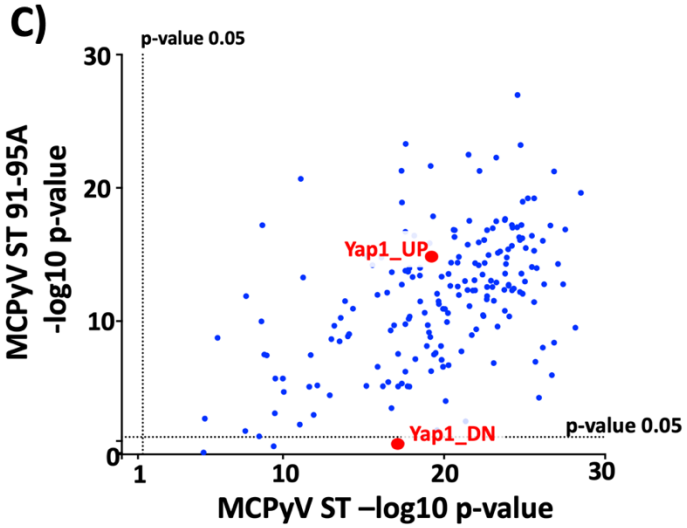
p-value 0.05
MCPyV ST 91-95A -log10 p-value
Yap1_UP
Yap1_DN
p-value 0.05
MCPyV ST –log10 p-value

D)

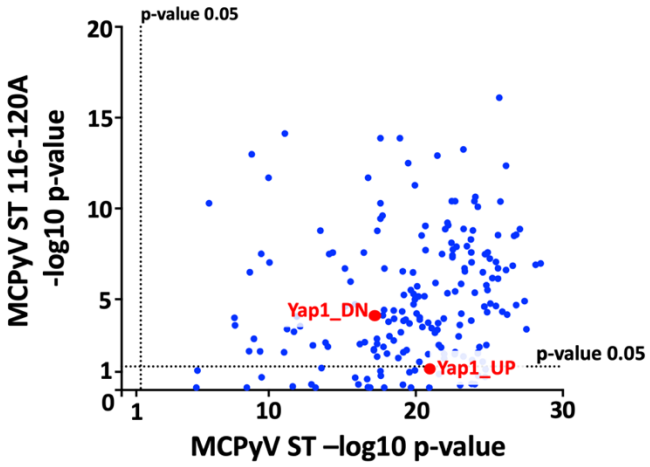
p-value 0.05
MCPyV ST 116-120A -log10 p-value
Yap1_DN
Yap1_UP
p-value 0.05
MCPyV ST –log10 p-value

E)

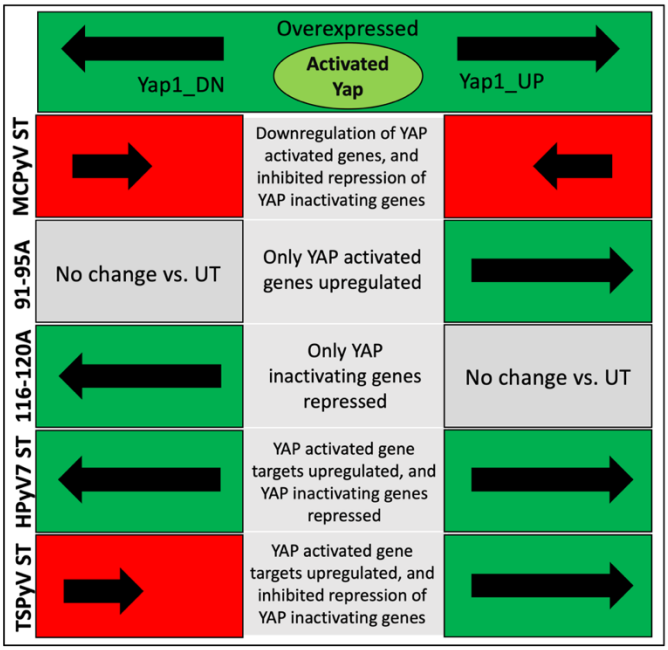
Overexpressed
Activated Yap
Yap1_DN
Yap1_UP
MCPyV ST
Downregulation of YAP activated genes, and inhibited repression of YAP inactivating genes
91-95A
No change vs. UT
Only YAP activated genes upregulated
116-120A
Only YAP inactivating genes repressed
No change vs. UT
HPyV7 ST
YAP activated gene targets upregulated, and YAP inactivating genes repressed
TSPyV ST
YAP activated gene targets upregulated, and inhibited repression of YAP inactivating genes

Figure 23. YAP target genes are deregulated in MCPyV ST expressing HFFs. Next generation RNA sequencing and gene set enrichment analysis (GSEA) was performed on RNA isolated from HFFs transduced with the transforming and non-transforming ST proteins (A). GSEA was performed for all individual genes with a FC>1.5 relative to the untransduced control. Differentially expressed gene sets within the oncogenic signatures (C6) collection were plotted by their p-value and average fold change for MCPyV ST expressing HFFs versus untransduced. Both Yap1_UP and Yap1_DN gene sets were found to be significantly downregulated in MCPyV ST expressing HFFs (B). P-values of the gene sets within the oncogenic signatures (C6) collection were compared between the non-transforming ST proteins and untrausduced HFFs. Both MCPyV MCPyV ST 91-95A, MCPyV ST116-120, HPyV7 ST and TSPyV ST were found to differentially regulate YAP target gene expression compared to MCPyV ST (B-E).

next generation RNA sequencing. Additionally, transcriptional changes of HFFs expressing the non-transforming MCPyV ST mutants (91-95A and 116-120A), or non-transforming HPyV ST proteins (HPyV7 ST and TSPyV ST), were also included in the analysis as tools to identify unique MCPyV ST perturbed pathways, or pathway perturbations that could be attributed to amino acids 91-95 and/or 116-120 (Fig. 23A).

Three biological replicates were created by transducing HFFs isolated from three independent donors with the transforming MCPyV ST, non-transforming MCPyV ST 91-95A, MCPyV ST 116-120A, HPyV7 ST, or TSPyV ST, or untransduced HFF control. RNA from each of these transduced HFFs were isolated and processed as an additional three experimental replicates, amounting to nine samples per ST transduced when accounting for both biological and experimental replicates. Next generation RNA sequencing was performed to compare individual gene expression levels between normal HFFs and those expressing the transforming or non-transforming ST proteins. Individual genes that were found to have a FC>1.5 in the ST expressing cells compared to untransduced were further analyzed by gene set enrichment analysis (GSEA), which was used to organize the data of individual genes into common sets or pathways. Individual genes with a FC>1.5 were grouped for hallmark gene sets (H), transcription factor targets (TFT), cancer gene neighborhoods (CGN), cancer modules (CM), and oncogenic signatures (C6) within the MSigDB collections. Gene sets within the oncogenic signatures (C6) collection that were significantly up- or down-regulated by MCPyV ST expression were plotted against their fold change and p-value.

Interestingly, MCPyV ST expression led to the downregulation of both YAP upregulated and downregulated genes (Yap1_DN and Yap1_UP) (Fig. 23B). When YAP, a potent transcriptional co-activator, is overexpressed in cells, a group of genes are found to be downregulated (Yap1_DN) and a group of genes are found to be upregulated (Yap1_UP). Expression of MCPyV ST repressed both Yap1_DN and Yap1_UP gene sets, suggesting MCPyV ST may inactivate YAP mediated transcription.

The p-values of gene sets significantly deregulated between MCPyV ST and untransduced expressing HFFs were further compared to the non-transforming ST expressing HFFs in an effort to identify gene sets and/or pathways that are unique to MCPyV ST or amino acids 91-95 and 116-120. Surprisingly, the deregulation of many gene sets was dependent on amino acids 91-95 and/or 116-120 of MCPyV ST, consistent with these domains being responsible for transformation by MCPyV ST. Unlike MCPyV ST which downregulated all YAP gene targets, expression of the non-transforming MCPyV ST 91-95A mutant led to no significant change in YAP downregulated genes, but increased expression of YAP upregulated genes; whereas the non-transforming MCPyV ST 116-120A mutant had the opposite effect YAP mediated gene expression (Fig. 23C and D). Together, these data suggest that both 91-95 and 116-120 may be responsible for targeting individual arms of YAP gene expression inactivation phenotype observed by MCPyV ST. Furthermore, in addition to YAP target genes, many gene sets were found to be uniquely deregulated by the transforming MCPyV ST, and not the non-transforming HPyV7 and TSPyV ST proteins (Fig. 23E). Together, these data suggest that MCPyV ST may uniquely target YAP, or a cellular component upstream of YAP, leading to repression of YAP gene expression.

5.2.2 ELUCIDATING THE ROLE OF YAP IN MCPYV ST MEDIATED CELLULAR TRANSFORMATION

5.2.1.1 MCPYV ST PERTURBS YAP LOCALIZATION AND PHOSPHORYLATION

YAP activity is regulated by three major factors: 1) the confluence of cells, 2) the subcellular localization of YAP, and 3) the phosphorylation status of YAP [143-145]. Briefly, in low confluence cells, YAP localizes to the nucleus in an unphosphorylated form, and interacts with transcription factors that induce transcription of genes important for cellular proliferation. In high confluence cells, YAP is localized to the cytoplasm in a phosphorylated form which leads to its proteasomal degradation or sequestration, ultimately inhibiting expression of genes responsible for cell cycle progression. Since YAP target gene expression was found to be deregulated in HFFs expressing MCPyV ST, and YAP was found to be an interactor of MCPyV ST, we next sought to further define the possible mechanism and role MCPyV ST perturbation of YAP may play in cellular transformation.

We first sought to determine whether MCPyV ST expression affects YAP subcellular localization by cell fractionation western blot. HFFs were plated at high and low confluency, both with and without MCPyV ST expression, and the amount of YAP in each subcellular fraction was compared for each condition. As expected, in low confluence HFFs, YAP primarily localized to the nucleus in low confluence cells, and to the cytoplasm in high confluence cells (Fig. 24A and B, lanes 2 and 3). Interestingly, expression of MCPyV ST in high confluence cells did not alter the proportion of YAP in the cytoplasm and nucleus; however, expression of MCPyV ST in low confluence cells led to an increase in cytoplasmic localization of YAP (Fig. 24A and B, lanes 2, 3, 6 and 7). Together, these data suggest MCPyV ST to preferentially localize YAP to the cytoplasm rather than the nucleus.

In addition to subcellular localization, YAP activity is also defined by its phosphorylation status. YAP can be phosphorylated at many residues, leading to either proteasomal degradation, or cytoplasmic sequestration, both of which can be thought of as inactivating phosphorylations as this

prevents nuclear localization of YAP and reduces induction of cell cycle progression gene expression [88, 143-145]. Namely, phosphorylation at S109 and S127 are important for suppressing YAP oncogenic activity, and nucleo-cytoplasmic shuttling. HFFs expressing MCPyV ST were plated at high and low confluence both with and without MCPyV ST expression. As expected, phosphorylation of YAP S109 and S127 increased in high confluence cells (Fig. 24C, lanes 1 and 3). However, expression of MCPyV ST decreased the amount of phosphorylated YAP in high confluence cells. Together, this suggests that MCPyV ST preferentially localizes YAP to the cytoplasm in an unphosphorylated, or stable, form.

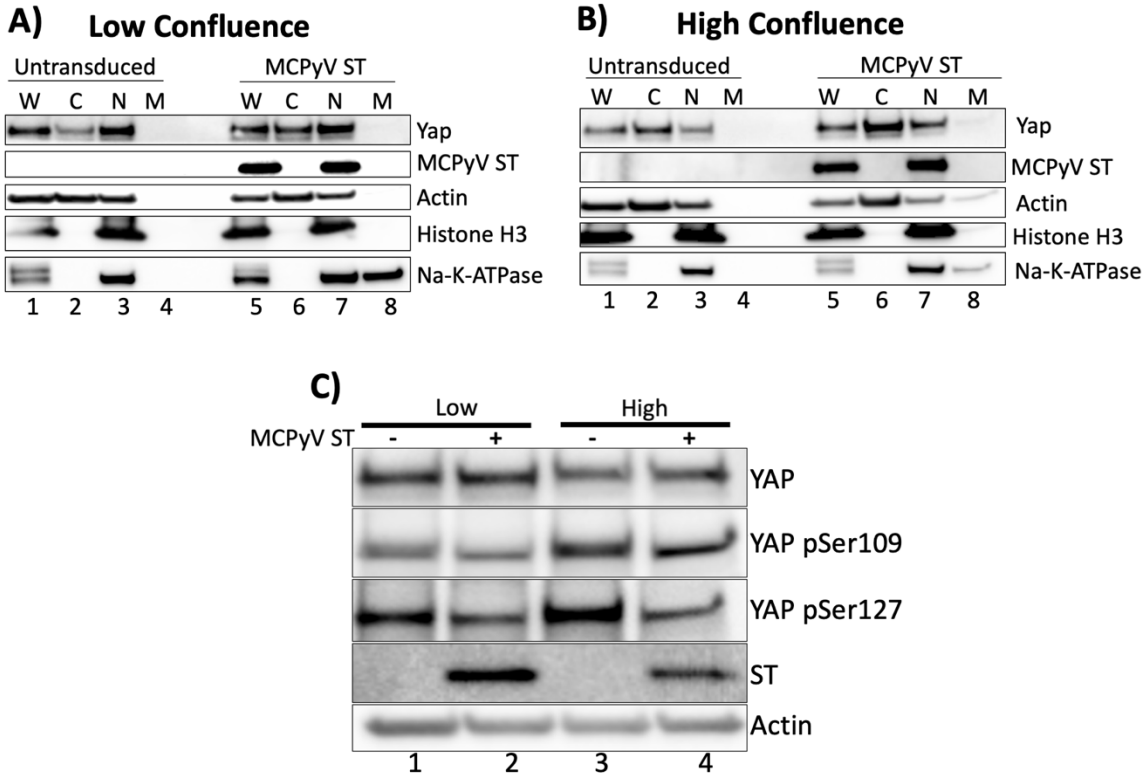

Figure 24. MCPyV ST alters the localization and phosphorylation status of YAP. YAP localization was assessed by a cell fractionation western blot in HFFs plated at low and high confluence both with and without MCPyV ST. YAP and MCPyV ST protein levels were assessed in the whole cell lysate (W), cytoplasmic fraction (C), nuclear fraction (N), and membrane (M). Actin immunoblotting was used to confirm cytoplasmic fractions. Histone H3 immunoblotting was used to confirm nuclear fractions. Na-K-ATPase immunoblotting was used to confirm membrane fractions. (A and B). YAP phosphorylation was also assessed in HFFs plated at high and low confluence both with and without MCPyV ST (C).

5.3 CONCLUSIONS AND FUTURE DIRECTIONS

Identification of ST as the robust and dominant transforming TAg of MCPyV makes further investigation into the binding partners and perturbed pathways paramount in our understanding of MCPyV mediated transformation and tumorigenesis. Previous investigation into the binding partners of MCPyV ST have proven unrewarding as no binding partners identified can account for the robust transforming capacity of MCPyV ST. For these reasons, we implemented a more modern mass spectrometry approach capable of identifying transient cellular interactors called TurboID. TurboID was utilized in relevant primary HFFs, which are transformed through MCPyV ST expression and a more relevant cell line than those used in previous mass spectrometry attempts. Through this approach, we successfully identified 8 novel MCPyV ST interactors with well-known associations to cancer development.

Although it is important to identify MCPyV ST interactors, our main priority is to identify protein-protein interactions with downstream consequences that result in cellular transformation. Next generation RNA sequencing and gene set enrichment analysis was performed to narrow down the list of MCPyV ST interactors to those with associated downstream consequences that could result in cellular transformation. Indeed, ST expression in HFFs led to transcriptional perturbations of a wide range of cellular processes and pathways connected to transformation and tumorigenesis, including YAP. The observed YAP transcriptional perturbations were unique to MCPyV ST, and not found to be a result of HPyV7 or TSPyV ST expression, making YAP a candidate for the unique MCPyV ST target responsible for transformation. Furthermore, these YAP transcriptional perturbations may be attributed to functions of the 91-95 and/or 116-120 domains, as mutation of these domains ablated the MCPyV ST mediated YAP transcriptional perturbations.

The decision to pursue YAP as a potential MCPyV ST binding partner important for transformation was based on several lines of evidence. First, both TurboID experiments identified

YAP as a novel MCPyV ST cellular interactor, increasing the validity of this interaction. In addition, TurboID also identified two known YAP interactors as potential MCPyV ST interactors: TAZ and AMOT, suggesting that binding of MCPyV ST to YAP may be part of a larger complex. YAP, TAZ and AMOT were also subsequently confirmed to interact with MCPyV ST in validation co-immunoprecipitation experiments.

The identification and validation of YAP as a MCPyV ST cellular interactor was exciting as YAP is a transcriptional co-activator with well-known association in the development of cancer. The canonical mechanism of YAP in the development of cancer most commonly can be attributed to untimely localization of YAP to the nucleus, leading to activation of transcription of genes important for cell cycle progression even when the cells are confluent. For these reasons, we were excited to find YAP target genes to be deregulated upon MCPyV ST expression, suggesting a downstream consequence of the interaction between MCPyV ST and YAP. To determine whether the interaction between YAP and MCPyV ST is necessary for transformation, soft agar analysis of YAP knockdown in HFFs expressing MCPyV ST are currently being conducted.

Over the past six years it has been found that perturbation of YAP appears to be a common mechanism of transformation by small DNA tumor viruses including SV40, adenovirus, MuPyV, and Human papilloma virus [91, 92, 94, 146, 147]. Although the mechanism by which all these small DNA tumor viruses perturb YAP differs, the downstream consequence of cellular transformation is similar in each case. For example, both MuPyV MT and ST, the two TAgs of MuPyV responsible for cellular transformation and tumor development, are capable of interacting with YAP through R103 (Fig. 25A). Excitingly, MCPyV ST contains a homologous arginine at position 102. Furthermore, it appears that MCPyV ST and MuPyV ST and MT contain a homologous domain surrounding R103 (RFCR), suggesting that this entire RFCR domain could be responsible for binding of YAP to these TAgs. Consistently, the two non-transforming HPyV ST proteins do not

contain R103 or the RFCR domain, which could explain the inability of these TAgs to transform HFFs (Fig. 25A). Currently, it is being investigated whether an MCPyV ST R102A mutant is capable of interacting with YAP, and is transforming in soft agar, doubling time, and saturation density assays.

Earlier, it was described that mutation of amino acids 91-95 or 116-120 ablated transformation by MCPyV ST. Therefore, we were interested spatially where these domains were located relative to the YAP binding RFCR domain. At the amino acid level the RFCR domain is

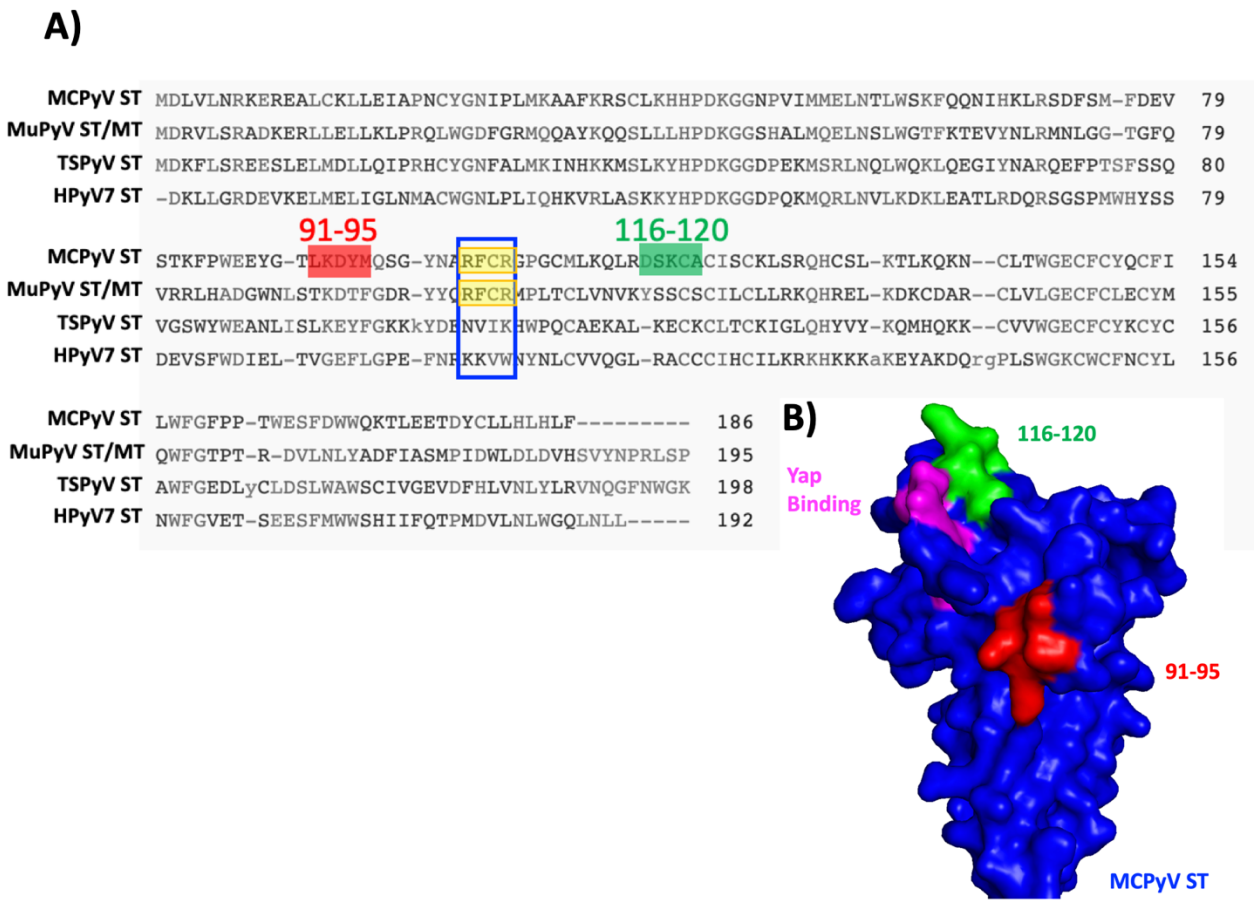

Figure 25. The YAP binding domain found in MuPyV ST and MT is conserved in MCPyV ST, but not HPyV7 and TSPyV ST. MuPyV MT and ST contain the same N-terminal amino acid sequence. MT and ST are known to interact with YAP through R103. Likewise, the transforming MCPyV ST contains R102, and also the domain surrounding the arginine (RFCR). This YAP binding domain is not conserved in TSPyV or HPyV7 ST antigens (A). At the amino acid level, the amino acids necessary for transformation, 91-95 and 116-120, are equally spaced around the RFCR domain; however, at the structural level, the YAP binding domains is in close proximity with amino acids 116-120 (B).

approximately equally space in-between the amino acids 91-95 and 116-120; however, at the structural level the RFCR domain directly interacts with amino acids 116-120 (Fig. 25B). Therefore, it is plausible that mutation of the 116-120 domain could causes structural disruptions in the RFCR domain. If so, the 116-120A mutant may actually be a YAP binding mutant, and therefore could explain why amino acids 116-120 are necessary, but not sufficient for transformation. Current studies are investigating the hypothesis of the 116-120A mutant as being a YAP binding mutant. In addition, a role of amino acids 91-95 in YAP binding is also being investigated. The unique conservation of the RFCR domain in the transforming MCPyV ST, but not the non-transforming HPyV7 and TSPyV ST proteins, could explain the unique transforming capacity of MCPyV ST compared to the ST antigen of other HPyVs. Therefore, current studies also include assessing whether the non-transforming HPyV7 and TSPyV ST proteins are capable of interacting with YAP, in addition to 'RFCR Swap' experiments to see if the RFCR YAP binding domain is both necessary and sufficient for transformation.

The perturbation of YAP by MuPyV MT and ST is several fold. First, MuPyV ST binds YAP and PP2A, leading to the dephosphorylation of YAP and subsequent stabilization and nuclear localization [92]. Although we likewise found MCPyV ST to lead to hypophosphorylated YAP, it is unlikely that this is through PP2A, as mutation of PP2A does not ablate transformation by MCPyV ST; however, it remains to be tested whether MCPyV ST mediated hypophosphorylation of YAP is dependent on PP2A binding. MuPyV MT perturbation of YAP is bimodal through direct interaction and activation of signaling pathways [94, 146]. MuPyV MT signaling through Src leads to YAP hyperphosphorylation, cytoplasmic localization, and degradation. MuPyV MT accounts for this by dephosphorylating YAP through PP2A binding. The binding of MT to YAP also leads to the localization of YAP to membranes, which is important for the contribution of YAP in transformation by MuPyV MT. As the localization of YAP to the membranes is contrary to the

known mechanism of YAP and cancer, this suggests that YAP promotes MT transformation via mechanisms that depart from YAP's canonical oncogenic transcriptional activation functions. We likewise found MCPyV ST to localize YAP to the cytoplasm in an unphosphorylated form, similar to MuPyV MT. Furthermore, these results are consistent with the next generation RNA sequencing data, in which YAP target genes were downregulated. These similar findings are comforting, as an oncogenic role for YAP in the cytoplasm has yet to be appreciated, and therefore opens the door for identification of a YAP transformation mechanism that departs from its known oncogenic functions.

The localization of YAP to the cytoplasm is reminiscent of another identified MCPyV ST cellular interactor: AMOT. AMOT is a more recently appreciated component of the Hippo pathway that has been found to inhibit YAP through phosphorylation-induced cytoplasmic retention and degradation [148]. AMOT is located at tight junction between cells, and also plays an important role in cell contact-inhibition. Therefore, it is plausible that the cytoplasmic localization of YAP by MCPyV ST may be connected to AMOT.

There is a great need for novel, efficacious therapies to treat MCC. The targeting of MCPyV TAg mechanisms necessary for tumorigenesis, such as YAP, could provide a specific, low off-target, and efficacious treatment for MCC. Currently, there are many known YAP-specific drugs that target various aspects, roles, and interactions necessary for the function of YAP in cancer [149]. Upon further elucidation of the mechanisms by which MCPyV ST perturbs YAP to accomplish cellular transformation, YAP-specific drugs for treatment MCC may be explored. As most, if not all, dividing cells in the body contain an active form of YAP, it is possible that the YAP-specific drugs may not be specific to MCC tumor cells expressing MCPyV ST, but may also target other actively dividing cells of the body, similar to chemotherapy. Therefore, the development of a small molecule to disrupt the interaction between MCPyV ST and YAP may decrease side-effects and also be more

specific for treatment of VP-MCC tumor cells. Upon proving that the interaction between MCPyV ST and YAP is vital for its transforming functions, a small molecule may be designed to bind to the face of MCPyV ST responsible for interacting with YAP, thereby disrupting the interaction. Since this small molecule would be designed to interact with MCPyV ST, its effects would be limited to cells expressing MCPyV ST, thereby decreasing potential side-effects. Furthermore, some cases of MCC have been found to be chemotherapy and/or immunotherapy resistant [99, 100]. As YAP has been implicated in causing both chemo- and immunotherapy resistance it is plausible that YAP-specific drugs or small molecule inhibitors may be used in combination with chemotherapy and/or immunotherapy [150]. Such combination therapy may prove efficacious in patients who would have otherwise not responded to chemotherapy and/or immunotherapy alone. The sensitivity of MCPyV ST mediated transformation to this disruption could be assessed in *in vivo* tumorigenesis assays, as well as MCC cell lines. Further, as various mutations that perturb the Hippo/YAP pathway in VN-MCC may be vital for the viability of these tumors, these studies may benefit both VP- and VN-MCC treatment.

Although many lines of evidence encourage further investigation into YAP, TAZ, and AMOT, it is important to remember that in addition to these 3 complex proteins, 5 other proteins were identified as MCPyV ST interactors with known associations to cancer. The ability of MCPyV ST to transform primary HFFs without additional cellular perturbations speaks to the strength of ST as a viral oncoprotein. Therefore, it is possible, if not likely, that MCPyV ST perturbs many pathways resulting in cellular transformation and tumorigenesis in addition to YAP. For these reasons, the investigation of the additional novel TurboID identified MCPyV ST binding partners is also of great interest.

Herein we described several lines of evidence that suggest MCPyV ST may be transforming through perturbation of YAP. Interestingly, the mechanism by which YAP is perturbed to

accomplish cellular transformation departs from the canonical mechanism of YAP and cancer; however, similar findings have been observed for MuPyV TAgs. Therefore, delineation of the mechanism by which MCPyV ST perturbs YAP functions resulting in transformation could prove vital in the development of targeted MCC therapeutics and in increasing our understanding of YAP cellular functions.

CHAPTER 6. CONCLUDING REMARKS AND FUTURE DIRECTIONS

The road to defining and understanding Merkel cell carcinoma has been winding, but also filled with many breakthroughs that inspire hope in treating this aggressive disease. Thirty-two years after the discovery and characterization of MCC, it was found that unlike other skin cancers, only 20% of MCC cases are caused by UV damage [17]. Contrarily, the majority of MCC cases (80%) are uniquely caused by the integration of MCPyV into the host genome of these tumors, and expression of the viral tumor antigens [151]. The dependency of VP-MCC on the expression of the MCPyV TAgs provides a unique and specific target to treat this aggressive disease, and therefore research into elucidating mechanisms of MCPyV driven transformation and tumorigenesis is paramount for the development of efficacious therapies.

Although MCPyV was discovered to be the etiologic agent of VP-MCC 12 years ago, our understanding of the mechanisms of transformation and tumorigenesis are still limited. This can be attributed to the absence of a relevant assay to assess the transformation capacity of the MCPyV TAgs, and the use of irrelevant methods and approaches. In this dissertation, we aimed to successfully elucidate mechanisms of transformation and tumorigenesis of MCPyV ST through 1) the creation of a relevant transformation assay, 2) stronger methodology, and 3) alternative approaches.

Our successful development of a novel, robust, and relevant transformation assay was based on the 2016 identification of human dermal fibroblasts as a probable host cell for natural MCPyV infection [30]. Although we found fibroblasts to be readily transformed by the expression of MCPyV ST, we do not see this finding as evidence to convincingly support fibroblasts as the progenitor cell of MCC; however, this finding does provide a powerful and more relevant tool to identify and investigate mechanisms of transformation by MCPyV TAgs.

There have been several methods employed in an effort to determine the mechanisms of transformation and tumorigenesis by MCPyV. One such method is based on the investigation and comparison of domains and mechanisms of transformation by other oncogenic polyomaviruses, such as SV40. Comparisons like these are responsible for the many years spent investigating MCPyV ST binding to PP2A, which has been found to be irrelevant for transformation by MCPyV ST [27, 82, 152]. Furthermore, comparisons between MCPyV and SV40 are behind the long-standing MCPyV ST Fbw7 perturbation mechanism, which data strongly suggest are not valid [95, 96, 153]. Contrary to this method, data presented in this dissertation suggests a stronger approach to delineate mechanisms of transformation by MCPyV ST is to do the exact opposite of previous approaches. Our finding that ST is the dominant transforming protein of MCPyV is opposite to SV40, in which ST plays only a supportive or accessory role. Further, we found MCPyV ST to be unique in its transformation capacity, as the ST of other HPyVs are non-transforming. These findings suggest that a stronger approach to identify the mechanism by which MCPyV ST is transforming is to assess the differences, rather than the similarities, between MCPyV ST and other ST proteins.

A second method that has been employed to identify mechanisms of transformation and tumorigenesis by MCPyV is to study VN-MCC [101]. Both VP- and VN-MCC tumors are identical, although the origin and mechanism of development of either VP- or VN-MCC varies dramatically. Therefore, others have hypothesized that the identification of common mutations in VN-MCC

would elucidate proteins and pathways perturbed by MCPyV TAgs leading to the development of VP-MCC. Although clever, this approach unfortunately has been lessfruitful. VN-MCC has the highest mutational burden of any cancer sequenced by the cancer genome atlas [26]. This makes it extremely difficult to distinguish between mutations necessary for the development of MCC and noise and is therefore not as informative as anticipated. Instead of using our understanding of VN-MCC to delineate the mechanisms of MCPyV TAgs in VP-MCC, I believe the opposite approach would prove more influential. By elucidating how MCPyV TAgs lead to the development of VP-MCC, this will deconvolute the slurry of mutations present in VN-MCC to the mutated pathways that are responsible for the development of VN-MCC. In addition, this approach may also prove influential in the development of novel therapeutics to treat both VP- and VN-MCC, as the targeting of central pathways responsible for the development of MCC, either perturbed by viral TAgs or mutations, may kill the tumor cells.

The findings presented in this dissertation have unequivocally proven the strength of these approaches. The utilization of a modern, more sensitive, mass spectrometry approach identified 8 cellular proteins, with known ties to cancer development, as MCPyV ST cellular interactors. One such binding partner, YAP, gained particular attention as YAP target genes were found to be deregulated specifically upon MCPyV ST expression, and not through the expression of the non-transforming ST mutants on HPyV ST proteins. This was exciting because not only is YAP a known cellular oncoprotein, but perturbation of YAP has also recently been implicated as a means of transformation by other oncogenic polyomaviruses such as SV40 and MuPyV, in addition to other small DNA tumor viruses including HPV and adenovirus [91, 92, 94, 146, 147]. Initially, our preliminary data finding MCPyV ST expression to relocalize YAP to the cytoplasm in an unphosphorylated form was perplexing, as this is contrary to the canonical mechanism of YAP mediated transformation [88, 143, 145]. However, upon finding that similar discoveries have been

reported by others for MT of MuPyV, this suggests that a subset of polyomaviruses may have evolved a novel mechanism of YAP perturbation that has not yet been described [146]. Novel cellular and molecular findings are not uncommon in polyomavirus research. For example, two potent tumor suppressors, Rb and p53 were identified through the studies of MuPyV and SV40, respectively [68, 80]. Therefore, the study of MCPyV ST may uncover additional cellular functions of YAP, that may also be targetable in both VP- and VN-MCC.

In conclusion, the novel assays, methods, and approaches pursued in this dissertation have enabled us to identify novel mechanisms of transformation by MCPyV ST. Additionally, these studies have laid the groundwork to gain additional insight into the function of YAP in the cell. Most importantly, the findings made possible through the utilization of the novel assays, methods, and approaches described in this dissertation have made great strides towards our goal of developing novel, targeted, efficacious therapeutics for the treatment of both VP- and VN-MCC.

REFERENCES

1. Becker J. Merkel cell carcinoma. Annals of Oncology. 2010;21(suppl_7):vii81-vii5.
2. Toker C. Trabecular carcinoma of ihe skin. Arch Dermatol. 1972;105:107-10.
3. Tang CK, Toker C. Trabecular carcinoma of the skin. An ultrastructural study. Cancer. 1978;42(5):2311-21.
4. Toker C. Trabecular carcinoma of the skin: a question of title. The American Journal of Dermatopathology. 1982;4(6):497-500.
5. Rywlin A. Malignant Merkel-cell tumor is a more accurate description than trabecular carcinoma. The American Journal of Dermatopathology. 1982;4(6):513-6.
6. Agelli M, Clegg LX, Becker JC, Rollison DE. The etiology and epidemiology of merkel cell carcinoma. Current problems in cancer. 2010;34(1):14-37.
7. Moshiri AS, Nghiem P. Milestones in the staging, classification, and biology of Merkel cell carcinoma. Journal of the National Comprehensive Cancer Network. 2014;12(9):1255-62.
8. Hodgson NC. Merkel cell carcinoma: changing incidence trends. Journal of surgical oncology. 2005;89(1):1-4.
9. Fitzgerald TL, Dennis S, Kachare SD, Vohra NA, Wong JH, Zervos EE. Dramatic increase in the incidence and mortality from Merkel cell carcinoma in the United States. The American surgeon. 2015;81(8):802-6.
10. Reichgelt B, Visser O. Epidemiology and survival of Merkel cell carcinoma in the Netherlands. A population-based study of 808 cases in 1993–2007. European journal of cancer. 2011;47(4):579-85.
11. Lyhne D, Lock-Andersen J, Dahlstrøm K, Drzewiecki K, Balslev E, Muhic A, et al. Rising incidence of Merkel cell carcinoma. Journal of plastic surgery and hand surgery. 2011;45(6):274-80.
12. Tejera-Vaquerizo A, Descalzo-Gallego M, Otero-Rivas M, Posada-García C, Rodríguez-Pazos L, Pastushenko I, et al. Skin cancer incidence and mortality in Spain: a systematic review and meta-analysis. Actas Dermo-Sifiliográficas (English Edition). 2016;107(4):318-28.
13. Paulson KG, Park SY, Vandeven NA, Lachance K, Thomas H, Chapuis AG, et al. Merkel cell carcinoma: Current US incidence and projected increases based on changing demographics. Journal of the American Academy of Dermatology. 2018;78(3):457-63. e2.
14. Veness M, Harris D. Role of radiotherapy in the management of organ transplant recipients diagnosed with non-melanoma skin cancers. Australasian radiology. 2007;51(1):12-20.
15. Garrett GL, Blanc PD, Boscardin J, Lloyd AA, Ahmed RL, Anthony T, et al. Incidence of and risk factors for skin cancer in organ transplant recipients in the United States. JAMA dermatology. 2017;153(3):296-303.
16. Wong SQ, Waldeck K, Vergara IA, Schröder J, Madore J, Wilmott JS, et al. UV-associated mutations underlie the etiology of MCV-negative Merkel cell carcinomas. Cancer research. 2015;75(24):5228-34.
17. Feng H, Shuda M, Chang Y, Moore PS. Clonal integration of a polyomavirus in human Merkel cell carcinoma. Science. 2008;319(5866):1096-100.

18. Engels EA, Frisch M, Goedert JJ, Biggar RJ, Miller RW. Merkel cell carcinoma and HIV infection. The Lancet. 2002;359(9305):497-8.
19. Gooptu C, Woollons A, Ross J, Price M, Wojnarowska F, Morris P, et al. Merkel cell carcinoma arising after therapeutic immunosuppression. British Journal of Dermatology. 1997;137(4):637-41.
20. Lanoy E, Engels EA. Skin cancers associated with autoimmune conditions among elderly adults. British journal of cancer. 2010;103(1):112-4.
21. Clarke CA, Robbins HA, Tatalovich Z, Lynch CF, Pawlish KS, Finch JL, et al. Risk of merkel cell carcinoma after solid organ transplantation. Journal of the National Cancer Institute. 2015;107(2):dju382.
22. Shuda M, Feng H, Kwun HJ, Rosen ST, Gjoerup O, Moore PS, et al. T antigen mutations are a human tumor-specific signature for Merkel cell polyomavirus. Proceedings of the National Academy of Sciences. 2008;105(42):16272-7.
23. Becker M, Dominguez M, Greune L, Soria-Martinez L, Pfleiderer MM, Schowalter R, et al. Infectious entry of Merkel cell polyomavirus. Journal of virology. 2019;93(6):e02004-18.
24. Carter JJ, Daugherty MD, Qi X, Bheda-Malge A, Wipf GC, Robinson K, et al. Identification of an overprinting gene in Merkel cell polyomavirus provides evolutionary insight into the birth of viral genes. Proceedings of the National Academy of Sciences. 2013;110(31):12744-9.
25. DeCaprio JA. Merkel cell polyomavirus and Merkel cell carcinoma. Philosophical Transactions of the Royal Society B: Biological Sciences. 2017;372(1732):20160276.
26. Goh G, Walradt T, Markarov V, Blom A, Riaz N, Doumani R, et al. Mutational landscape of MCPyV-positive and MCPyV-negative Merkel cell carcinomas with implications for immunotherapy. Oncotarget. 2016;7(3):3403.
27. Shuda M, Kwun HJ, Feng H, Chang Y, Moore PS. Human Merkel cell polyomavirus small T antigen is an oncoprotein targeting the 4E-BP1 translation regulator. The Journal of clinical investigation. 2011;121(9).
28. Sunshine J, Jahchan N, Sage J, Choi J. Are there multiple cells of origin of Merkel cell carcinoma? Oncogene. 2018;37(11):1409-16.
29. Tilling T, Moll I. Which are the cells of origin in merkel cell carcinoma? Journal of skin cancer. 2012;2012.
30. Liu W, Yang R, Payne AS, Schowalter RM, Spurgeon ME, Lambert PF, et al. Identifying the target cells and mechanisms of Merkel cell polyomavirus infection. Cell host & microbe. 2016;19(6):775-87.
31. Lemasson G, Coquart N, Lebonvallet N, Boulais N, Galibert M-D, Marcorelles P, et al. Presence of putative stem cells in Merkel cell carcinomas. Journal of The European Academy of Dermatology and Venereology. 2012;26(6):789-95.
32. Visscher D, Cooper P, Zarbo R, Crissman J. Cutaneous neuroendocrine (Merkel cell) carcinoma: an immunophenotypic, clinicopathologic, and flow cytometric study. Modern pathology: an official journal of the United States and Canadian Academy of Pathology, Inc. 1989;2(4):331-8.
33. zur Hausen A, Rennspiess D, Winnepenninckx V, Speel E-J, Kurz AK. Early B-cell differentiation in Merkel cell carcinomas: clues to cellular ancestry. Cancer research. 2013;73(16):4982-7.

34. Sauer C, Haugg A, Chteinberg E, Rennspiess D, Winnepenninckx V, Speel E-J, et al. Reviewing the current evidence supporting early B-cells as the cellular origin of Merkel cell carcinoma. Critical reviews in oncology/hematology. 2017;116:99-105.
35. Kolarsick PA, Kolarsick MA, Goodwin C. Anatomy and physiology of the skin. Journal of the Dermatology Nurses' Association. 2011;3(4):203-13.
36. Sidhu GS, Chandra P, Cassai ND. Merkel cells, normal and neoplastic: an update. Ultrastructural pathology. 2005;29(3-4):287-94.
37. Gross L. A filterable agent, recovered from Ak leukemic extracts, causing salivary gland carcinomas in C3H mice. Proceedings of the Society for Experimental Biology and Medicine. 1953;83(2):414-21.
38. Stewart SE, Eddy BE, Gochenour AM, Borgese NG, Grubbs GE. The induction of neoplasms with a substance released from mouse tumors by tissue culture. Virology. 1957;3(2):380-400.
39. Sweet BH, Hilleman MR. The vacuolating virus, SV 40. Proceedings of the Society for Experimental Biology and Medicine. 1960;105(2):420-7.
40. Eddy BE, Borman GS, Berkeley WH, Young RD. Tumors induced in hamsters by injection of rhesus monkey kidney cell extracts. Proceedings of the Society for Experimental Biology and Medicine. 1961;107(1):191-7.
41. Eddy BE, Borman GS, Grubbs GE, Young RD. Identification of the oncogenic substance in rhesus monkey kidney cell cultures as simian virus 40. Virology. 1962;17(1):65-75.
42. Shein HM, Enders JF. Transformation induced by simian virus 40 in human renal cell cultures, I. Morphology and growth characteristics. Proceedings of the National Academy of Sciences of the United States of America. 1962;48(7):1164.
43. Rabson AS, Kirschstein RL. Induction of malignancy in vitro in newborn hamster kidney tissue infected with simian vacuolating virus (SV40). Proceedings of the Society for Experimental Biology and Medicine. 1962;111(2):323-8.
44. Rabson AS, O'Conor GT, Kirschstein RL, Branigan WJ. Papillary Ependymomas Produced in Rattus (Masfomys) Natalensis inoculated With Vacuolating Virus (SV40). Journal of the National Cancer Institute. 1962;29(4):765-87.
45. Shah KV. SV40 and human cancer: a review of recent data. International journal of cancer. 2007;120(2):215-23.
46. Rotondo JC, Mazzoni E, Bononi I, Tognon M, Martini F. Association Between Simian Virus 40 and Human Tumors. Frontiers in oncology. 2019;9.
47. Poulin DL, DeCaprio JA. Is there a role for SV40 in human cancer? Journal of clinical oncology. 2006;24(26):4356-65.
48. Gardner S, Field A, Coleman D, Hulme B. New human papovavirus (BK) isolated from urine after renal transplantation. The Lancet. 1971;297(7712):1253-7.
49. Padgett B, Zurhein G, Walker D, Eckroade R, Dessel B. Cultivation of papova-like virus from human brain with progressive multifocal leucoencephalopathy. The Lancet. 1971;297(7712):1257-60.
50. Prado JCM, Monezi TA, Amorim AT, Lino V, Paladino A, Boccardo E. Human polyomaviruses and cancer: an overview. Clinics. 2018;73.
51. DeCaprio JA, Garcea RL. A cornucopia of human polyomaviruses. Nature reviews Microbiology. 2013;11(4):264-76.

52. Buck CB, Van Doorslaer K, Peretti A, Geoghegan EM, Tisza MJ, An P, et al. The ancient evolutionary history of polyomaviruses. PLoS pathogens. 2016;12(4).
53. Dilworth S, editor Cell alterations induced by the large T-antigens of SV40 and polyoma virus. Seminars in cancer biology; 1990.
54. Du W, Searle JS. The rb pathway and cancer therapeutics. Current drug targets. 2009;10(7):581-9.
55. Chan HM, Smith L, La Thangue NB. Role of LXCXE motif-dependent interactions in the activity of the retinoblastoma protein. Oncogene. 2001;20(43):6152-63.
56. Dyson N, Bernards R, Friend SH, Gooding L, Hassell J, Major E, et al. Large T antigens of many polyomaviruses are able to form complexes with the retinoblastoma protein. Journal of virology. 1990;64(3):1353-6.
57. Stubdal H, Zalvide J, Campbell KS, Schweitzer C, Roberts TM, DeCaprio JA. Inactivation of pRB-related proteins p130 and p107 mediated by the J domain of simian virus 40 large T antigen. Molecular and cellular biology. 1997;17(9):4979-90.
58. Sullivan CS, Cantalupo P, Pipas JM. The molecular chaperone activity of simian virus 40 large T antigen is required to disrupt Rb-E2F family complexes by an ATP-dependent mechanism. Molecular and cellular biology. 2000;20(17):6233-43.
59. Kazem S, Van Der Meijden E, Wang RC, Rosenberg AS, Pope E, Benoit T, et al. Polyomavirus-associated trichodysplasia spinulosa involves hyperproliferation, pRB phosphorylation and upregulation of p16 and p21. PLoS One. 2014;9(10).
60. Hesbacher S, Pfitzer L, Wiedorfer K, Angermeyer S, Borst A, Haferkamp S, et al. RB1 is the crucial target of the Merkel cell polyomavirus Large T antigen in Merkel cell carcinoma cells. Oncotarget. 2016;7(22):32956.
61. Houben R, Adam C, Baeurle A, Hesbacher S, Grimm J, Angermeyer S, et al. An intact retinoblastoma protein-binding site in Merkel cell polyomavirus large T antigen is required for promoting growth of Merkel cell carcinoma cells. International journal of cancer. 2012;130(4):847-56.
62. Schrama D, Hesbacher S, Angermeyer S, Schlosser A, Haferkamp S, Aue A, et al. Serine 220 phosphorylation of the M erkel cell polyomavirus large T antigen crucially supports growth of Merkel cell carcinoma cells. International journal of cancer. 2016;138(5):1153-62.
63. O'Shea CC, Fried M. Modulation of the ARF-p53 pathway by the small DNA tumor viruses. Cell Cycle. 2005;4(3):449-52.
64. Zindy F, Williams RT, Baudino TA, Rehg JE, Skapek SX, Cleveland JL, et al. Arf tumor suppressor promoter monitors latent oncogenic signals in vivo. Proceedings of the National Academy of Sciences. 2003;100(26):15930-5.
65. Lowe SW, Sherr CJ. Tumor suppression by Ink4a–Arf: progress and puzzles. Current opinion in genetics & development. 2003;13(1):77-83.
66. Mor O, Read M, Fried M. p53 in polyoma virus transformed REF52 cells. Oncogene. 1997;15(25):3113-9.
67. Lane DP, Crawford LV. T antigen is bound to a host protein in SY40-transformed cells. Nature. 1979;278(5701):261-3.
68. Linzer DI, Levine AJ. Characterization of a 54K dalton cellular SV40 tumor antigen present in SV40-transformed cells and uninfected embryonal carcinoma cells. Cell. 1979;17(1):43-52.

69. Ahuja D, Rathi AV, Greer AE, Chen XS, Pipas JM. A structure-guided mutational analysis of simian virus 40 large T antigen: identification of surface residues required for viral replication and transformation. Journal of virology. 2009;83(17):8781-8.
70. Kierstead T, Tevethia M. Association of p53 binding and immortalization of primary C57BL/6 mouse embryo fibroblasts by using simian virus 40 T-antigen mutants bearing internal overlapping deletion mutations. Journal of virology. 1993;67(4):1817-29.
71. Moule MG, Collins CH, McCormick F, Fried M. Role for PP2A in ARF signaling to p53. Proceedings of the National Academy of Sciences. 2004;101(39):14063-6.
72. Lomax M, Fried M. Polyoma virus disrupts ARF signaling to p53. Oncogene. 2001;20(36):4951-60.
73. Cheng J, Rozenblatt-Rosen O, Paulson KG, Nghiem P, DeCaprio JA. Merkel cell polyomavirus large T antigen has growth-promoting and inhibitory activities. Journal of virology. 2013;87(11):6118-26.
74. Borchert S, Czech-Sioli M, Neumann F, Schmidt C, Wimmer P, Dobner T, et al. High-affinity Rb binding, p53 inhibition, subcellular localization, and transformation by wild-type or tumor-derived shortened Merkel cell polyomavirus large T antigens. Journal of virology. 2014;88(6):3144-60.
75. Houben R, Dreher C, Angermeyer S, Borst A, Utikal J, Haferkamp S, et al. Mechanisms of p53 restriction in Merkel cell carcinoma cells are independent of the Merkel cell polyoma virus T antigens. Journal of Investigative Dermatology. 2013;133(10):2453-60.
76. Park DE, Cheng J, Berrios C, Montero J, Cortés-Cros M, Ferretti S, et al. Dual inhibition of MDM2 and MDM4 in virus-positive Merkel cell carcinoma enhances the p53 response. Proceedings of the National Academy of Sciences. 2019;116(3):1027-32.
77. Rozenblatt-Rosen O, Deo RC, Padi M, Adelmant G, Calderwood MA, Rolland T, et al. Interpreting cancer genomes using systematic host network perturbations by tumour virus proteins. Nature. 2012;487(7408):491-5.
78. Alberts AS, Thorburn AM, Shenolikar S, Mumby MC, Feramisco JR. Regulation of cell cycle progression and nuclear affinity of the retinoblastoma protein by protein phosphatases. Proceedings of the National Academy of Sciences. 1993;90(2):388-92.
79. Schönthal AH. Role of serine/threonine protein phosphatase 2A in cancer. Cancer letters. 2001;170(1):1-13.
80. Andrabi S, Hwang JH, Choe JK, Roberts TM, Schaffhausen BS. Comparisons between murine polyomavirus and Simian virus 40 show significant differences in small T antigen function. Journal of virology. 2011;85(20):10649-58.
81. Walter G, Ruediger R, Slaughter C, Mumby M. Association of protein phosphatase 2A with polyoma virus medium tumor antigen. Proceedings of the National Academy of Sciences. 1990;87(7):2521-5.
82. Rodriguez-Viciana P, Collins C, Fried M. Polyoma and SV40 proteins differentially regulate PP2A to activate distinct cellular signaling pathways involved in growth control. Proceedings of the National Academy of Sciences. 2006;103(51):19290-5.
83. Yeh E, Cunningham M, Arnold H, Chasse D, Monteith T, Ivaldi G, et al. A signalling pathway controlling c-Myc degradation that impacts oncogenic transformation of human cells. Nature cell biology. 2004;6(4):308-18.

84. Yu Y, Kudchodkar SB, Alwine JC. Effects of simian virus 40 large and small tumor antigens on mammalian target of rapamycin signaling: small tumor antigen mediates hypophosphorylation of eIF4E-binding protein 1 late in infection. Journal of virology. 2005;79(11):6882-9.
85. Ogris E, Mudrak I, Mak E, Gibson D, Pallas DC. Catalytically inactive protein phosphatase 2A can bind to polyomavirus middle tumor antigen and support complex formation with pp60c-src. Journal of virology. 1999;73(9):7390-8.
86. Wu JH, Simonette RA, Nguyen HP, Rady PL, Tyring SK. Molecular mechanisms supporting a pathogenic role for human polyomavirus 6 small T antigen: Protein phosphatase 2A targeting and MAPK cascade activation. Journal of medical virology. 2017;89(4):742-7.
87. Wu J, Narayanan D, Simonette R, Rady P, Tyring S. Dysregulation of the MEK/ERK/MNK 1 signalling cascade by middle T antigen of the trichoydsplasia spinulosa polyomavirus. Journal of the European Academy of Dermatology and Venereology. 2017;31(8):1338-41.
88. Piccolo S, Dupont S, Cordenonsi M. The biology of YAP/TAZ: hippo signaling and beyond. Physiological reviews. 2014;94(4):1287-312.
89. Ma S, Meng Z, Chen R, Guan K-L. The Hippo pathway: biology and pathophysiology. Annual review of biochemistry. 2019;88:577-604.
90. Han Y. Analysis of the role of the Hippo pathway in cancer. Journal of translational medicine. 2019;17(1):116.
91. Nguyen HT, Hong X, Tan S, Chen Q, Chan L, Fivaz M, et al. Viral small T oncoproteins transform cells by alleviating hippo-pathway-mediated inhibition of the YAP proto-oncogene. Cell reports. 2014;8(3):707-13.
92. Hwang JH, Fernando ATP, Faure N, Andrabi S, Hahn WC, Schaffhausen BS, et al. Polyomavirus small T antigen interacts with yes-associated protein to regulate cell survival and differentiation. Journal of virology. 2014;88(20):12055-64.
93. Dilworth SM, Brewster CE, Jones MD, Lanfrancone L, Pelicci G, Pelicci PG. Transformation by polyoma virus middle T-antigen involves the binding and tyrosine phosphorylation of Shc. Nature. 1994;367(6458):87-90.
94. Shanzer M, Ricardo-Lax I, Keshet R, Reuven N, Shaul Y. The polyomavirus middle T-antigen oncogene activates the Hippo pathway tumor suppressor Lats in a Src-dependent manner. Oncogene. 2015;34(32):4190-8.
95. Kwun HJ, Chang Y, Moore PS. Protein-mediated viral latency is a novel mechanism for Merkel cell polyomavirus persistence. Proceedings of the National Academy of Sciences. 2017;114(20):E4040-E7.
96. Kwun HJ, Shuda M, Feng H, Camacho CJ, Moore PS, Chang Y. Merkel cell polyomavirus small T antigen controls viral replication and oncoprotein expression by targeting the cellular ubiquitin ligase SCFFbw7. Cell host & microbe. 2013;14(2):125-35.
97. Verhaegen ME, Mangelberger D, Harms PW, Vozheiko TD, Weick JW, Wilbert DM, et al. Merkel cell polyomavirus small T antigen is oncogenic in transgenic mice. Journal of Investigative Dermatology. 2015;135(5):1415-24.
98. Kwun HJ, Chang Y, Moore PS. Protein-mediated viral latency is a novel mechanism for Merkel cell polyomavirus persistence. Proceedings of the National Academy of Sciences. 2017:201703879.

99. Harms PW, Harms KL, Moore PS, DeCaprio JA, Nghiem P, Wong MK, et al. The biology and treatment of Merkel cell carcinoma: current understanding and research priorities. Nature Reviews Clinical Oncology. 2018;15(12):763-76.
100. Nghiem PT, Bhatia S, Lipson EJ, Kudchadkar RR, Miller NJ, Annamalai L, et al. PD-1 blockade with pembrolizumab in advanced Merkel-cell carcinoma. New England Journal of Medicine. 2016;374(26):2542-52.
101. Starrett GJ, Marcelus C, Cantalupo PG, Katz JP, Cheng J, Akagi K, et al. Merkel cell polyomavirus exhibits dominant control of the tumor genome and transcriptome in virus-associated Merkel cell carcinoma. MBio. 2017;8(1):e02079-16.
102. Borowicz S, Van Scoyk M, Avasarala S, Rathinam MKK, Tauler J, Bikkavilli RK, et al. The soft agar colony formation assay. JoVE (Journal of Visualized Experiments). 2014;(92):e51998.
103. Fluck MM, Schaffhausen BS. Lessons in signaling and tumorigenesis from polyomavirus middle T antigen. Microbiol Mol Biol Rev. 2009;73(3):542-63.
104. Ahuja D, Sáenz-Robles MT, Pipas JM. SV40 large T antigen targets multiple cellular pathways to elicit cellular transformation. Oncogene. 2005;24(52):7729-45.
105. Cheng J, DeCaprio JA, Fluck MM, Schaffhausen BS, editors. Cellular transformation by simian virus 40 and murine polyoma virus T antigens. Seminars in cancer biology; 2009: Elsevier.
106. Liu W, Krump NA, MacDonald M, You J. Merkel cell polyomavirus infection of animal dermal fibroblasts. Journal of virology. 2018;92(4):e01610-17.
107. Schrama D, Hesbacher S, Angermeyer S, Schlosser A, Haferkamp S, Aue A, et al. Serine 220 phosphorylation of the Merkel cell polyomavirus large T antigen crucially supports growth of Merkel cell carcinoma cells. International journal of cancer. 2016;138(5):1153-62.
108. Kwun HJ, Shuda M, Camacho CJ, Gamper AM, Thant M, Chang Y, et al. Restricted protein phosphatase 2A targeting by Merkel cell polyomavirus small T antigen. Journal of virology. 2015;89(8):4191-200.
109. Fewell SW, Pipas JM, Brodsky JL. Mutagenesis of a functional chimeric gene in yeast identifies mutations in the simian virus 40 large T antigen J domain. Proceedings of the National Academy of Sciences. 2002;99(4).
110. Cho US, Morrone S, Sablina AA, Arroyo JD, Hahn WC, Xu W. Structural basis of PP2A inhibition by small t antigen. PLoS biology. 2007;5(8).
111. An P, Sáenz Robles MT, Pipas JM. Large T antigens of polyomaviruses: amazing molecular machines. Annual review of microbiology. 2012;66:213-36.
112. Cheng J, Park DE, Berrios C, White EA, Arora R, Yoon R, et al. Merkel cell polyomavirus recruits MYCL to the EP400 complex to promote oncogenesis. PLoS pathogens. 2017;13(10):e1006668.
113. Griffiths DA, Abdul-Sada H, Knight LM, Jackson BR, Richards K, Prescott EL, et al. Merkel cell polyomavirus small T antigen targets the NEMO adaptor protein to disrupt inflammatory signaling. Journal of virology. 2013;87(24):13853-67.
114. Neumann F, Borchert S, Schmidt C, Reimer R, Hohenberg H, Fischer N, et al. Replication, gene expression and particle production by a consensus Merkel Cell Polyomavirus (MCPyV) genome. PloS one. 2011;6(12):e29112.
115. Schowalter RM, Reinhold WC, Buck CB. Entry tropism of BK and Merkel cell polyomaviruses in cell culture. PloS one. 2012;7(7).

116. Tsang SH, Wang X, Li J, Buck CB, You J. Host DNA damage response factors localize to Merkel cell polyomavirus DNA replication sites to support efficient viral DNA replication. Journal of virology. 2014;88(6):3285-97.
117. Paulson KG, Lemos BD, Feng B, Jaimes N, Peñas PF, Bi X, et al. Array-CGH reveals recurrent genomic changes in Merkel cell carcinoma including amplification of L-Myc. Journal of Investigative Dermatology. 2009;129(6):1547-55.
118. Shuda M, Velásquez C, Cheng E, Cordek DG, Kwun HJ, Chang Y, et al. CDK1 substitutes for mTOR kinase to activate mitotic cap-dependent protein translation. Proceedings of the National Academy of Sciences. 2015;112(19):5875-82.
119. Welcker M, Clurman BE. FBW7 ubiquitin ligase: a tumour suppressor at the crossroads of cell division, growth and differentiation. Nature reviews Cancer. 2008;8(2):83.
120. Welcker M, Orian A, Grim JA, Eisenman RN, Clurman BE. A nucleolar isoform of the Fbw7 ubiquitin ligase regulates c-Myc and cell size. Current Biology. 2004;14(20):1852-7.
121. Davis RJ, Welcker M, Clurman BE. Tumor suppression by the Fbw7 ubiquitin ligase: mechanisms and opportunities. Cancer cell. 2014;26(4):455-64.
122. Welcker M, Larimore EA, Swanger J, Bengoechea-Alonso MT, Grim JE, Ericsson J, et al. Fbw7 dimerization determines the specificity and robustness of substrate degradation. Genes & development. 2013;27(23):2531-6.
123. Welcker M, Clurman BE. Fbw7/hCDC4 dimerization regulates its substrate interactions. Cell division. 2007;2(1):7.
124. Hao B, Oehlmann S, Sowa ME, Harper JW, Pavletich NP. Structure of a Fbw7-Skp1-cyclin E complex: multisite-phosphorylated substrate recognition by SCF ubiquitin ligases. Molecular cell. 2007;26(1):131-43.
125. Welcker M, Clurman BE. The SV40 large T antigen contains a decoy phosphodegron that mediates its interactions with Fbw7/hCdc4. Journal of Biological Chemistry. 2005;280(9):7654-8.
126. Koepp DM, Schaefer LK, Ye X, Keyomarsi K, Chu C, Harper JW, et al. Phosphorylation-dependent ubiquitination of cyclin E by the SCFFbw7 ubiquitin ligase. Science. 2001;294(5540):173-7.
127. Welcker M, Singer J, Loeb KR, Grim J, Bloecher A, Gurien-West M, et al. Multisite phosphorylation by Cdk2 and GSK3 controls cyclin E degradation. Molecular cell. 2003;12(2):381-92.
128. Yada M, Hatakeyama S, Kamura T, Nishiyama M, Tsunematsu R, Imaki H, et al. Phosphorylation-dependent degradation of c-Myc is mediated by the F-box protein Fbw7. The EMBO journal. 2004;23(10):2116-25.
129. Kwun HJ, Wendzicki JA, Shuda Y, Moore P, Chang Y. Merkel cell polyomavirus small T antigen induces genome instability by E3 ubiquitin ligase targeting. Oncogene. 2017;36(49):6784.
130. Welcker M, Orian A, Jin J, Grim JA, Harper JW, Eisenman RN, et al. The Fbw7 tumor suppressor regulates glycogen synthase kinase 3 phosphorylation-dependent c-Myc protein degradation. Proceedings of the National Academy of Sciences of the United States of America. 2004;101(24):9085-90.

131. Kõivomägi M, Valk E, Venta R, Iofik A, Lepiku M, Balog ERM, et al. Cascades of multisite phosphorylation control Sic1 destruction at the onset of S phase. Nature. 2011;480(7375):128-31.
132. Kitagawa M, Hatakeyama S, Shirane M, Matsumoto M, Ishida N, Hattori K, et al. An F-box protein, FWD1, mediates ubiquitin-dependent proteolysis of β-catenin. The EMBO journal. 1999;18(9):2401-10.
133. Brägelmann J, Böhm S, Guthrie MR, Mollaoglu G, Oliver TG, Sos ML. Family matters: How MYC family oncogenes impact small cell lung cancer. Cell Cycle. 2017;16(16):1489-98.
134. Kim D-W, Wu N, Kim Y-C, Cheng PF, Basom R, Kim D, et al. Genetic requirement for Mycl and efficacy of RNA Pol I inhibition in mouse models of small cell lung cancer. Genes & development. 2016;30(11):1289-99.
135. Hershko A, Ciechanover A. The ubiquitin system. Annual Reviews 4139 El Camino Way, PO Box 10139, Palo Alto, CA 94303-0139, USA; 1998.
136. Martin-Lluesma S, Schaeffer C, Robert EI, Van Breugel PC, Leupin O, Hantz O, et al. Hepatitis B virus X protein affects S phase progression leading to chromosome segregation defects by binding to damaged DNA binding protein 1. Hepatology. 2008;48(5):1467-76.
137. Liu B, Hong S, Tang Z, Yu H, Giam C-Z. HTLV-I Tax directly binds the Cdc20-associated anaphase-promoting complex and activates it ahead of schedule. Proceedings of the National Academy of Sciences of the United States of America. 2005;102(1):63-8.
138. Scheffner M, Huibregtse JM, Vierstra RD, Howley PM. The HPV-16 E6 and E6-AP complex functions as a ubiquitin-protein ligase in the ubiquitination of p53. Cell. 1993;75(3):495-505.
139. Ali SH, Kasper JS, Arai T, DeCaprio JA. Cul7/p185/p193 binding to simian virus 40 large T antigen has a role in cellular transformation. Journal of virology. 2004;78(6):2749-57.
140. Isobe T, Hattori T, Kitagawa K, Uchida C, Kotake Y, Kosugi I, et al. Adenovirus E1A inhibits SCFFbw7 ubiquitin ligase. Journal of Biological Chemistry. 2009;284(41):27766-79.
141. Larochelle M, Bergeron D, Arcand B, Bachand F. Proximity-dependent biotinylation mediated by TurboID to identify protein–protein interaction networks in yeast. Journal of cell science. 2019;132(11):jcs232249.
142. Moens U, Macdonald A. Effect of the Large and Small T-Antigens of Human Polyomaviruses on Signaling Pathways. International journal of molecular sciences. 2019;20(16):3914.
143. Boopathy GT, Hong W. Role of hippo pathway-Yap/Taz signaling in angiogenesis. Frontiers in cell and developmental biology. 2019;7.
144. Varelas X. The Hippo pathway effectors TAZ and YAP in development, homeostasis and disease. Development. 2014;141(8):1614-26.
145. Gumbiner BM, Kim N-G. The Hippo-YAP signaling pathway and contact inhibition of growth. Journal of cell science. 2014;127(4):709-17.
146. Rouleau C, Fernando ATP, Hwang JH, Faure N, Jiang T, White EA, et al. Transformation by polyomavirus middle T antigen involves a unique bimodal interaction with the Hippo effector YAP. Journal of virology. 2016;90(16):7032-45.
147. Zemke NR, Gou D, Berk AJ. Dedifferentiation by adenovirus E1A due to inactivation of Hippo pathway effectors YAP and TAZ. Genes & development. 2019;33(13-14):828-43.
148. Zhao B, Li L, Lu Q, Wang LH, Liu C-Y, Lei Q, et al. Angiomotin is a novel Hippo pathway component that inhibits YAP oncoprotein. Genes & development. 2011;25(1):51-63.

149. Pobbati AV, Hong W. A combat with the YAP/TAZ-TEAD oncoproteins for cancer therapy. Theranostics. 2020;10(8):3622.
150. Nguyen CD, Yi C. YAP/TAZ signaling and resistance to cancer therapy. Trends in cancer. 2019.
151. Houben R, Shuda M, Weinkam R, Schrama D, Feng H, Chang Y, et al. Merkel cell polyomavirus-infected Merkel cell carcinoma cells require expression of viral T antigens. Journal of virology. 2010;84(14):7064-72.
152. Sablina AA, Hector M, Colpaert N, Hahn WC. Identification of PP2A complexes and pathways involved in cell transformation. Cancer research. 2010;70(24):10474-84.
153. Dye KN, Welcker M, Clurman BE, Roman A, Galloway DA. Merkel cell polyomavirus Tumor antigens expressed in Merkel cell carcinoma function independently of the ubiquitin ligases Fbw7 and β-TrCP. PLoS pathogens. 2019;15(1):e1007543.